KYB

Our Precision, Your Advantage

KAYABA Corporation

KAYABA TECHNICAL REVIEW No. 64 APR. 2022

KAYABA TECHNICAL REVIEW

ISSN 1880-7410

APR. 2022

No.64

KYB Corporation

KYB Corporation adopted the common name of KAYABA Corporation on April 1, 2022.

As of January 1, 2022

Head Office World Trade Center Building South Tower 28F, 2-4-1, Hamamatsu-cho, Minato-ku, Tokyo 105-5128, Japan Tel：(81)3-3435-3511

Basic Technology R&D Center	1-12-1, Asamizodai, Minami-ku, Sagamihara-shi, Kanagawa 252-0328, Japan	TEL:(81)42-745-8111
Production Technology R&D Center	60, Dota, Kani-shi, Gifu 509-0206, Japan	TEL:(81)574-26-1453
Developmental Center	1185 Aza-shirasuna, Kashio, Kawabe-cho, Kamo-gun, Gifu 509-0307, Japan	TEL:(81)574-52-1323
Machine Tools Center	60, Dota, Kani-shi, Gifu 509-0206, Japan	TEL:(81)574-26-5310
North Kanto Branch	2-8-4, Bijogi kita, Toda-shi, Saitama 335-0038, Japan	TEL:(81)48-499-0859
South Kanto Branch	1-12-1, Asamizo-dai, Minami-ku, Sagamihara-shi, Kanagawa 252-0328, Japan	TEL:(81)42-746-5587
Nagoya Branch	Meieki Nishikibashi Bldg. 2F, 5-27-13, Meieki, Nakamura-ku, Nagoya-shi, Aichi 450-0002, Japan	TEL:(81)52-587-1760
Osaka Branch	2nd TEK Bldg. 3F, 1-23-20, Esaka-cho, Suita-shi, Osaka 564-0063, Japan	TEL:(81)6-6387-3221
Fukuoka Branch	Yasukawa-Sangyo Bldg. 5F, 2-6-26, Hakataekihigashi, Hakata-ku, Fukuoka-shi, Fukuoka, 812-0013, Japan	TEL:(81)92-411-2066
Hiroshima Sales Office	Hiroshima Bldg. 4F, 1-12-16 Hikari-machi, Higashi-ku, Hiroshima-shi, Hiroshima, 732-0052, Japan	TEL:(81)82-567-9166
SAGAMI PLANT	1-12-1, Asamizodai, Minami-ku, Sagamihara-shi, Kanagawa 252-0328, Japan	TEL:(81)42-746-5511
KUMAGAYA PLANT	2050, Nagazaike, Fukaya-shi, Saitama 369-1193, Japan	TEL:(81)48-583-2341
GIFU NORTH PLANT	2548, Dota, Kani-shi, Gifu 509-0298, Japan	TEL:(81)574-26-5111
GIFU SOUTH PLANT	505, Dota, Kani-shi, Gifu 509-0297, Japan	TEL:(81)574-26-1111
GIFU EAST PLANT	60, Dota, Kani-shi, Gifu 509-0206, Japan	TEL:(81)574-26-2135
MIE PLANT	1129-11, Kumozunagatsune-cho, Tsu-shi, Mie 514-0396, Japan	TEL:(81)59-234-4111
KYB Stage Engineering Co., Ltd.	1129-11, Kumozunagatsune-cho, Tsu-shi, Mie 514-0396, Japan	TEL:(81)59-234-9260
KYB TRONDULE Co., Ltd.	3909, Ura, Nagaoka-shi, Niigata, 949-5406, Japan	TEL:(81)258-92-6903
TAKAKO Industries, INC.	1-32-1 Hosononishi, Seika-cho, Souraku-gun, Kyoto, 619-0240, Japan	TEL:(81)774-95-3336
KYB Kanayama Co., Ltd.	4350-130, Aza-Funeno Tobe, Kanayama-cho, Gero-shi, Gifu, 509-1605, Japan	TEL:(81)576-35-2201
KYB-YS Co., Ltd.	9165 Sakaki, Sakaki-machi, Hanishina-gun, Nagano, 389-0688, Japan	TEL:(81)268-82-2850
KYB Motorcycle Suspension Co., Ltd.	2548, Dota, Kani-shi, Gifu 509-0298, Japan	TEL:(81)574-27-1170
KYB Logistics Co., Ltd.	2-16, Himegaoka, Kani-shi, Gifu 509-0249, Japan	TEL:(81)574-26-6427
JAPAN ANALYSTS Co., Ltd.	KYB Corporation SAGAMI PLANT 1-12-1, Asamizodai, Minami-ku, Sagamihara-shi, Kanagawa 252-0328, Japan	TEL:(81)42-749-7512
Kensiyuu Co., Ltd.	2-8-4, Bijogi kita, Toda-shi, Saitama 335-0038, Japan	TEL:(81)48-499-9336

Overseas Subsidiaries and Affiliates

【Americas】

KYB Americas Corporation
2625 North Morton, Franklin, Indiana 46131, U.S.A.
TEL: (1)317-736-7774

Takako America Co., Inc.
715 Corey Road Hutchinson, Kansas 67504-1642, U.S.A.
TEL: (1)620-663-1790

KYB International America, Inc.
2625 North Morton, Franklin, Indiana 46131, U.S.A.
TEL: (1)317-346-6719

KYB Mexico S.A. de C.V.
Circuito San Roque Norte #300 Santa Fe II, Puerto Interior, Silao Guanajuato, CP 36275, Mexico
TEL: (52)472-748-5000

KYB Latinoamerica, S.A. de C.V.
Blvd. Manuel Avila Camacho No. 32, Int. 403, Col. Lomas de Chapultepec, Del. Miguel Hidalgo, DF, 11000, Mexico
TEL: (52)55-5282-5770

KYB Manufacturing do Brasil Fabricante de Autopeças S.A.
Rua Francisco Ferreira da Cruz, 3000, Fazenda Rio Grande-Parana, CEP 83820-293, Brazil
TEL: (55)-41-2102-8200

Comercial de AutopeÇas KYB do Brasil Ltda.
Rua Cyro Correia Pereira, 2400 Suite 07-Cidade Industrial, Curitiba-PR, 81460-050, Brazil
TEL: (55)41-3012-3620

【Europe】

KYB Europe GmbH
Langfeldstrasse.11 80939 Munich, Germamy
TEL: (49)-89-5480188-0

KYB Suspensions Europe, S.A.U.
Ctra, Irurzun S/No, 31171 Ororbia Navarra, Spain
TEL: (34)948-421700

KYB Advanced Manufacturing Spain, S.A.U.
Poligono Industrial Perguita Calle B, No. 15, 31210 Los Arcos Navarra, Spain
TEL: (34)948-640336

KYB Manufacturing Czech, s.r.o.
U Panasonicu 277, Stare Civice, 530 06 Pardubice, Czech Republic
TEL: (420)466-812-233

KYB CHITA Manufacturing Europe s.r.o.
Prumyslova 1421, 53701 Chrudim, Czech Republic
TEL: (420)469-363-302

LLC KYB Eurasia
117638 Odesskaya street 2 building A, Moscow, Russian Federation
TEL: (7)495-7716010

【Asia】

KYB Steering (Thailand) Co., Ltd.
700/829 Moo 6, T. Nongtamlueng Amphur Panthong, Chonburi 20160,Thailand
TEL: (66)3-818-5559

KYB(Thailand)Co., Ltd.
700/363 Moo 6, Amata Nakorn Industrial Park2, Bangna-Trad Road, K.M. 57, Tambol Don Hua Roh, Amqhur Muang, Chonburi 20000, Thailand
TEL: (66)3-846-9999

KYB Asian Pacific Corporation Ltd.
No. 4345 Bhiraj Tower at BITEC, Unit 1209-1211, 12th Floor, Sukhumvit Road, Bangnatai Sub-District, Bangna District, Bangkok 10260, Thailand
TEL: (66)2-300-9777

KYB-UMW Malaysia Sdn. Bhd.
Lot 8, Jalan Waja 16, Telok Panglima Garang, 42500 Kuala Langat, Selangor, Malaysia
TEL: (60)3-3322-0800

PT. KYB Hydraulics Manufacturing Indonesia
JL. Irian X blok RR2 Kawasan MM2100, Cikarang Barat 17520, Indonesia
TEL: (62)21-28080145

PT. Kayaba Indonesia
JL, Jawa Blok ii No. 4 Kawasan MM2100, Cikarang Barat 17520, Indonesia
TEL: (62)21-8981456

PT. Chita Indonesia
JL, Jawa Blok ii No. 4 Kawasan MM2100, Cikarang Barat 17520, Indonesia
TEL: (62)21-89983737

KYB Manufacturing Vietnam Co., Ltd.
Plot I 10-I 11-I 12, Thang Long Industrial Park, Dong Anh District, Hanoi, Vietnam
TEL: (84)24-3881-2773

Takako Vietnam Co., Ltd.
27 Dai Lo Doc Lap, Vietnam Singapore Industrial Park, Thuan An District, Binh Duong, Vietnam
TEL: (84)274-378-2954

永華機械工業股份有限公司
KYB Manufacturing Taiwan Co., Ltd.
No. 493, Guang Hsing Road, Bade District, Taoyuan City, 33454, Taiwan
TEL: (886)3-368-3123

KYB Motorcycle Suspension India Pvt. Ltd.
Pilot No. 6, Sipcot Industrial Park, Vallam Vadagal Village, Sriperumbudur Taluk, Kancheepuram District 631604 Tamil Nadu, India
TEL: (91)44-3012-4301

KYB-Conmat Pvt. Ltd.
702-703, Beside N. H. No. 8, Por, Vadodara 391243, Gujatat, India
TEL: (91)960-1551608

KYB Corporation Chennai Branch
No. 408, Height 1, Temple Green Project, Mathur Village, Sriperumbudur Taluk, Kancheepuram District, India 602105
TEL: (91)2568-0501

【China】

凱迩必(中国)投資有限公司
KYB (China) Investment Co., Ltd.
No. 121, Wei 3 Road, Dingmao, Zhenjiang New Zone, Zhenjiang, Jiangsu, 212009, China
TEL: (86)511-8558-0300

凱迩必機械工業(鎮江)有限公司
KYB Industrial Machinery (Zhenjiang) Ltd.
No. 38, Wei 3 Road, Dingmao, Zhenjiang New Zone, Zhenjiang, Jiangsu, 212009, China
TEL: (86)511-8889-1008

無錫凱迩必拓普減震器有限公司
Wuxi KYB Top Absorber Co., Ltd.
No. 2 Xikun North Road, Singapore Industrial Zone, Xinwu District, Wuxi, Jiangsu, 214028, China
TEL: (86)510-8528-0118

常州朗鋭凱迩必減振技術有限公司
Changzhou KYB Leadrun Vibration Reduction Technology Co., Ltd.
No. 19 Shunyuan Road, New District, Changzhou, Jiangsu 213125 China
TEL: (86)519-8595-7206

湖北恒隆凱迩必汽車電動転向系統有限公司
Hubei Henglong & KYB Automobile Electric Steering System Co., Ltd.
108 Shacen Road, Economic and Technological Development Zone, Jingzhou, Hubei, China. 434000
TEL: (86)716-416-7951

知多弾簧工業(鎮江)有限公司
CHITA KYB Manufacturing (Zhenjiang) Co., Ltd.
No. 8 Building-1F, New Energy Industrial Park (North Park), No. 300, Gangnan Road, Zhenjiang New District, Jiangsu 212132, China
TEL: (86)511-8317-2570

KAYABA TECHNICAL REVIEW

No. 64 APR. 2022

CONTENTS

Foreword

Future of High Value Manufacturing

(Evolution from Ultimate Form Generation to Function Generation)

KURIYAGAWA Tsunemoto*

1. Introduction

In Japan, it is important to discuss a vision for Monozukuri (creative design and manufacturing), which is the country's industrial base.

However, Monozukuri that has long contributed to the prosperity of Japan with mass production and volume consumption is almost coming to an end. We will face circumstances that require us to develop another type of Monozukuri responding to various senses of values in the future.

For example, we need to take measures for achieving carbon neutral or supporting super-aging of society. It is being internationally discussed to develop novel technologies to accomplish these goals as an urgent challenge.

Besides technological innovation, economic and societal innovations are also indispensable. For these ends, we should have a broad range of knowledge and insight covering areas from human and social sciences to natural science. In recent years, some attempts have been actively made to establish a cross-sectional innovation and eco systems in which industry, academia and government can talk together through coalition. Then, what the Monozukuri field can do to help them achieve the ends. One is to develop even higher-accuracy, even higher-value-added products that cannot be achieved with foreign technologies. What is significant to achieve this is not only the existing simple Form Generation, but also Function Generation that creates a structure for expressing functions on the surface or internally. The author named this "Function Generation Machining" and has promoted its research and development to be one of the technologies for "High Value Manufacturing".

2. What Is Function Generation Machining?

Machined parts are normally evaluated for their machining accuracy with two criteria: form accuracy and surface roughness. Requirements for machining accuracy have recently become more intense with some of them exceeding nano order to reach pico order. To achieve such ultimate machining accuracy, comprehensive research and development has already been started covering machining principles, tooling, machine tools, evaluation and measurement methodologies, materials, assembly methods, and design theory. Function Generation Machining produces microscopic structures on an ultra-precision machined surface achieved with these techniques or controls crystal structures in the proximity of the machined surface, thereby expressing new functions.

In this way, a combination of form generation and function generation is used to try to achieve high-value-added generation. This type of Monozukuri is called Function Generation Machining. In other words, the conventional simple form generation should be merged with function generation into a new style of Monozukuri.

To achieve this, it is indispensable to scientifically make clear how the machining works in the molecular or atomic level and to establish a new machining process for realizing pico-precision machining. Specifically, this comprehensive technology to be established must leverage pico/nano/micro/macro or so-called multi-scale mechanical system design theory that supports pico-precision machining to complete a device or even a system, and tool design engineering, pico-level in-situ measurement and evaluation techniques, cooperation of machining simulators and systems, pico-level implementation for precision assembly of microscopic structures, and material generation and strength reliability evaluation for ensuring safety and security.

3. The Keyword Is “Hybrid”

Many function generation products have a hybrid structure. For example, μm-order diffraction grating is formed on an aspherical lens surface, and furthermore a several hundred nm-pitch moth-eye structure is superimposed to be a high-function hybrid refraction-diffraction optical device with nonreflective function. Such a hybrid structure can often be fabricated by combining different machining methods, not using them independently, to express significantly higher efficiency and/or special functions. These examples include ultrasonic-assisted grinding that combines ultrasonic machining and grinding, laser-assisted micro machining that combines laser cutting and grinding, and ultrasonic vibration assisted

*Professor, Tohoku University

electrochemical grinding that combines three techniques: ultrasonic machining, grinding and electrolysis. In addition, one of the technologies recently developed is one that uses ultrafine bubble (UFB) machining fluid to simultaneously achieve improved machinability and surface modification. In this type of machining, the chip removal mechanism will be greatly affected by chemical factors because chips are as fine as nano order. Particularly where electrolysis, discharge, laser and UFB-assisted process are combined, nano-order physico-chemical phenomena must be understood not only from the mechanical engineering aspect, but also from the chemical and quantum aspects.

4. In Closing

This paper has introduced Function Generation Machining for achieving high-value-added Monozukuri that may be significant in discussing future Monozukuri. To implement a machining technique for future Monozukuri, scientific and rational Monozukuri based on understanding of what's really happening in the nano-order world is indispensable.

It is also important not to heavily depend on development of innovative mechanical solutions, namely, advanced hardware. Of course, hardware development is important, but software development is also essential in that hardware items cannot be combined and used efficiently without quality software. Furthermore, Monozukuri must essentially take into account production, disposal and recycling (including reuse) to be a recycling-based technology. In the life stream of "materials" (the syllable "mono" of Mono-zukuri literally means "material" in Japanese), greenhouse gases including CO2 are generated. Therefore, it is also needed to design and accomplish life cycle assessment to minimize the greenhouse gases.

Finally, needless to say, it is important to develop human resources with capability and spirit to overcome various difficulties in societally implementing novel technologies, the so-called Devil River, Valley of Death, and Darwinian Sea. It is strongly desired to establish a corporate environment for such human resources development to be realized in house as well. Simultaneously, I expect young engineers to develop and deliver entrepreneurship themselves for jumping into a world they have never seen before. I am really looking forward to seeing how Monozukuri (creative design and manufacturing) will evolve in future.

Editorial

Microstructure and Mechanical Properties of Cast Iron

HIRATSUKA Sadato*

1. Introduction

Cast iron is an important structural material of castings. Japan produced about 3 million tons of cast iron in 2020. Of the annual production, 63.7% was used for transportation machinery (including automobiles, railroads and ships), 23.7% for general or electric machinery (including industrial machinery and equipment, construction machinery, metal working tools & machine tools, and electric machinery), 7.8% for cast iron pipes, and the remaining 4.7% for other applications (including couplings, kitchen appliances and craftwork) [1].

Fig. 1 shows an example of hydraulic equipment for regular/compact excavators manufactured by Kayaba Industry Co., Ltd. [2] The compact hydraulic excavator has control valves whose body is made of cast iron.

Both cast iron and steel are classified into iron-carbon (Fe-C) alloys. They are differentiated from each other by carbon content. Steel has a carbon content of not more than approximately 2 mass% (hereinafter expressed in "%" only) while cast iron has a higher carbon content than the level. Practical cast iron is usually considered as Fe-C-Si alloys because of its carbon content as high as 3% to 4% and its silicon (Si) content of around 1% to 3%. With a higher percentage of carbon than 2%, carbide forms in iron (Fe) in the cast iron. In this sense, cast iron may be considered as a composite material consisting of steel and graphite in various forms.

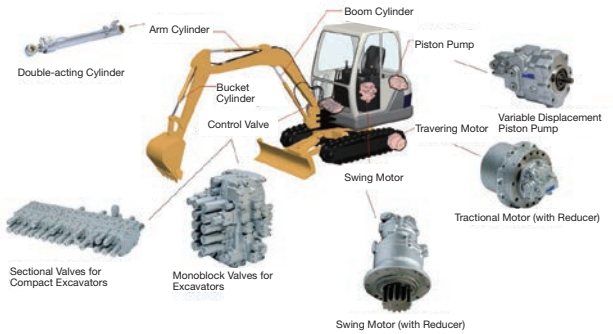

Fig. 1 Example of hydraulic equipment for regular/compact excavators

*Professor, Research Center for Casting Technology, Iwate University

The lower carbon content of cast iron compared to steel results in a substantially low solidifying (or melting) temperature and good fluidity. Cast iron also features good castability because of its low solidification shrinkage or less shrinkage cavities attributable to volume expansion taking place when the graphite is crystallized during solidification. In addition, the presence of graphite and the high silicone content give cast iron excellent industrial properties including vibration absorption, machineability, wear resistance, thermal conductivity, corrosion resistance and oxidization resistance.

This paper describes the microstructure and mechanical properties of cast iron that may affect its characteristics.

2. Microstructure of Cast Iron

The microstructure of cast iron greatly varies by the chemical composition of the molten iron, the solidification condition, and heat treatment given. What microstructure the solidified cast iron will have is a critical issue because cast iron is used in the as-cast condition in most cases; however, this does not matter a lot for steel because it is subjected to deformation processing, such as rolling, and heat treatment after solidification. The microstructure of cast iron can be roughly divided into graphite and matrix microstructures. The combination of these two microstructures greatly affects the mechanical, physical and chemical properties of the cast iron.

2.1 Graphite Microstructure

Fig. 2 shows how graphite can appear in iron castings. This classification was proposed by the technical committee in the World Foundry Congress held in 1962 in the U.S. [3]

Form I is flake graphite. Cast iron with graphite flakes is classified by the Japanese Industrial Standard (JIS) G5501 into gray cast iron. Form II is spheroidal graphite with pointed ends that is likely to appear when a spheroidizing agent such as magnesium (Mg) is added in an excessive amount during production of nodular graphite cast iron. Form III is quasi-flake graphite that may appear with a lack of graphite spheroidizing agent. This type of graphite forms in CV graphite cast iron. Form IV is massive graphite that may appear in malleable cast iron or graphite steel. Form V is quasi-spheroidal graphite. Form VI is com-

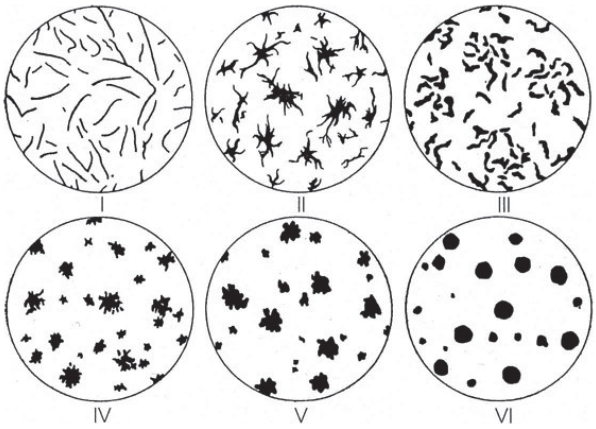

Fig. 2 Classification of graphite forms

pletely spheroidal graphite that often appears in nodular graphite cast iron. Among these, the forms II to VI are uniform graphite in a random distribution in most cases. However, form I, namely, flake graphite, changes in form and distribution depending on the chemical composition of the cast iron, its melting history and/or cooling rate during solidification. American Society for Testing Materials (ASTM) A247 classifies this category of graphite into Types A to E by distribution as shown in Fig. 3. Type A shows random flake graphite in a uniform distribution, which is the most optimally distributed flake graphite. Type B is called rosette flake graphite. Type C shows hypereutectic cast iron with coarse pro-eutectic graphite. Type D is called eutectic graphite that is likely to appear in titan (Ti)-added or undercooled molten iron. Type E is called interdendritic flake graphite.

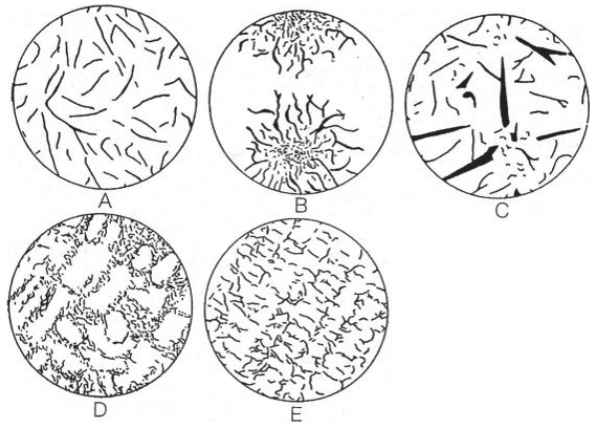

Fig. 3 Types of flake graphite by distribution [ASTM A247]

2.2 Matrix Microstructure

The matrix microstructure of cast iron varies by the cooling rate during solidification, the alloy element content, and/or heat treatment given. This section introduces three typical matrices:

(i) Ferrite

The ferrite matrix, which is also known as α-Fe or α solid solution, is soft iron with a trace quantity of carbon having a body-centered cubic crystal structure with a density of 7.9, a tensile strength of 200 MPa to 400 MPa, and a Brinell hardness of 90 HB to 150 HB. Ferrite in iron castings is called silico-ferrite because silicon (Si) incorporates into the ferrite to form a solid solution. The ferrite matrix with more silicon offers higher tensile strength and higher hardness.

(ii) Cementite

Cementite is a rhombic composition consisting of three Fe atoms and a C atom with a density of 7.7 and a Brinell hardness of 550 HB. This is the hardest and brittlest among all the cast iron microstructures.

(iii) Pearlite

Austenite breaks down (transforms) into ferrite and cementite during metastable eutectoid transformation. These two phases are generated in the form of a stack of sheets alternately overlayed with each other. They can be identified as a layered or banded structure under an optical microscope. It is a very tough microstructure with a density of 7.8, a tensile strength of 800 MPa to 900 MPa, and a Brinell hardness of 200 HB to 240 HB.

Nodular graphite cast iron normally has a so-called bull's-eye microstructure in which ferrite and pearlite coexist as shown in Fig. 4.

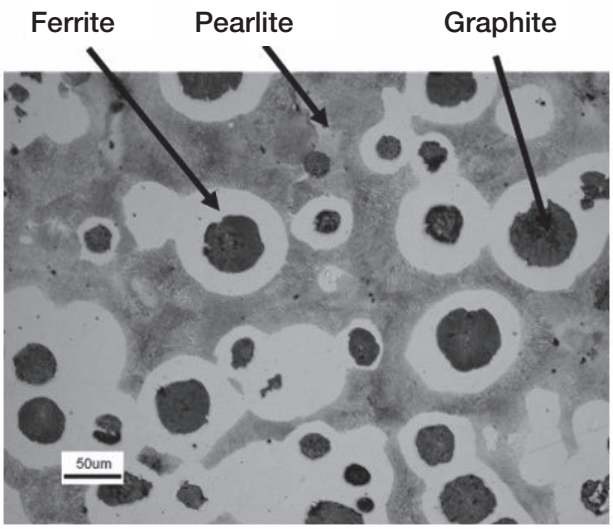

Fig. 4 Bull's eye microstructure of nodular graphite cast iron

3. Mechanical Properties of Cast Iron

Mechanical properties of material including tensile strength, hardness, elongation and fatigue strength are collectively called generalized strength. Any of these properties is a measure of resistance to deformation or fracture.

The strength of a metallic material is decided by its microstructure. In the case of cast iron, the strength is governed by the graphite, matrix and other microstructures.

3.1 Strength of Flake Graphite Cast Iron

As compared to the matrix, the graphite microstructure

can easily fracture with a substantially lower force because of its tensile strength of around as low as 20 MPa. Therefore, the strength of cast iron is decided by the strength, form, and continuity of the matrix except graphite particles.

In other words, cast iron with fine graphite (Type A or E) may offer a high strength. Those with long-type graphite (Type A, B or C) usually have a low strength because of their low continuity of the matrix.

Fig. 5 illustrates how two types of flake graphite cast iron can fracture when they are applied with a tensile force: one has a ductile matrix (a) and the other a brittle matrix (b). [4] The former (a) with a ductile matrix will have a number of ductile cracks and partial ruptures. These will be connected with each other along the graphite flakes, thereby accelerating rupture.

The latter (b) with a brittle matrix in turn will accelerate rupture when brittle cracks occurring at the ends of the graphite flakes propagate.

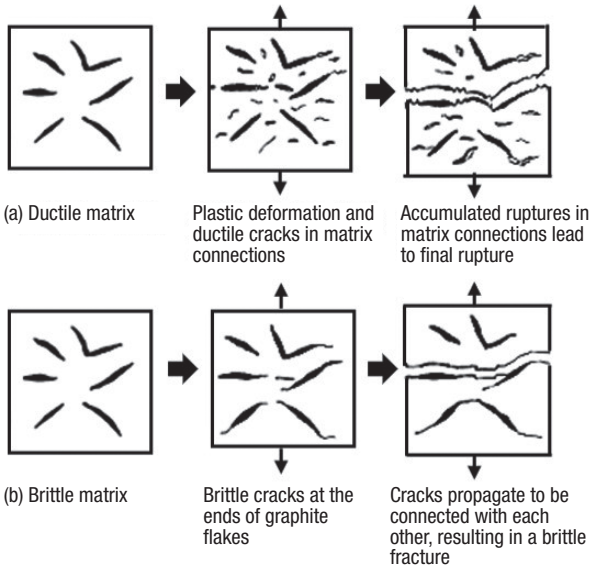

Fig. 5 How flake graphite cast iron fails with tensile fracture

Fig. 6 shows stress-strain curves of flake graphite cast iron. [5] The continuously warped curves include no obvious yield behavior. Determining the 0.2% yield point (or yield strength) will not make sense to flake graphite cast iron. Rather, it is necessary to define the yield strength against a small distortion as low as 0.05% or even smaller.

3.2 Strength of Nodular Graphite Cast Iron

Nodular graphite cast iron has a matrix with substantially higher continuity than that of the flake graphite type. The extent of continuity hardly varies by minor changes in form (the degree of spheroidization) or particle size of graphite as long as the degree of spheroidization is higher than a certain level (generally 0.7).

Fig. 7 illustrates how two types of nodular graphite cast iron can fracture when they are applied with a tensile force: one has a ductile matrix (a) and the other a brittle matrix (b). [6]

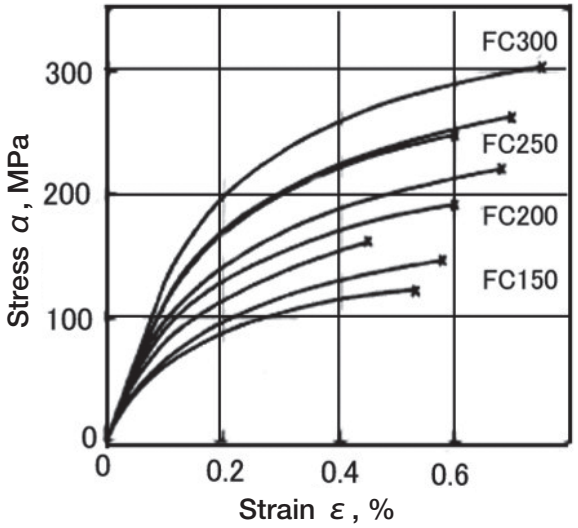

Fig. 6 Stress-strain curves of flake graphite cast iron

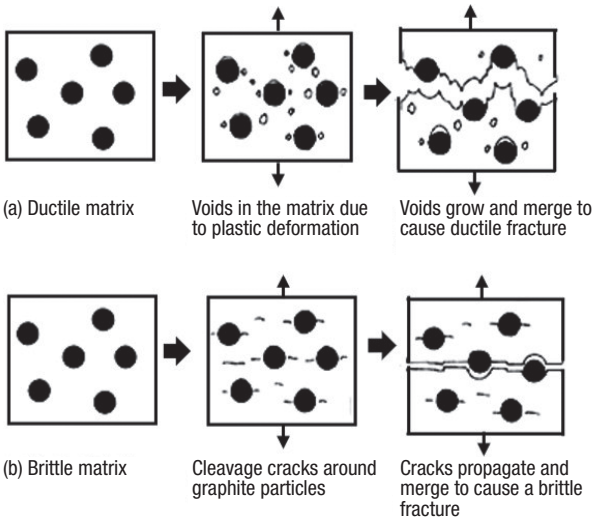

Fig. 7 How nodular graphite cast iron fails with tensile fracture

The former (a) with a ductile matrix involves sufficient plastic deformation. Many cracks occurring around the graphite particles merge into voids as deformation progresses. Voids also occur in the grain boundaries and inclusions within the matrix. These voids are connected with each other and merge into bigger voids, resulting in a rupture.

In this rupture development process, cracks tend to develop in a zigzag manner bridging the closest graphite particles or the weakest parts of the largest graphite particles.

For the latter (b) with a brittle matrix in turn, cleavage cracks occurring around the graphite particles will grow to cause rapid crack propagation, resulting in a rupture.

Fig. 8 shows the relationship between the tensile strength and the carbon equivalent (CE) value of nodular, compacted and flake graphite cast iron. [7] According to the figure, the strength of flake graphite cast iron greatly varies by the CE value while that of nodular graphite cast

iron seldom depends on the CE value. The figure also implies that compacted graphite cast iron is almost midway between the two. This is because the strength of flake graphite cast iron heavily depends on the matrix continuity (i.e., to what extent the matrix among graphite flakes is sound with no break), in other words, the form and distribution of graphite flakes. For nodular graphite cast iron consisting of distributed independent spheroidal graphite particles (approximately 10 vol%) and a matrix (approximately 90 vol%) in turn, the matrix shows considerably higher continuity than for flake graphite cast iron. Naturally, the strength of nodular graphite cast iron heavily depends on the matrix microstructure and is seldom affected by the CE value.

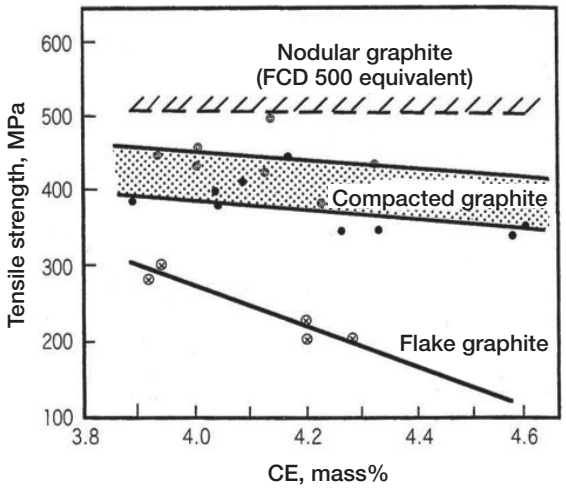

Fig. 8 Effect of CE value on the tensile strength of a variety of cast iron

Fig. 9 shows stress-strain curves of four types of nodular graphite cast iron with different matrix microstructures. [8] Specifically, these curves indicate the stress-strain relationship of austempered ductile irons (ADI) with ferrite matrix (curve 1), with ferrite and pearlite matrix (bull's eye microstructure) (curve 2), with pearlite matrix (curve 3), and with bainite matrix (curve 4). The curve 1 for ferrite matrix shows high elongation. As pearlite occupies a larger area of the matrix in order of the curves 2, 3, the stress-strain curve tends to show higher stress.

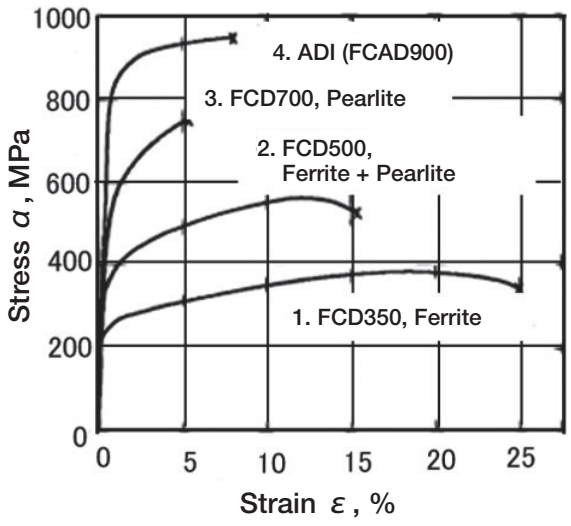

Fig. 9 Stress-strain curves of nodular graphite cast iron

Fig. 10 shows the correlation among pearlite area, tensile strength and elongation of nodular graphite cast iron. [9] As the pearlite area increases, the tensile strength goes up. By contrast, as the pearlite area slightly increases, elongation rapidly decreases and then tends to decrease gradually.

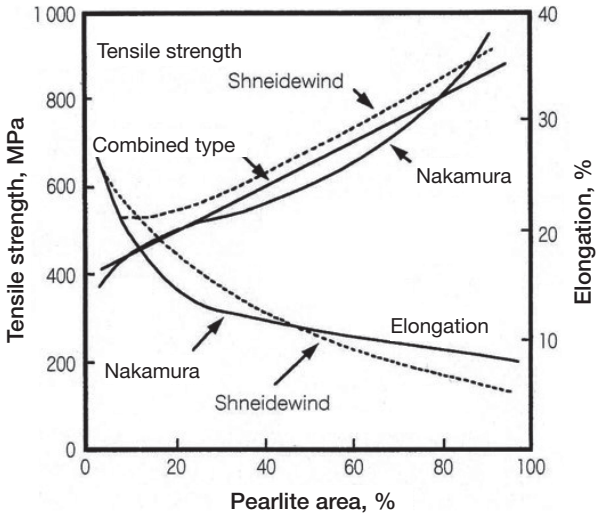

Fig. 10 Relationship among pearlite area, tensile strength and elongation of nodular graphite cast iron

4. In Closing

Cast iron can be considered as a composite material consisting of graphite and steel. Its strength is governed by the graphite, matrix and other microstructures.

The strength of flake graphite cast iron is primarily affected by the form of graphite flakes, namely, the matrix continuity between graphite flakes, and secondarily by the matrix microstructure.

In nodular graphite cast iron in turn, the matrix continuity is substantially higher than for flake graphite cast iron. This means that the strength of nodular graphite cast iron heavily depends on the matrix microstructure.

Iron castings can deliver excellent mechanical, physical and chemical properties when their graphite and matrix microstructures are properly controlled. High-strength, high-function cast iron whose microstructure has been suitably controlled can be expected to be applied to a variety of industrial applications. I hope this paper will help manufacturers achieve this.

References

1) SOKEIZAI Annual Industrial Report: SOKEIZAI Vol.62 (2021) 8.
2) KYB Hydraulics Products Guide (Construction equipment, industrial vehicles, agricultural equipment, and other industrial equipment).
3) A.B. Everest: Trans. Amer. Foundrym. Soc., 70 (1962) 210.

4) NOGUCHI Toru: Journal of Japan Foundry Engineering Society, Volume 77 (2005) 794.
5) NOGUCHI Toru: Journal of Japan Foundry Engineering Society, Volume 76 (2004) 333.
6) HARADA Shoji, NOGUCHI Toru: Evaluation of strength of nodular graphite cast iron, AGNE Gijutsu Center Inc. (1999) 52.
7) Japan Foundry Engineering Society (editor): Foundry Engineering Handbook (Maruzen Publishing Co., Ltd.) (2002) 254.
8) HARADA Shoji, NOGUCHI Toru: Evaluation of strength of nodular graphite cast iron, AGNE Gijutsu Center Inc. (1999) 50.
9) NAKAMURA Koukichi, SUMIMOTO Haruyoshi: Castings 39 (1967) 480.

Technology Explanation

Building the Foundation for MES Services in the New Era

YUBUKI Kento, GABRIELLA Anak Magin

Abstract

With the advancement of digital technology, the manufacturing industry is becoming increasingly digitalized. Companies all over the world are using the Internet of Things (IoT) to build “smart factories” where each device in the factory is connected to the Internet to improve the efficiency of the manufacturing process.

Japan’s manufacturing industry has maintained quality through improvement activities and worker training. For this reason, there has been little progress in digitalization efforts. However, in recent years, with the decline in the working population and rapid changes in the international market, production systems need to be more productive and flexible than ever before. This is why MES, which analyzes data from manufacturing processes to improve productivity and support workers, and SCADA, which monitors and automatically controls equipment data, are attracting attention.

KYB is also working on MES and SCADA, and has several systems in operation to acquire and utilize data from production lines and equipment. In order to collect, accumulate, analyze, and utilize data, an analysis platform called “IoT Platform” has been developed in-house. However, the systems that have been in operation for a long time are not linked to the IoT Platform, so only limited analysis can be done within the systems, and they are not being fully utilized.

Therefore, in this development, we have developed a new service that solves these problems by first linking the IoT Platform to a single production data collection system. This system utilizes IoT and cloud technologies to build its functions. This paper describes the integration with the IoT Platform and the functions we have developed to utilize data in the manufacturing process.

1 Introduction

With the recent rapid advancement in digital technology, the world's manufacturing industry has changed significantly. Companies are actively introducing digital technology to use the Internet of Things (IoT) [Note 1)] for building "smart factories" [Note 2)] where all devices and equipment are connected with each other via the Internet. Such a smart factory can collect and accumulate data from its manufacturing process and analyze it using advanced technologies including artificial intelligence (AI) [Note 3)]. This system can be expected to provide the following effects:

- To identify any inefficient parts of the manufacturing process and solve problems, achieving higher productivity, higher product quality, and lower cost
- To create a database of techniques and expertise of skilled technicians to allow for automation and transfer of their skills to younger technicians
- To use the accumulated data to predict the demand and supply and plan predictive maintenance

However, Japan's manufacturing industry has been left behind on digitalization. Japan's manufacturing (often called "Monozukuri") has maintained quality through human efforts including (skilled technicians' improvement activities leveraging their skills and experience and worker training to enforce workplace discipline. Only a few companies have heavily invested in digitalization programs. Quality maintenance has mainly been assured with human-based approaches relying on the expertise of technicians. In recent years, however, Japan has failed to successfully deal with the decline in the working population with fewer children and aged adults as well as the rapid changes in the international market, resulting in lower competitiveness. Owing to such situation, digitalization efforts are attracting attention in the Japanese manufacturing industry as well.

Today, many systems to promote enterprise digitalization are available. Among them, the following three are considered significant in the manufacturing industry:

- Enterprise Resource Planning (ERP)
- Manufacturing Execution System (MES)
- Supervisory Control And Data Acquisition (SCADA)

The ERP is the integrated management of main business processes. The ERP system centralizes management of business resources including humans, things, money and information. General systems to collect and control information necessary for financial, customer, inventory

and human resource management are packed in an ERP system to help companies make decisions.

The MES is used to identify, manage and support manufacturing processes. The system makes use of data on production equipment, production control and product quality for improving productivity and quality and for supporting workers. While the ERP system covers management of an entire enterprise, the MES can be said to be a management system tailored to its manufacturing process. With this difference in mind, the MES can be linked to the higher-order ERP system to allow decision making based on real-time data collected from the manufacturing process.

The SCADA system monitors and controls manufacturing processes. It monitors how production devices are being operated and measured and, if necessary, controls them. While the MES analyzes and utilizes production data, the SCADA system monitors what is happening in the manufacturing process in real time. With this difference in mind, the SCADA system can be linked to the higher-order MES to allow for management of the manufacturing process and its automatic control in case of abnormality.

These three systems linked to each other will enable all employees and management to get a whole grasp of data from upstream to downstream and to carry out various activities based on the data, including decision making, improvement, and new business development.

KYB has also promoted efforts to manage and utilize data collected from its production lines and devices from an earlier time. The typical systems of this kind include the Point of Production Information Collection System (POPICS) and the line monitoring system (the details of these systems will be described in the following chapter). These systems that collect and utilize operation data from production lines and devices are considered to be positioned within the production system as shown in Fig. 1. Our POPICS has certainly achieved data sharing among the ERP, MES and SCADA regions, but only to a limited extent. Our line monitoring system is being reviewed to provide various functions for the SCADA region by introducing new technologies. However, its integration with higher-order systems such as MES or ERP has not yet been discussed, resulting in insufficient use of data from the manufacturing process.

We have built a foundation to provide new MES services (Fig. 1) using a SCADA collecting data from the line monitoring system linked to an MES that has been designed to be able to have additional functions. The following describes the details of the foundation and its related systems.

Note 1) An acronym for Internet of Things. The IoT refers to general attempts to connect things to the Internet and utilize them.

Note 2) A factory where devices therein are connected with each other via the Internet to improve the manufacturing process and enhance the operation efficiency. Data collected from the devices is analyzed and utilized in a sophisticated manner to optimize the factory/production management.

Note 3) An acronym for Artificial Intelligence.

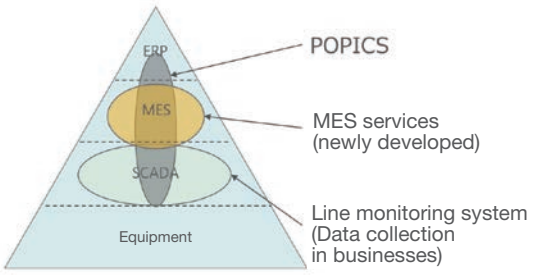

Fig. 1 Scheme of systems for MES services (KYB's effort)

2 Current Systems in KYB

2.1 POPICS (Fig. 2)

KYB developed and introduced a production line data collection system called POPICS 20 or more years ago [1].

Via panel computers installed on the production lines, POPICS transfers production instructions and other data from higher-order systems, collects cycle time data using device I/O, and collects nonconformance reports by operators and other data from lower-order systems. POPICS summarizes collected data into KPIs [Note 4] such as productivity and presents them to manager-class personnel using a visualization application program.

Part of POPICS has already been linked to higher-order systems so that POPICS data can also be viewed on the systems that manage cost data and inventory control information.

A problem is that POPICS only collects data in production lines. Collected data for each line is not sufficient to develop measures against device failures or conduct improvement activities, failing to satisfy user needs.

Note 4) An acronym for Key Performance Indicator. This major performance evaluation indicator is intended to evaluate achievements against goals.

Fig. 2 Example of POPICS window (sample data shown)

2.2 Line Monitoring System

KYB is promoting Innovative Monozukuri mainly on the production lines in its factories for manufacturing shock absorbers, which are one of the company's key products. This activity aggressively makes use of AI and IoT technologies to recreate a manufacturing system from design to production, with the aim to achieve the following goals:

① To double productivity
② To halve design-to-production lead time
③ To achieve zero nonconformance

Then, KYB introduced IoT technology to the production lines and developed a new line monitoring system for visualizing the manufacturing process in an easy-to-understand way to ensure higher productivity and higher quality. This system was developed in 2017 as an improved version of the POPICS described in the previous section and has been sequentially introduced to KYB facilities. While the conventional POPICS can only collect data in production lines, the new line monitoring system can collect data in production devices, thereby enabling real-time monitoring of individual devices.

In this line monitoring system, PLCs Note 5) for individual devices collect operation data, which will be put together by a general PLC installed on each line and stored in a database (DB) built on a line server. Furthermore, a visualization software program running on the line server displays data on a large-sized monitor in an easy-to-understand way (see section 4.3 for the system configuration).

The monitor displays data as shown in Fig. 3. Production information including KPIs and the operating status of each device, quality information including measurements, and processing condition information can be viewed on the screen. Note 6) Personnel can easily view these types of information in real time to identify any anomaly in each device and take appropriate measures.

However, the current line monitoring system cannot provide line comparison or long-time data analysis, posing a challenge of diversified analysis to be available.

Fig. 3 Example of display on the line monitor screen (sample data shown)

Note 5) An acronym for Programmable Logic Controller. This control device developed as an alternate to a relay circuit is often used to control production devices.

Note 6) The information includes undisclosed information that has been intentionally deleted or blurred.

2.3 KYB-IoT Platform (Fig. 4)

In order to analyze and utilize all in-house data, KYB internally developed a data analysis base called KYB-IoT Platform Note 7) in 2020. The Platform was developed under the concept that "anyone can easily analyze and use data anywhere anytime". Storage of collected data as well as data analysis and use with AI or BI Note 8) can be started easily and quickly.

The KYB-IoT Platform has been built on the public cloud Amazon Web Service (AWS) where the storage and processing capability can be scaled up/down depending on data volume and throughput. The cloud-based platform can be used anywhere and can easily be deployed throughout the world. Leveraging the abundant cloud services available on the AWS will efficiently develop new services and provide additional functions.

One of the systems operating on the KYB-IoT platform is the equipment predictive maintenance system. [2] This system collects data for identifying the equipment status such as vibration and temperature and then analyze it with AI, thereby enabling prediction of failure signs. The results are visualized with BI tools to be available to the department users belong to, implementing predictive maintenance.

In this case example, saving, AI analysis and visualization with BI tools of collected data are all implemented on the KYB-IoT Platform. Beside these, the platform implements the function that issues an alarm when a failure exceeds a threshold level and has an improved visualization monitor. The KYB-IoT Platform has thus been added with new functions and has been improved as necessary.

Note 7) A system base to collect, visualize, analyze and control large volume of data from IoT devices connected to the network.

Note 8) An acronym for Business Intelligence. It refers to collecting, accumulating and analyzing data to support decision making on enterprise activities.

2.4 Problems with the Current Internal Systems

KYB has different systems shown in Fig. 5. However, it cannot be said that these systems are properly interfaced to each other so as to optimize the company's total operation. If these systems could share and exchange data, we would be able to identify more clearly what the company is actually doing or what we have not noticed so far. The company should leverage the potential of the systems.

Some production systems have been developed and deployed recently, including the line monitoring system described in section 2.2 and the KYB-IoT Platform described in section 2.3. Unfortunately, these systems have not been linked to each other, failing to use data effectively.

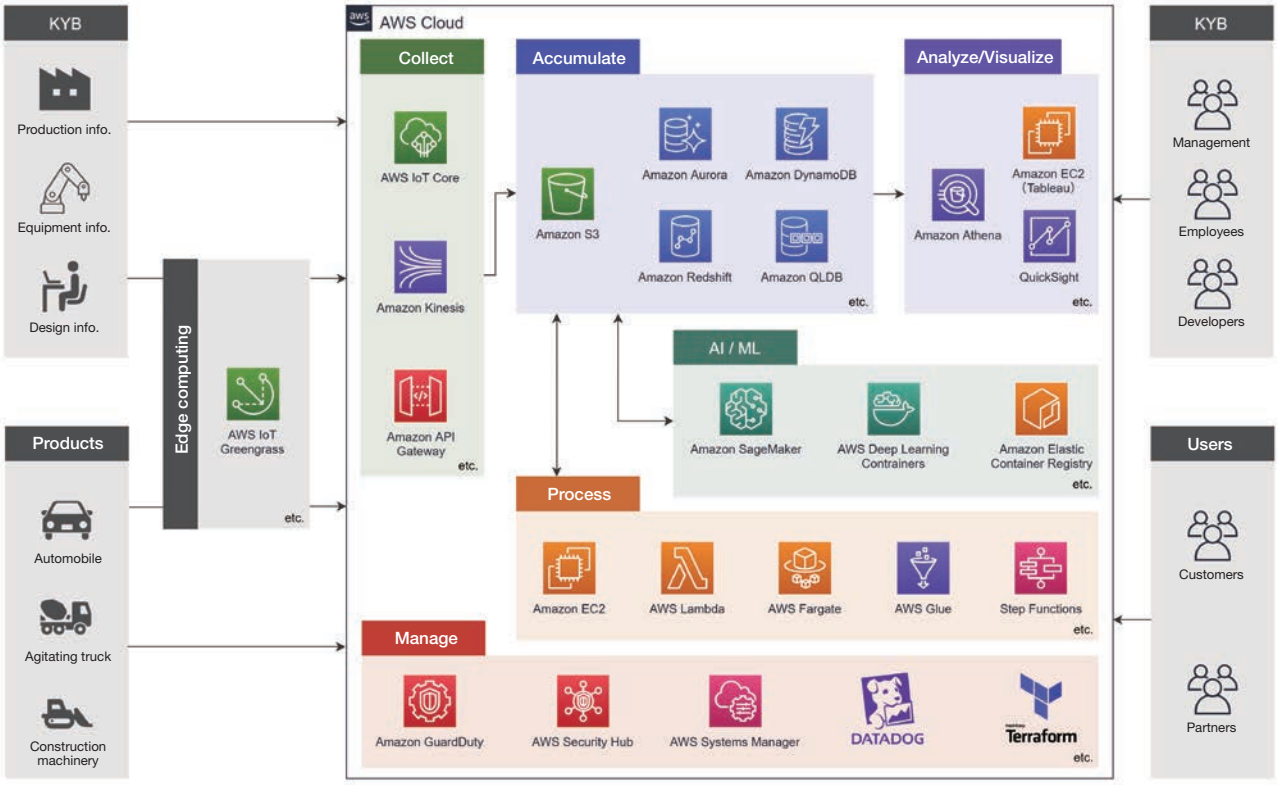

Fig. 4 Overview of IoT Platform

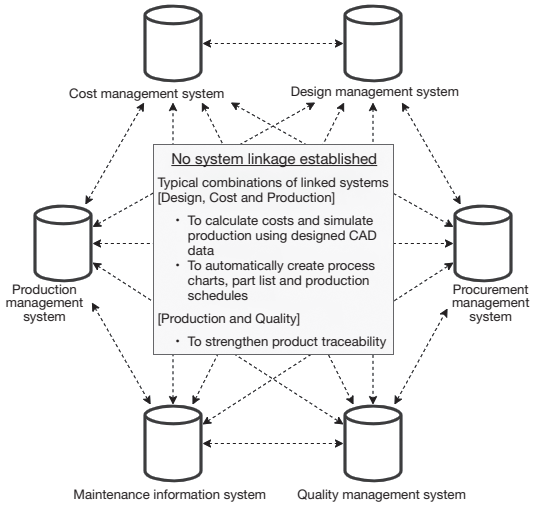

Fig. 5 Current internal systems

In addition to the line monitoring system, the company has also discussed or developed other data collection systems to be deployed in internal source locations. Still, these systems have been designed to display and store data in different ways because they use their own data formats. This is one of the reasons why the systems can hardly share data.

To overcome these challenges, KYB is discussing to centralize data in the KYB-IoT Platform. In addition, to solve the problem that several data collection systems gather different data items from internal source locations, it is necessary to decide what data is to be collected in what format, such as the standard data set including "CT [Note 9], MT [Note 10] and anomaly time".

In this development, we have built a foundation of a total system to centralize manufacturing process data in the KYB-IoT Platform and to link the platform to other systems. The following sections explain it in detail.

Note 9) An acronym for Cycle Time. It refers to the operation cycle time from when a task is completed to when a next task is completed.

Note 10) An acronym for Machine Time. It refers to the machining time of machine tools.

3 Requirements

The following shows the requirements for ensuring that the total system is operated properly for effective use of production data:

① To standardize data items to be collected so that collected data can be saved in the KYB-IoT Platform
② To ensure that all necessary data items are collected and accumulated in the KYB-IoT Platform
③ To enable data analysis in devices and long-time data analysis
④ To link the KYB-IoT Platform to other internal systems to share design and cost information
⑤ To build a total universal system for global use
⑥ To ensure that horizontal deployment of and function addition to the system can easily be done

4 Development of MES Services

4.1 System Overview

This development has the purpose of building a total system linking the aforementioned KYB-IoT Platform to the line monitoring system for analyzing and utilizing manufacturing process data. The development is underway with another future goal of achieving company-wide and even global deployment of the total system.

Fig. 6 illustrates how the total system is configured. The line monitoring system collects data from individual devices and save the data in a predetermined format. All the collected data is saved in the KYB-IoT Platform for centralized control of company-wide production data. Once saved, the data will be immediately visualized to be available for analysis.

The KYB-IoT Platform can easily be linked to other systems because of its collective data management and can also provide diversified analysis using data from other systems.

This development roughly covers the following four major tasks. The details will be explained in the following sections:

- To standardize data to be collected and data format
- To determine how to collect/transfer data
- To determine how to save data
- To determine how to display and analyze data

4.2 Standardizing Data to Be Collected and Data Format

We have standardized data to be collected to ensure that data collection systems at various source locations can write common data items to the KYB-IoT Platform in the same data format. This makes it possible to utilize data for analysis with a unified set of indicators. We have selected important data items needed by all locations to carry out improvement activities. These data items can be categorized by data collection timing and data content into four groups shown in Table 1. We have specified a data format for each data group, achieving standardization of data collection.

The first data group is production results (including actual CT & MT and setup change time) to be stored in the KYB-IoT Platform. With these types of data available, the user can find possible causes of lower production while viewing CT/MT, setup change time and availability data on the screen.

The second data group is equipment alarm (including alarm date and time, alarm type and downtime) to be stored in the KYB-IoT Platform. With these types of data available, the user can narrow down equipment alarms to be handled in higher priority and check the equipment alarm log.

The third one is jig and tool change data (including date and time of change and the remaining number of times of use) to be stored in the KYB-IoT Platform. With these types of data available, user can identify what caused the jigs and tools to be changed.

The fourth one is measurement data (including measurement values and items) to be stored in the KYB-IoT Platform. With these types of data available, the user can manage the daily data trend using control charts and find possible causes of an anomaly in connection with the alarm information. In addition, some devices may measure and save multiple measurement items at the same time. The style of tables accepting data in this case has been standardized to "vertical" Note 11), thereby enabling the user to easily switch over devices and measurement items or to analyze data more conveniently.

On the other hand, some source locations may collect data in a data format other than that stated above in some cases. Then, we, in this development, have decided to save data collected from individual source locations in a common file format. In the format, first comes the identification information including production line, production device, date and time of data collection, and type of data collected. This general information is followed by source-specific data. Although data items to be collected and the number of data items vary by target device or object, the KYB-IoT Platform identifies data and executes subsequent processing (including pretreatment and DB storage).

Note 11) A kind of data table structure. It refers to a type of tables where data is added in the longitudinal (line) direction.

Table 1 Data to be collected

Data group	Data to be collected
Production	• Actual CT • Actual MT • Setup change time
Equipment alarm	• Date and time of alarm • Type of alarm • Downtime
Jig change	• Date and time of change • Remaining number of times of use after change
Measurement data	• Measurement item • Measurement value

4.3 Data Collection/Transfer

This section explains the line monitoring system, although several other data collection systems are being discussed in various sites. It should be noted that any data collection system could be linked to the KYB-IoT Platform even if the system does not have the same configuration as that of the line monitoring system.

The line monitoring system is generally configured as shown in the Data Collection region in Fig. 6. The line monitoring system centralizes operation data held by the equipment PLCs to the general PLC and stores data in the database (DB) built in each line server. By using a visualization software program running on each line server, the system displays data on a large monitor in real time. It also transfers data from the general PLC to the KYB-IoT

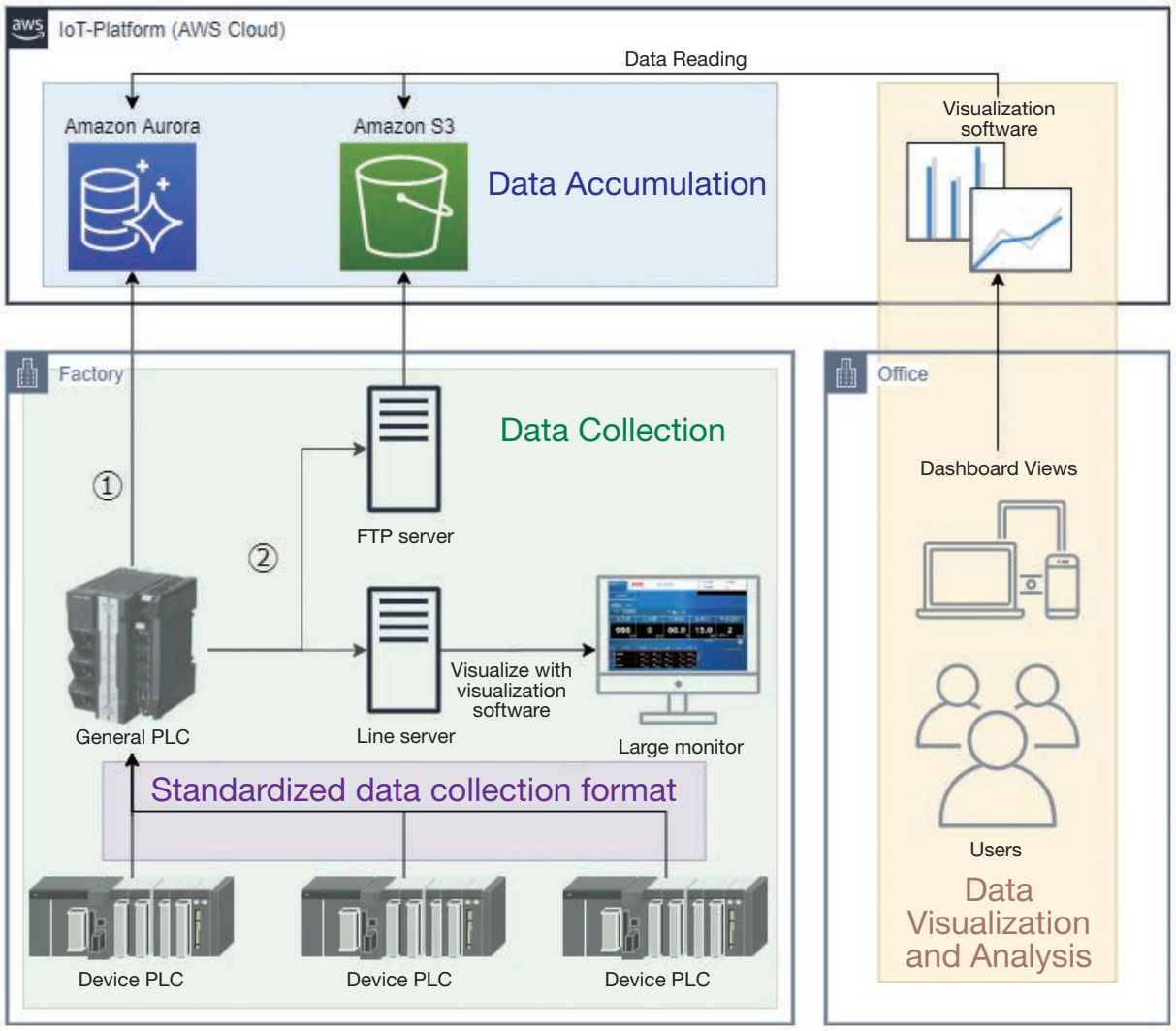

Fig. 6 Configuration of MES services (overview)

Platform in the following two methods to store data in the Platform (Fig. 6, ① and ②):

① Directly write data from the general PLC into the DB on the KYB-IoT Platform

② Transfer file data in CSV or other format created in the general PLC by using the file transfer protocol (FTP)

The method ① should be selected for structured data Note 12) occurring infrequently (in several seconds) that will be utilized frequently (i.e., accessed) after saved. Specifically, CT, MT and equipment alarms will be transferred in this method and written into the DB on the Platform one by one when the equipment cycle is completed or any alarm is reset. It should be remembered that this method can only be used with a PLC that supports data writing to a database. It is thus necessary to prepare in advance a PLC supporting the data writing.

In method ②, the system saves data gathered by the general PLC in a file format and transfers it to an internal FTP server using the FTP before saving in the storage on the KYB-IoT Platform. This method should be selected for data that cannot be accepted by the DB, for example, data that is generated in a large size per unit time such as millisecond or non-structured data. Specifically, measurement data and equipment machining condition data (current and temperature) will be recorded in the general PLC as required at a certain sampling rate. Several data sets will be put together to be saved in a file when a setup change or a production session has been completed. Such files will be periodically transferred using the FTP. In fact, this type of data saved in files can be viewed at a lower retrieval speed than that for the DB. Still, our understanding is that no significant problem with system operation will arise because data utilization (access) has been assumed to take place infrequently. This method has been verified to be supported by a wide range of PLCs. How to store data in these two methods will be described in detail in the following section.

Note 12) "To structure data" means to preliminarily define the type and sequence of data items and arrange them in a specified structure.

4.4 Data Storage

As described in the previous section, we have established two different ways of storing data (Fig. 6).

For method ① in Fig. 6, a database (DB) has been

created on the KYB-IoT Platform (cloud) to store acquired data. The DB uses an AWS fully managed [Note 13)] high-performance RDB [Note 14)] service called "Amazon Aurora" featuring high performance, high expandability, high safety and high availability. Thanks to its high data reading performance, Amazon Aurora allows user to quickly retrieve data by linking multiple data sets using SQL. [Note 15)]

Method ② in Fig. 6 uses a cloud storage service called "Amazon S3" (hereinafter "S3") to store data saved by the general PLC in files. This service features high durability, high safety and high availability. Furthermore, S3 can offer many other benefits including virtually infinite storage capacity and lower cost than Amazon Aurora. One disadvantage is that the data retrieval service for S3 is not designed to allow the user to easily retrieve data in an advanced way, resulting in lower retrieval speed than for RDB.

Furthermore, it costs more for S3 to store large amounts of data than for Aurora as shown in Table 2. The data storage cost may be reduced by changing where to store data depending on the data use frequency. It is vital to select a better one from these two destinations with consideration given to frequency of data occurrence and frequency of data use.

Table 2 Comparison of data storage

	Aurora	S3
Data volume	Low	High
Frequency of use	High	Low
Storage cost [Note 16)]	0.12 USD/GB/month	0.025 USD/GB [Note 17)]

Note 13) AWS undergoes server/operating system (OS) management and failure correction for users. Users can focus on their use of service, leading to higher development efficiency and lower operation cost.

Note 14) An acronym for Relational Data Base. An RDB manages data in multiple tables and defines the relationships among the tables to be able to handle the relation among complex data sets.

Note 15) An acronym for Structured Query Language. SQL is an internationally standardized database language used to operate and control the RDB management software.

Note 16) The figure shows the price in Tokyo Region as of December 21, 2021. The figure for Aurora only indicates the data storage cost.

Note 17) The price for S3 becomes lower in stages as the data capacity becomes lower. The figures shown in the table indicate the service fee for 50 TB/month.

4.5 Data Visualization and Analysis

We have developed a data display system using a BI tool called Tableau [Note 18)] to visualize and analyze collected data.

This visualization and analysis system reads data on the KYB-IoT Platform. Once data is saved in the system, the data immediately becomes available on the screens. Fig. 7 shows how these screens are configured. All the screens shown in Fig. 7 are standard views for all the sites. A total of 18 screens are available at this moment. Some of these screens cover two or more types of data to allow for diversified analysis. The screens are linked with each other so that the user can view several screens to find more detailed analysis screens for deeper analysis. This section will explain some of these screens we have developed.

Note 18) This industry's leading BI tool allows the user to easily visualize and analyze data. KYB is also introducing and deploying the tool.

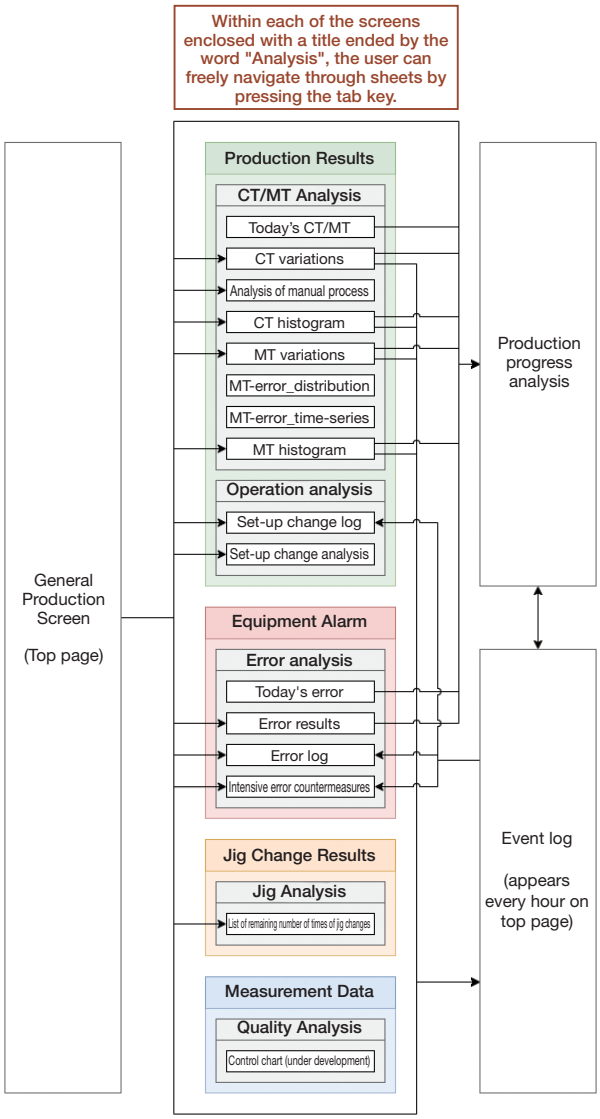

Fig. 7 Linkage of visualization and analysis screens

4.5.1 General Production Screen (Top Page)

Fig. 8 shows the general production screen where the user can view actual results of production. Views showing CT, MT, setup change, availability, alarm and jig changes for each device are tiled on the screen, enabling the user to narrow down possible causes of any lower productivity from various angles. [Note 19)] This screen displays how daily-compiled data changes day by day. The user can look at the graphs on the screen to be able to easily identify any

data showing an anomaly (for example, longer CT or more errors than the criteria). If this is the case, the user can move on to another analysis screen linked to the top page for deeper investigation.

Note 19) The information on the screen includes undisclosed information that has been intentionally deleted or blurred.

Fig. 8 General production screen (Top page)

4.5.2 CT Histogram Screen

Fig. 9 shows the CT histogram screen that displays the CT results over a specified period of time in the form of a time-series two-dimensional histogram. The upper half of the screen provides the CT histogram over a specified period with the X-axis showing CT bins in the unit of one second and with the Y-axis showing the magnitude. The lower half of the screen indicates how CT changes by each day in light and dark in color. A dark colored cell represents a high magnitude. The Y-axis shows the date in units of one day (time elapses from top to bottom with the top oldest and the bottom newest), representing daily CT variations (distribution in a day). User can first identify normal CT on the histogram over the entire period and then check variations for each day to determine whether any worse CT than the normal level is attributable to a spontaneous or chronic cause. If spontaneous, it is advisable to narrow down possible causes on the screen stated in the previous section and take appropriate measures. For chronic ones, it is effective to review the work and machining programs and check any other chronic error.

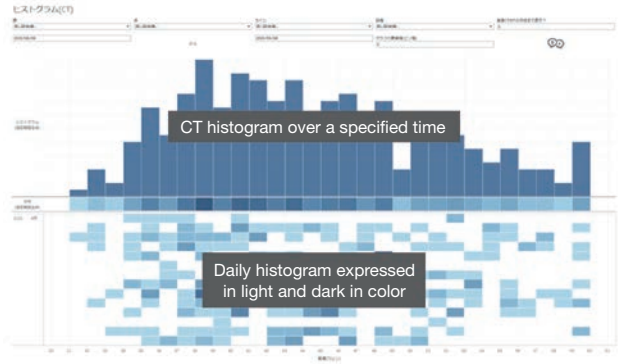

Fig. 9 CT histogram screen

4.5.3 Alarm Screen for Intensive Measures

Fig. 10 shows the alarm screen for intensive measures where the user can identify device alarms in the form of Pareto charts. The Pareto charts are intended to show the occurrences of device alarms (the left chart on the screen) and their downtime (the right chart on the screen). If a device has an alarm of frequent occurrence involving short downtime, the device should have been frequently stopped. If a device has an alarm of non-frequent occurrence involving long downtime, the device should have been troubled with major stoppages. As a general rule, focusing frequent alarms involving long downtime will relatively easily improve productivity. First, it is good to narrow down device alarms into those involving poor productivity. Once this is done, you can now tackle improvement activities including device adjustment and work improvement.

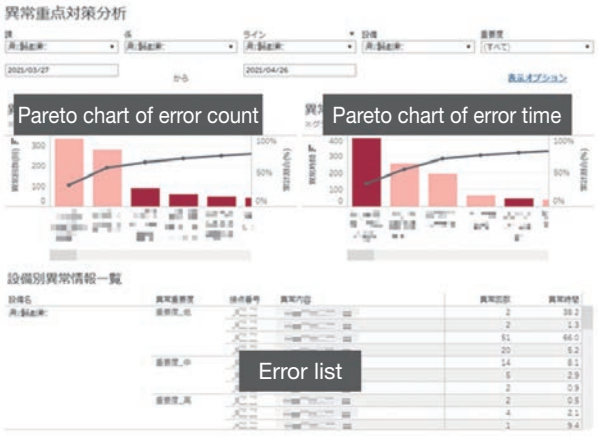

Fig. 10 Alarm screen for intensive measures

4.5.4 Screen Customization

The visualization screen system we have developed provide standard screens for all sites. Only using these standard screens allows for basic data analysis, but some sites may have to carry out more detailed analysis. For such sites, an environment is available for users to be able to create their own necessary visualization screens using Tableau. Once having created a visualization screen, the user can easily share it with personnel from other departments via the Internet or easily download any screens created by personnel from other departments and then customize them so that they can easily use within their own department.

The screen creation procedure (how to use Tableau) has been designed so that users can build programs as they like as a scheme of developing human capital [Note 20)] is established to promote evolvement of this system.

Note 20) KYB uses the term "human capital", instead of "human resources".

5 Future Prospects

Through this development, we have built the foundation of a system that utilizes manufacturing process data. We are now improving the system and adding functions to it based on user feedback on the lines whose data is saved on the KYB-IoT Platform. We are also promoting the linkage between the system and other data collection systems than the line monitoring system, thereby enabling us to collect data from existing devices that have long been operated and then to utilize the data.

From now on, we will further improve the system and add functions to it while promoting its global deployment. In promoting the global deployment, we are facing some challenges. As the global deployment progresses, data will be saved more frequently, which will require us to review the processing capacity and the way of writing data from data collection terminals. The visualization screen system is also anticipated to have lower display speed and lower operability as it handles more data. These possible problems will have to be discussed as required.

We are also going to discuss establishing a linkage between the system and other systems. The systems that have already been put into service and have collected data should be put together to collectively save their data on the KYB-IoT Platform. For systems to be built and introduced in future, we will sequentially develop their linkage mechanisms.

Our final goal is to establish a comprehensive scheme to centrally control data sets from different functions of the company, closely link these data sets, and allow the user to utilize the data as necessary and make decisions based on the data. Through the scheme, we will aim at strengthening the engineering chain including strengthening the inter-functional connection and reducing the production lead time as well as at strengthening the supply chain including enhancing the product reliability and making the production scheme flexible.

6 Concluding Remarks

Through this development, we have successfully established a scheme to utilize manufacturing process data. MES can connect upstream systems and downstream devices in promoting digitalization of manufacturing industry. The function we have developed is part of the MES in the production management system. With this in mind, we will continue promoting the system improvement and function addition and the linkage with other systems, contributing to the higher productivity and higher quality.

Finally, we would like to take this opportunity to sincerely thank all those concerned from internal related functions who extended great support and cooperation to this development project.

References

1) YAMAMOTO: Establishment of a Process Management System, KYB Technical Review No. 14 (April 1997).
2) FURUKAWA, ISASHI: Development of an Equipment Predictive Maintenance System, KYB Technical Review No. 63 (October 2021).

Author

YUBUKI Kento

Joined the company in 2016.
DX Dept., Engineering Div.
Engaged in development of analysis screen systems using BI tools

GABURIELLA Anak Magin

Joined the company in 2015.
Group 2, Production Engineering Sect. No. 2, SA Production Engineering Dept., Automotive Components Operations.
Engaged in production preparation

Technology Explanation

Research on Technology to Control Air Bubble Content in Hydraulic Fluid

KITAMURA Yoshiaki, KODERA Yasuhiro

Abstract

In hydraulic pumps used in Continuously Variable Transmission (CVT) of automobiles, air is mixed from the surface of hydraulic fluid due to vibration of the hydraulic circuit, and also the dissolved the air appears in the working oil due to the cavitation. In CVT pumps, 10% to more than 30% of air bubbles are contained in the hydraulic fluid in the hydraulic circuit under the operating environment. These bubbles cause many problems such as pump discharge performance reduction, as well as degradation related to vibration, noise, and durability.

Therefore, when developing a pump, it is necessary to evaluate its performance under actual operating conditions, taking into account the bubble content. However, in general, there are no devices or methods to stably adjust the bubble content.

To solve this problem, KYB has developed a device and method to control the bubble content in the hydraulic fluid. First, we focused on a method using a swirling flow as a technique for removing bubbles from oil, and fabricated a bubble separation device. Second, we analytically and experimentally confirmed that the bubble separation effect of this device was sufficient.

Furthermore, we installed the bubble separator in the actual pump test equipment and verified whether the bubble removal effect could be obtained. Finally, to automatically control the bubble content, we verified it was possible to obtain the desired bubble content ratio by controlling the opening and closing of the valve on the outlet side of the bubble separator. In this report, the results of the above verification are described.

1 Introduction

A hydraulic fluid usually contains several percentages of air dissolved therein under atmospheric pressure. Inside a hydraulic pump like the one shown in Photo 1, the hydraulic circuit may have a local decrease in pressure to cause cavitation, generating voids or air bubbles (Fig. 1). Tiny bubbles appearing in this way will stay in the fluid for a certain period of time and may need considerable time to be dissolved in the fluid again or float up to collapse. The air can also be mixed into the hydraulic fluid from the outside of the fluid due to entrainment (sloshing) that occurs when the hydraulic circuit or the oil tank vibrates. The hydraulic circuit for continuously variable transmissions (hereinafter "the CVT") of automobiles is a typical example of those exposed to frequent opportunities for air intrusion in this mechanism. It is said that this type of hydraulic fluid contains 10% to, in some case, even more than 30% bubbles. The fluid with a high bubble content looks whitish as shown in Photo 2 compared to when it has a low bubble content. These bubbles contained in the fluid are often known as the third contaminant [2] of machinery, next to the particulates and water, and may cause the machinery to have vibration, noise or mechanical failure. The presence of air bubbles in the hydraulic fluid reduces the apparent elasticity of the fluid to impair the responsivity of the system. Research [3] has verified that aggressively decreasing the bubble content of the fluid will eventually lower the amount of air dissolved in the fluid to reduce cavitation. Taking into account the fact that

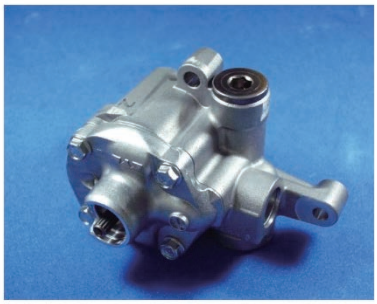

Photo 1 Example of KYB hydraulic pump

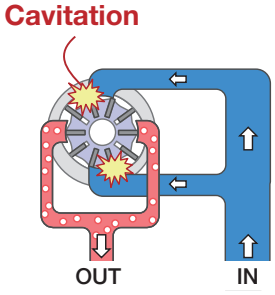

Fig. 1 How cavitation occurs (example)

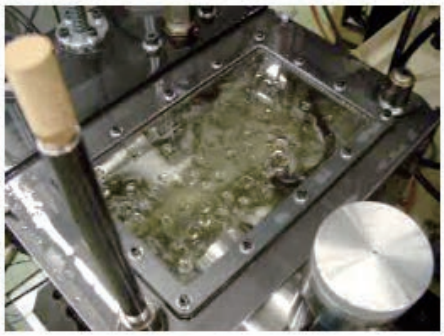

(a) 0% bubble content

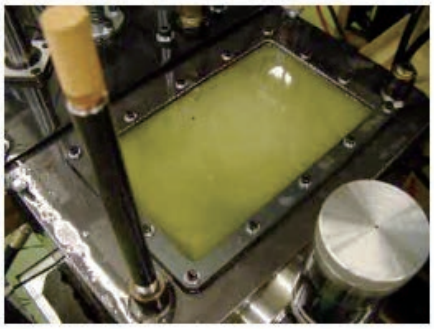

(b) 10% bubble content

Photo 2 Bubbles in a tank in a hydraulic circuit

one of the major causes of failures of hydraulic machinery elements is erosion caused by cavitation, reducing the bubble content of the hydraulic fluid will definitely help prevent machinery failures.

A question: what is the fluid's bubble content that degrades the machinery performance to eventually cause a failure? Such a quantitative indication has not yet been determined. This is because you can barely measure or adjust the bubble content of the fluid in real time at a high accuracy under the present circumstances. Conventionally, the bubbles in the fluid have been removed predominantly by negative methods, such as spontaneous air purge of the oil tank or addition of anti-foam agent to the fluid.

In such situation, modern automobiles are required to have intermittent runs or stops of their engine more frequently for higher fuel efficiency. Accordingly, hydraulic pumps connected to the engines need to be started or stopped frequently as well. Air bubbles contained in the hydraulic oil are likely to stay or merge in various locations within the hydraulic circuit, which may cause the automobiles to generate noise or may make the hydraulic system unstable during the initial stage of the start-up process. The need to determine the effect of the bubble content of the fluid and to take measures has become urgent.

To respond to the need, we first tackled technical development to implement techniques for stable adjustment of the bubble content of the fluid. This report proposes a bubble separation device using a swirling flow and a method to control the bubble content of the fluid entering the separator. The separator has an air purge valve whose operation (closing/opening) can be controlled to adjust the bubble content of the fluid leaving the separator. Furthermore, the report explains the adequacy of this method by introducing the results of an experimental verification test.

2 Design and Fabrication of a Bubble Separator

2.1 Bubble Separator Using a Swirling Flow

Fig. 2 shows the operating principle and structure of a bubble separation device that uses a swirling flow to draw bubbles, which are distributed throughout the hydraulic fluid, and puts them together to be separated and removed by a simple mechanism. Using a swirling flow, the separator can draw bubbles distributed in the fluid and build them up around the central axis in a time as short as approximately 100 msec. The separator can remove and discharge these collected bubbles from a purge outlet to the outside by utilizing a slight difference in pressure between the fluid outlet and the purge outlet. [4] To implement this, a control valve should be installed downstream of the purge outlet to adjust the air purge by valve opening/closing. Controlling the period of time for the valve to be open or closed and/or the operation timing will adjust the volume of bubbles to be separated from the fluid. In this development, we began to fabricate the separator for building a system that can control the bubble content of the fluid at the fluid outlet of the separator.

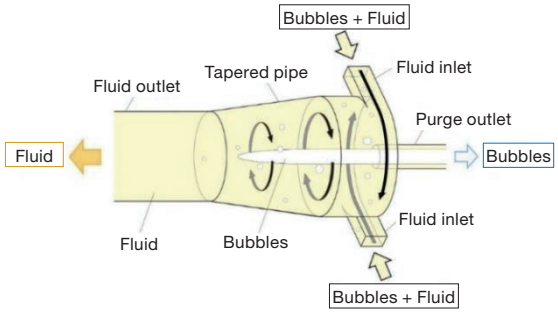

Fig. 2 Operating principle and structure of bubble separator

2.2 Simulation of Bubble Separation

For the method to be verified in this research, we set up a target range of the bubble content between 1% and 40%. To achieve this goal, the bubble separator must provide adequate bubble removal performance within the range. Since the performance of the separator heavily depends on the geometry of the fluid inlet and the diameter of the purge outlet, [5] it is very important to select appropriate parameters for flow conditions in designing the separator.

To verify the operating principle and select optimal geometry parameters, we used the computational fluid dynamics (CFD) to simulate and verify the bubble separation. For the purpose of CFD, we used a fluid duct shown in Fig. 3 and simulation conditions listed in Table 1. Within the target range, 20%, 30% and 40% bubble

content levels were selected as examples for analysis purpose.

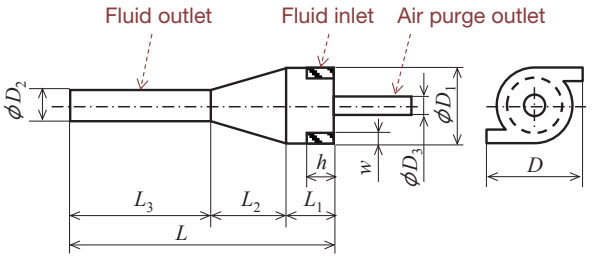

Fig. 3 Fluid duct for computational simulation

Table 1 Computational simulation conditions

Item		Value
Fluid flow at inlet (L/min)		30
Size of bubble particles (mm)		0.1
Physical properties of hydraulic fluid	Density (g/cm^3)	0.8474
	Dynamic viscosity (mm^2/sec.)	9.189
Bubble content (%)		20, 30, 40

The bubbles entering the separator via the fluid inlet has a higher flow rate around the perimeter of the inlet port and a lower flow rate in the center of the same as shown in Fig. 4(a). The figure represents how a swirling flow occurs. The volume fraction of the bubbles for the bubble content levels of 20%, 30% and 40% is higher in the center of the duct for any of the bubble content levels as shown in Fig. 4(b). It was verified that the bubbles flowed towards the purge outlet efficiently to be separated and removed from the fluid.

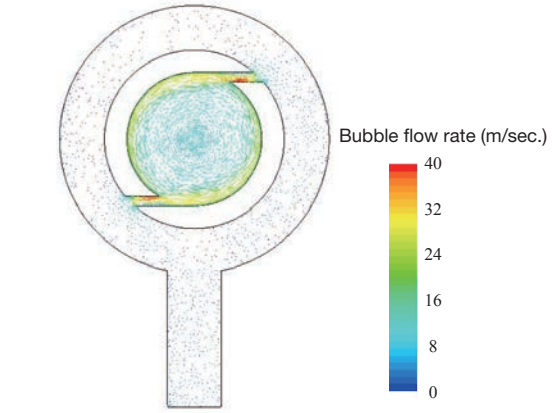

(a) Distribution of bubble flow rate (for fluid with 40% bubble content)

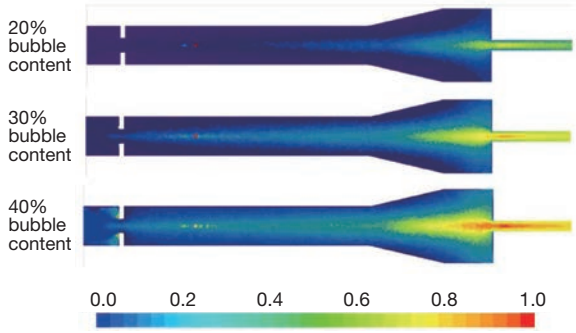

(b) Volume fraction of bubbles

Fig. 4 Computational simulation of bubble flow

As a result of the CFD, an optimal set of geometry parameters for the bubble separator was obtained as shown in Table 2. Fig. 5 shows the resultant bubble removal rate of the separator with its fluid inlet sized to be 2.18 mm (width) x 4.35 mm (height), its air purge outlet sized to have an inside diameter of φ4.4 mm, and its fluid outlet sized to have an inside diameter of φ16 mm for the bubble content cases of 20%, 30% and 40%. Note that the bubble removal rate here refers to what percentage of the bubbles have been removed from the fluid that is discharged from the fluid outlet, not from the air purge outlet. The CFD proved that the simulated bubble separator with the optimal geometry parameters delivered a bubble removal performance as high as 90% or more for all the cases. These results were used as design parameters for an experimental bubble separation device.

Table 2 Optimal geometry parameters for bubble separator

Geometry parameter	Value [mm]
Inside diameter of tapered pipe section φD_1	30.0
Inside diameter of fluid outlet φD_2	16.0
Inside diameter of air purge outlet φD_3	4.4
Total Length L	150.0
Length of fluid inlet pipe L_1	20.0
Length of tapered pipe section L_2	30.0
Length of fluid outlet pipe L_3	100.0
Width of fluid inlet w	2.18
Height of fluid inlet h	4.35

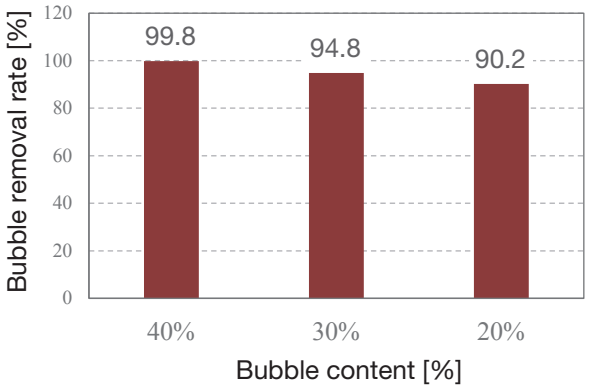

Fig. 5 Results of simulation of bubble separation

2.3 Separator Design and Fabrication

Based on the results of the CFD analysis stated in the previous section, we designed and fabricated a bubble separation device to be used in experiments of controlling the bubble content of the hydraulic fluid. Fig. 6 shows the bubble separator. The separator was designed in modulars so that the geometry parameters including the fluid inlet

size, the fluid outlet size and the air purge outlet size can be adjusted later to be suited to the test conditions. Pieces of this modular device can be first inserted into a casing and then fixed together from both sides to be a one-piece structure. The peripheral casing and inserts are made of transparent acrylic.

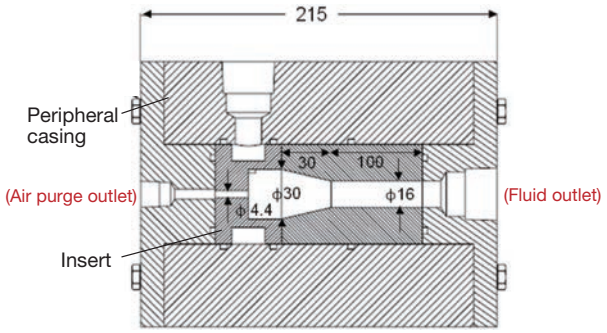

Fig. 6 Design and fabrication of bubble separator

3 Evaluation of Performance of Bubble Separator

To verify the bubble separation performance of the fabricated separator, a preliminary test was first conducted.

Fig. 7 shows the hydraulic circuit used in the preliminary test. The bubble separator was installed on the fluid circuit. A manually operated needle valve was mounted on the circuit line of the purge outlet side of the separator and a Coriolis-type flowmeter was on the circuit line of the fluid outlet side of the separator. The hydraulic fluid was forcefully mixed with bubbles from the air blown by an air compressor located on the discharge side of the pump. While the air was being blown into the fluid, the needle valve was manually controlled to deliver the fluid from the separator at different bubble content levels. The bubble content of the fluid was determined by measuring the density of the fluid at the fluid outlet against the degree of opening of the needle valve. [6] The fluid pressure at the fluid inlet of the separator was maintained at 0.5 MPa.

Photo 3 shows what happened inside the bubble separator during the preliminary test. With the purge outlet fully closed, the fluid looks whitish with great amounts of air bubbles over the entire duct in the separator as shown in Photo 3 (a) (Bubble separation with the purge outlet closed). With the purge outlet fully open, the air bubbles flowing into the separator from the fluid inlet quickly flowed toward the purge outlet. Few bubbles stayed in the separator for a while and then flowed toward the fluid outlet as shown in Photo 3 (b) (Bubble separation with the purge outlet open).

Fig. 8 shows the results of the preliminary test: the relationship between the degree of opening of the needle valve and the bubble content of the fluid at the fluid outlet. In fact, the specifications of the needle valve used in the test made it difficult to achieve precise control of the flow rate at the purge outlet by varying the degree of opening of the valve. Unfortunately, just slightly opening the valve at the purge outlet actually caused the separator to deliver the bubble removal effect more than expected, resulting in a substantially lower bubble content of the fluid at the fluid outlet. However, it was verified that the bubble content of the fluid at the fluid outlet can be controlled by changing the degree of opening of a valve installed at the purge outlet.

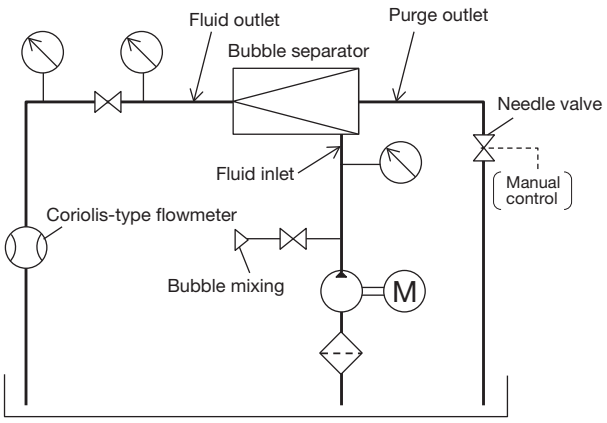

Fig. 7 Hydraulic circuit for testing of manual control of bubble content

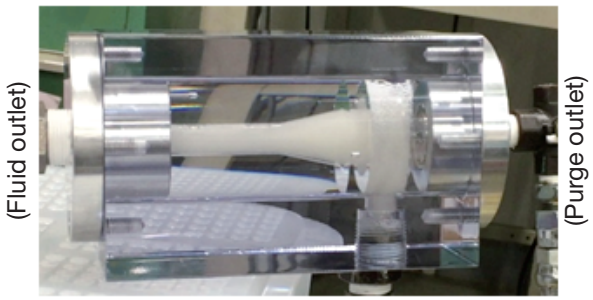

(a) Purge outlet closed

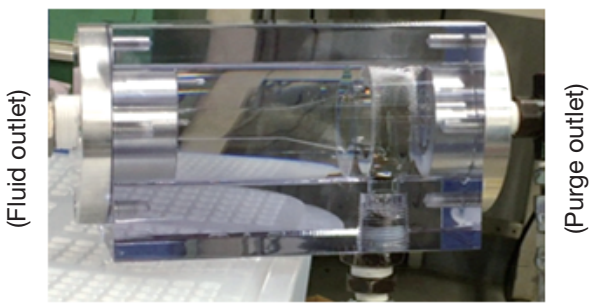

(b) Purge outlet open

Photo 3 Inside the bubble separator

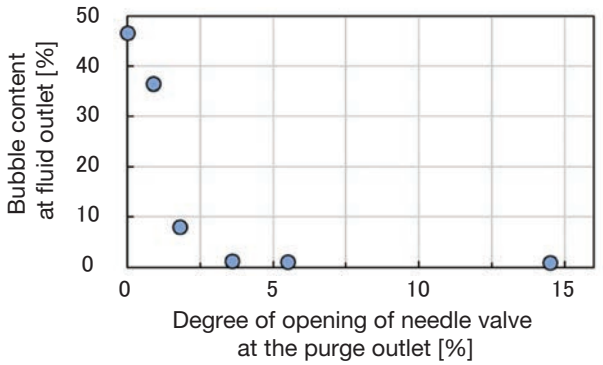

Fig. 8 Manually controlled bubble content

4 Evaluation of Performance of Bubble Separator on Actual Machine

To verify that the bubble separator developed can also be applied to evaluation of actual pumps, we carried out an experimental test on the bubble separator installed on an actual pump test unit. Note that the bubble separator used for this test was another unit made of metal, not the original separator.

Fig. 9 shows the hydraulic circuit of the actual machine test equipment. In order to determine the effect of the bubble content of the hydraulic fluid on the pump, a device to mix the air into the hydraulic fluid in a tank upstream of the target pump to be evaluated was provided to increase the bubble content of the fluid. This air mixing device was designed to be able to control the air discharge rate for mixing. The bubble separator was installed downstream of the target pump. On the purge outlet line a needle valve was provided to be able to be opened or closed freely in the same manner as for the preliminary test. On the fluid outlet side an orifice of any round shape was inserted as a back pressure control. Further downstream, an inline impedance-type bubble content measuring device was installed to measure the bubble content in real time. The oil temperature was maintained at 100°C by a cooler and a heater provided on the circuit.

As an example of verification of the bubble removal effect, Fig. 10 shows changes in bubble content of the fluid over time for the case of a constant mixing rate of bubbles in the tank, a fluid outlet size of φ10, and a pump discharge rate of 18 L/min. At the time point of 0 seconds, the separator has its purge outlet closed and the duct contains the fluid with bubbles mixed in as sufficient as around 30% with the mixing tank being operated. When the purge outlet is opened, the bubble content immediately dropped and became stable at around 10% about 4 minutes later.

This bubble content level was obtained when the bubble mixing device in the tank and the bubble separator were both operated. The air content of the hydraulic fluid may be adjusted to any given level by controlling the air mixing rate and/or the air purge rate of the bubble separator.

Now we have verified that using the bubble separator in the actual pump test unit enables quick, stable adjustment of the bubble content of the fluid in the circuit.

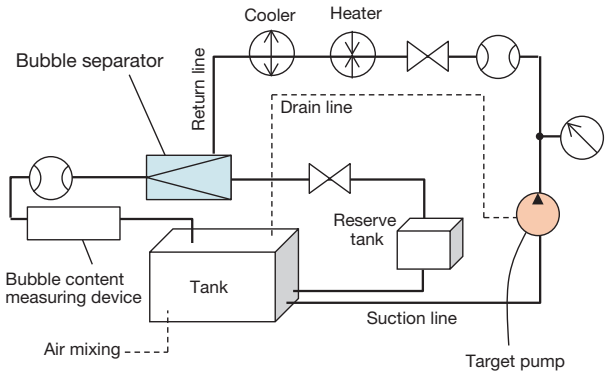

Fig. 9 Hydraulic circuit of actual machine test equipment

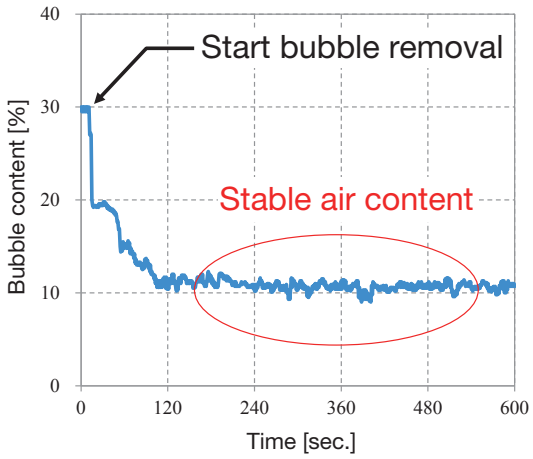

Fig. 10 Bubble content of hydraulic fluid on actual machine

5 Evaluation of Performance of Automatic Bubble Content Control

After verifying that controlling the degree of opening of the purge outlet of the bubble separator can adjust the bubble content of the hydraulic fluid in the circuit, we further tried to determine the possibility of automatically controlling the bubble content to any given level. To this end, we installed an on-off control solenoid at the purge outlet and carried out a test to control the bubble content of the fluid at the fluid outlet by adjusting the on/off time or the switching timing of the solenoid.

Fig. 11 shows the hydraulic circuit used in the control test. The bubble separator was installed on the fluid circuit similar to the one shown in Fig. 7. A Coriolis-type flowmeter was installed at the fluid inlet and a bubble content measuring device installed at the fluid outlet. Then, the bubble content of the fluid was measured in real time for various cases. Air mixing into the fluid was attained by keeping the suction port of the pump open to the atmosphere. An on-off control solenoid was installed at the

purge outlet of the separator. The solenoid control (opening/closing) was implemented by a sequencer using a relay according to the deviation of bubble content measurements at the fluid outlet from the target level.

Fig. 12 shows an example of the results of the bubble content control tests. When the incoming fluid had about 29% bubble content, the outgoing fluid had about 28% bubble content with the purge outlet closed. Then, the target bubble content was set to 18%. With the on-off control solenoid operation frequency 1s and the duty ratio between 10% and 100%, the bubble separator automatically controlled the duty ratio to attain the target level as indicated by the figure. Table 3 shows the average bubble content for each duty ratio and its relative deviation from the target bubble content for a certain period of time (19.2 seconds to 25 seconds) after the bubble content became stable at around the target level. In general, the smaller the duty ratio is, the lower the control accuracy and responsivity are. However, this test demonstrated that the relative deviation from the target level was within 9.4% for small duty ratios, proving a certain level of control accuracy.

For some duty ratio settings, however, the bubble content may fail to be stable at around the target level and may continue fluctuating in some cases. This is because the on-off solenoid at the purge outlet can only deliver low responsivity while the bubble separator has highly responsive bubble removal performance. This can be probably improved by using a more responsive proportional valve.

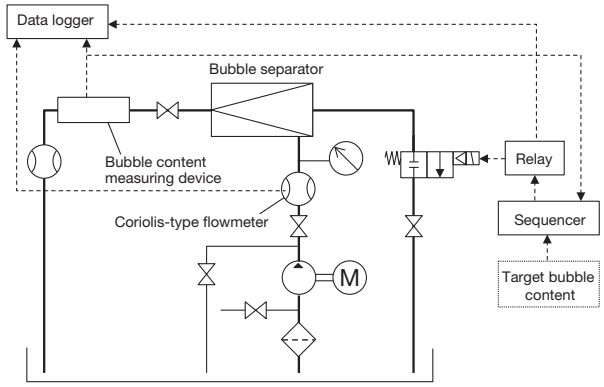

Fig. 11 Hydraulic circuit for automatic bubble control test

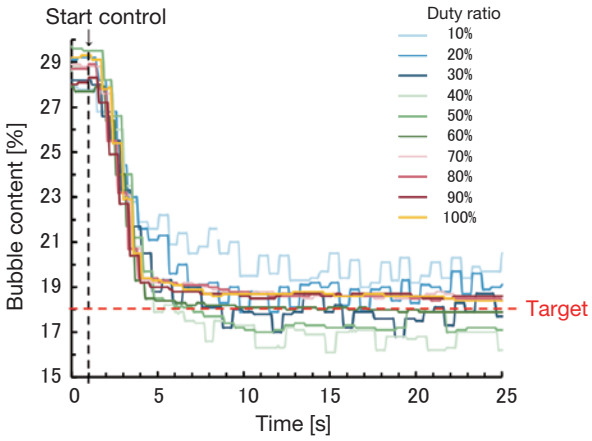

Fig. 12 Automatically controlled bubble content

Table 3 Bubble content for various duty ratios

Duty ratio [%]	Average [%]	Relative deviation [%]
10	19.7	9.4
20	18.8	4.4
30	17.9	0.5
40	16.8	6.7
50	17.3	3.9
60	18.0	0.0
70	18.6	3.3
80	18.6	3.3
90	18.6	3.3
100	18.6	3.3

6 Future Prospects

We will apply the technology that controls the bubble content of the hydraulic fluid developed in this research to evaluation of our pumps under actual operating conditions, thereby developing high-function and high-quality products, although the control stability is still a challenge.

On the other hand, we aim to deploy the technology in such a manner that our pump products including CVT could be improved in performance by focusing the feature of the technology that can remove the bubbles contained in the fluid, which may be called "the third contamination" as stated in the beginning of this report.

By improving our capability of technical development like this, we will be able to offer even-higher-efficiency pumps that could improve the fuel efficiency of automobiles for instance. These products will help create a carbon neutral society or achieve the sustainable development goals (SDGs).

7 Concluding Remarks

This report has introduced the verification of the method that freely controls the bubble content of the hydraulic fluid with the bubble removal technology using a swirling flow, toward establishment of such a bubble content control system. The verification has produced the following conclusions:

(1) A bubble separator has been developed and fabricated that can adequately remove air bubbles from the hydraulic circuit to obtain a bubble content between 1% and 40%.

(2) It has been verified that the bubble separator mounted on the actual pump test unit can control the bubble content in the hydraulic circuit quickly and stably.

(3) Testing has proven that adjusting the flow rate at the purge outlet of the bubble separator can control the bubble content of the fluid at the fluid outlet of the separator.

This research was carried out in cooperation with Professor TANAKA Yutaka, Hosei University, who designed the bubble separation device using a swirling flow, and Associate Professor SAKAMA Sayako, Aoyama Gakuin University (currently belonging to National Institute of Advanced Industrial Science and Technology), who carried out various element tests. Finally, we would like to take this opportunity to sincerely thank them.

References

1) SAKAMA S, et.al: Air Bubble Separation and Elimination from Working Fluids for Performance Improvement of Hydraulic Systems, Proc. IFPE 2014, Paper No. 27.1 (2014).
2) SEKIDO Makiko, MIZUMURA Atsushi: How to select and use filters and their trouble cases, Basic Hydraulic Technology Class - How to select and use peripheral equipment, Japan Industrial Publishing Co., Ltd. (2016).
3) GOTO H, SAKAMA S, SUZUKI R, TANAKA Y: Reduction of Cavitation Damage by Elimination of Bubbles in Oil Reservoir, Proc. FLUCOME2013, OSI-02-4. (2013).
4) TANAKA Y, et.al.: Visualization of Flow Fields in a Bubble Eliminator, J. of Visualization, Vol. 4, No. 1, pp. 81-90. (2001).
5) SAKAMA Sayako, TANAKA Yutaka, SUZUKI Ryushi: Research on design and evaluation of bubble separation devices (Report #2), Transactions of The Japan Fluid Power System Society Vol. 45, No. 5, pp. 79-84. (2014).
6) GOTO Hiroyuki, SAKAMA Sayako, TANAKA Yutaka: Measurement of bubble content of hydraulic oil using Coriolis-type flowmeter, Transactions of FY2015 Annual Assembly Lectures of the Japan Society of Mechanical Engineers (JSME), No.15-1, S1150302, (2015).

Author

KITAMURA Yoshiaki

Joined the company in 2013.
Mechanical Component Engineering Sect., Basic Technology R&D Center, Engineering Div.
Engaged in research and development of hydraulic pumps and power steering

KODERA Yasuhiro

Joined the company in 2009.
Developmental Experiment Sect., Developmental Center, Engineering Headquarters, Automotive Components Operations
Engaged in development of hydraulic pumps

Technical Article

Research on Particle Assemblage Damper

TOYOUCHI Atsushi

Abstract

Dampers are devices which suppress vibrations that cause harm to vehicles, buildings, and the like. There are various types of dampers, depending upon the application. However, each type of damper comes with its own problems. Typical examples of such problems are that in the case of oil dampers, liquid leakage may occur, and the damping force may be dependent on temperature. Particle dampers suppress vibrations by generating resistance force through the use of particles in place of oil or the like. These dampers can be exemplified as a possible solution to the abovementioned problems. In this study, an investigation and examination were carried out in order to clarify the generative force characteristics and force generation factors of a separated dual chamber single rod-type particle damper which employs a particulate elastomer*. This type of damper holds the possibility of solving these problems by means of a simple structure.

With regard to the damper used in this study, a particle chamber within the cylinder was divided in two by a piston. It was found that when one chamber of the damper was filled with particles, the generative force had the characteristic of being gradually hardening with hysteresis, with great influence exerted by elastic force in the normal direction and frictional force in the tangential direction. The elastic force in this case was mainly accounted for by repulsion force under compression generated by the compression of the particles, and the frictional force was generated by sliding friction between the cylinder and the particles. Furthermore, it was found that in particular, the packing fraction and Young's modulus, which affects the material, exerted a large effect on the maximum generative force and the hysteresis.

When both chambers were filled with particles, contrary to the findings of single-chamber filling, it was found that the frictional force was generated by the sliding friction between the cylinder and rod and the particles, whereby, due to the friction of the rod, a waveform of the generative force was asymmetrical with respect to the origin.

These results were demonstrated by means of simulations of generative force and particle behavior using the distinct element method, as well as by experiments. The simulation results and the experimental results were in good agreement with one another both qualitatively and quantitatively, and it was confirmed that the simulations were able to reliably reproduce the phenomena which occurred in the experiments.

*"Elastomer" is a generic term for a polymer having elasticity. Rubber and the like correspond to this term.

1 Introduction

The particle assemblage damper is a damper filled with small steel or elastomer balls in place of a fluid such as oil as in oil dampers. These spherical particles that fill the damper are fluidized by the movement of a piston to yield a resistive force. [1, 2] The existing oil damper involves problems including liquid leakage and temperature-dependent damping force. One of the possible solutions to the problems is the use of particle dampers. A particle damper using particles of a larger size than the clearance of the sliding part of the damper is free from leakage. For a particle damper using small elastomer balls (hereinafter "elastomer particles"), using elastomer material with excellent heat/cold resistance whose glass transition temperature is low can reduce the temperature dependence of the generative force.

This study used a separated dual chamber single rod-type particle damper which had two chambers divided by a piston and employed elastomer particles. An investigation was carried out to clarify the generative force characteristics and force generation factors or mechanism for two different cases: with particles filling only one of the two chambers and with particles filling both chambers. Elastomer particles were selected with an aim at delivering a high generative force by densely filling them, which was possible thanks to their high elastic deformation. The investigation used two approaches: one is to develop a damping theory based on the distinct element method and the other to simulate generative force and particle behavior. The simulation results were compared with those obtained from experiments using an actual machine to determine the generative force characteristics and mechanism and to verify the adequacy of the developed theory.

Please note that this damper generates a combined elastic and viscous force, although the term "damper" might cause you to imagine a damper that can suppress vibration by exerting a damping force attributable to a pressure loss or viscous resistance of the fluid used. That's why the force generated by this damper is called a "generative force", not a damping force, for clarification purposes.

2 Generative Force Characteristics of Particle Damper with One of the Chambers Filled

2.1 Damper Structure

Fig. 1 shows the general structure of the damper used in simulations and experiments. The internal void of the damper is divided into two chambers by a piston and only the chamber without the rod is filled with spherical particles. The clearance between the piston perimeter and the cylinder bore is very small so that no particles can move freely between the chambers. Friction in the sliding part is negligible as it is considerably smaller than the generative force of the damper. The piston displacement of this damper described in the following sections refers to the movement of the piston in the direction of the z-axis shown in Fig. 1.

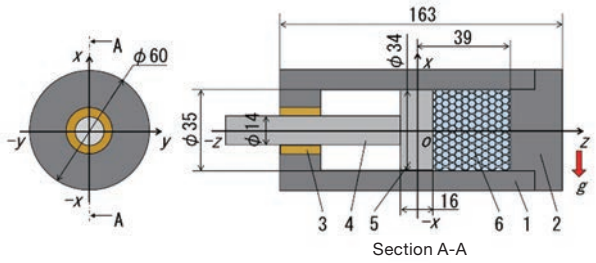

Fig. 1 Damper structure
1. Cylinder, 2. End cover, 3. Bearing, 4. Rod, 5. Piston, 6. Elastomer particles, Unit: mm

2.2 Simulations and Experiments

2.2.1 Distinct Element Method

Simulations were conducted by using the distinct element method (hereinafter "DEM") to clarify the particle behavior, generative force characteristics, and components of the force. DEM is a method for computing the behavior of particles by sequentially calculating the equation of the motion of particles for their translational motion and rotation at individual time points, with consideration given to contact interactions of particles.

2.2.2 Primitive Equation

DEM can be used to determine the velocity and position of a particle by solving the equation of motion expressed in Equation (1) and the equation of angular motion expressed in Equation (2) by taking into account the contact force of each particle.

$$m_i \frac{d^2 \boldsymbol{r}_i}{dt^2} = \boldsymbol{F}_i \tag{1}$$

$$I_i \frac{d\boldsymbol{\Omega}_i}{dt} = \boldsymbol{T}_i \tag{2}$$

where:
i is particle number;
t is time;
m_i is particle mass;
$\boldsymbol{r}_i$ is position vector of the particle;
$\boldsymbol{F}_i$ is the sum total of contact forces;
I_i is inertia moment;
$\boldsymbol{\Omega}_i$ is angular velocity vector of the particle, and;
$\boldsymbol{T}_i$ is the sum total of torques applied to the particle.

$\boldsymbol{F}_i$, $\boldsymbol{T}_i$ and I_i can be expressed in Equations (3) to (5) below:

$$\boldsymbol{F}_i = \boldsymbol{F}_{cn} + \boldsymbol{F}_{ct} + m_i \boldsymbol{g} \tag{3}$$

$$\boldsymbol{T}_i = \boldsymbol{r}_i \times \boldsymbol{F}_{ct} \tag{4}$$

$$I_i = \frac{8}{15} \rho \pi r^5 \tag{5}$$

In the equations above, the subscript n indicates the normal direction at the point of contact and the subscript t the tangential direction at the point of contact. $\boldsymbol{F}_{cn}$ and $\boldsymbol{F}_{ct}$ are the contact force in the normal and tangential directions, respectively. m_i is particle mass, g is gravitational acceleration, p is particle density, and r is particle radius. The concept of contact force was proposed by Cundall and Strack [3]. They used an analysis model consisting of three elements shown in Fig. 2: a spring, a dashpot and a friction slider. The model can be expressed in Equations (6) and (7). Fig. 3 shows a conceptual rendering of the force applied in the normal direction and the force applied in the tangential direction.

$$\boldsymbol{F}_{cn} = \left(-K_n \delta_n^{1.5} - C_n \boldsymbol{V}_{ij} \cdot \boldsymbol{n}_i \right) \boldsymbol{n}_i \tag{6}$$

$$\boldsymbol{F}_{ct} = -K_t \boldsymbol{\delta}_t - C_t \boldsymbol{V}_{fij} \tag{7}$$

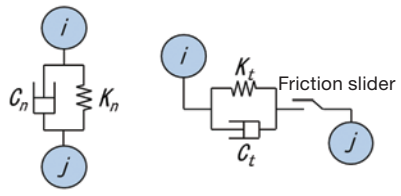

Fig. 2 Contact model
(a) Normal direction, (b) Tangential direction

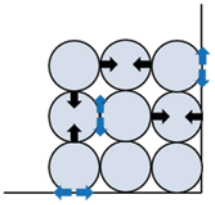

Fig. 3 Conceptual rendering of forces in the normal and tangential directions

In the equations above, K_n and K_t indicate elastic modulus in the normal and tangential directions, respectively, and C_n and C_t are viscosity coefficients in the normal and tangential directions, respectively. δ_n is displacement in the normal direction at the point of contact and $\boldsymbol{\delta}_t$ displacement vector in the tangential direction at the point of contact between the particles i and j. $\boldsymbol{n}_i$ is the unit vector in the normal direction from the particle i to the particle j at their contact point. $\boldsymbol{V}_{ij}$ is the relative velocity vector of the particle i against the particle j. $\boldsymbol{v}_i$ and $\boldsymbol{v}_j$ are velocity vectors of the particles i and j, respectively. $\boldsymbol{V}_{fij}$ is the relative velocity vector in the tangential direction of the particle i against the particle j at their contact point. $\boldsymbol{V}_{ij}$, $\boldsymbol{V}_{fij}$ and $\boldsymbol{\delta}_t$ can be expressed in Equations (8) to (10):

$$\boldsymbol{V}_{ij}=\boldsymbol{v}_i-\boldsymbol{v}_j \tag{8}$$

$$\boldsymbol{V}_{fij}=\boldsymbol{V}_{ij}-(\boldsymbol{V}_{ij}\cdot\boldsymbol{n}_i)\boldsymbol{n}_i+2a(\boldsymbol{\omega}_i-\boldsymbol{\omega}_j)\times\boldsymbol{n}_i \tag{9}$$

$$\boldsymbol{\delta}_t=\Delta t-\boldsymbol{V}_{fij} \tag{10}$$

In the equations above, a is the particle radius, and $\boldsymbol{\omega}_i$ and $\boldsymbol{\omega}_j$ are angular velocity vectors of the particles i and j. Elastic modulus in the tangential direction can be expressed in Equations (11) to (14) using the Hertzian contact theory:

$$K_{nij}=\frac{4}{3\pi}\left(\frac{1}{2\delta_i}\right)\sqrt{\frac{a\delta_n}{2}} \tag{11}$$

$$K_{niw}=\frac{4}{3\pi}\left(\frac{1}{\delta_i+\delta_w}\right)\sqrt{a\delta_n} \tag{12}$$

$$\delta_i=\frac{1-\nu_i^2}{E_i\pi} \tag{13}$$

$$\delta_w=\frac{1-\nu_w^2}{E_w\pi} \tag{14}$$

In the equations above, the subscript w indicates that the relevant amount is related to the wall surface of the cylinder bore (hereinafter "the cylinder wall"). K_{nij} indicates the elastic modulus K_n of the particles during their contact. K_{niw} indicates the elastic modulus K_n of the particle when it makes contact with the cylinder wall. E_i and E_w are the modulus of longitudinal elasticity of the particle and the wall, respectively. ν_i and ν_w are Poisson ratios of the particle and the wall, respectively. The elastic modulus in the tangential direction is based on an assumption that no slide occurs at the point of contact and can be expressed in Equations (15) and (16) in accordance with the Mindlin [4] theory:

$$K_{tij}=\frac{2\sqrt{2a}\,G_i}{2-\nu_i}\delta_n^{0.5} \tag{15}$$

$$K_{tiw}=\frac{8\sqrt{a}\,G_i}{2-\nu_j}\delta_n^{0.5} \tag{16}$$

In the equations above, K_{tij} is the elastic modulus of the particles during their contact. K_{tiw} is the elastic modulus of the particle and the wall during their contact. G_i is the modulus of transverse elasticity of the particle and can be expressed in Equation (17):

$$G_i=\frac{E_i}{2(1+\nu_i)} \tag{17}$$

C_n and C_t can be expressed in Equations (18) and (19):

$$C_n=\alpha\sqrt{m_iK_n}\,\delta_n^{0.25} \tag{18}$$

$$C_t=\alpha\sqrt{m_iK_t}\,\delta_{ct}^{0.25} \tag{19}$$

$$\alpha=2.2\sqrt{\frac{\ln(e)^2}{\ln(e)^2+\pi}} \tag{20}$$

α is a dimensionless constant that decides the magnitude of viscous force and can be expressed in Equation (20). e in Equation (20) is the repulsion coefficient of the particle. If the relative velocity vector in the tangential direction of the particle on the contact surface is more than zero (0) or the contact force in the tangential direction is higher than the frictional force, it is considered that particle sliding has occurred along the contact surface. The phenomenon can be expressed in Equations (21) to (23):

If $|\boldsymbol{V}_{fij}|=0$ and $\boldsymbol{F}_{ct}\leqq\mu_f|\boldsymbol{F}_{cn}|$,

$$\boldsymbol{F}_{ct}=\boldsymbol{F}_{ct} \tag{21}$$

If $\boldsymbol{F}_{ct} > \mu_f \mid \boldsymbol{F}_{cn} \mid$,

$$\boldsymbol{F}_{ct} = -\mu f \mid \boldsymbol{F}_{cn} \mid \boldsymbol{t}_i \tag{22}$$

If $|\boldsymbol{V}_{fij}| > 0$,

$$\boldsymbol{F}_{ct} = -\mu f \mid \boldsymbol{F}_{cn} \mid \boldsymbol{t}_i \tag{23}$$

$$t_i = \frac{\boldsymbol{V}_{fij}}{|\boldsymbol{V}_{fij}|} \tag{24}$$

$\boldsymbol{t}_i$ is unit vector in the $\boldsymbol{V}_{fij}$ direction of the particle and can be expressed in Equation (24). μ_f is the friction coefficient of the particle.

Thus, the analysis model was designed to consider elastic and viscous forces in the normal direction and, in addition to these forces, frictional force as well in the tangential direction. This analysis also applied the second-order accurate Adams-Bashforth method to time-stepping of displacement, velocity and angular velocity.

2.2.3 Simulation and Experimental Conditions

The overview of the experiment equipment is shown in Fig. 4. The simulation conditions are shown in Table 1 and the experimental conditions are shown in Table 2. The particles used in the experiments are shown in Photo 1.

Table 1 Simulation conditions

Particle material	Silicone rubber (TSE 3466 made by Momentive Performance Materials), nitrile rubber (NBR made by Inaba Rubber)
Particle size [mm]	3, 5
Packing fraction [-]	0.60, 0.70
Number of particles	1,339, 1,562
Stroke [mm]	10
Excitation frequency [Hz]	1, 5
Time increments [sec.]	5.0×10^{-9}
Excitation waveform	Sinusoidal
Particle density [kg/m^3]	1.10×10^3
Poisson ratio of particle ν_i	0.5
Friction coefficient μ_f (wall-particle)	0.5
Friction coefficient μ_f (between particles)	0.5
Young's modulus E_w [GPa] (wall)	210
Young's modulus E_i [MPa] (particle)	4.08 (TSE3466), 17.6 (NBR)
Viscosity coefficient α	0.5311

Table 2 Experimental conditions

Particle material	Silicone rubber (TSE 3466), nitrile rubber (NBR)
Young's modulus E_i [MPa] (particle)	4.08(TSE3466), 17.6(NBR)
Particle size [mm]	3, 5
Packing fraction [-]	0.60, 0.70
Stroke [mm]	10
Excitation frequency [Hz]	1, 5

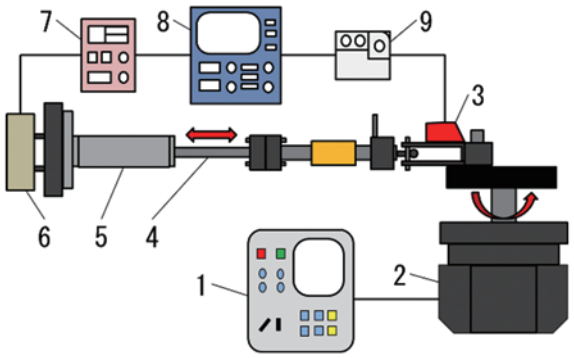

Fig. 4 Experiment equipment
1. Controller, 2. Motor, 3. Laser displacement gauge, 4. Rod, 5. Damper, 6. Load cell, 7. Dynamic distortion amplifier. 8, Oscilloscope, 9. Displacement gauge amplifier unit

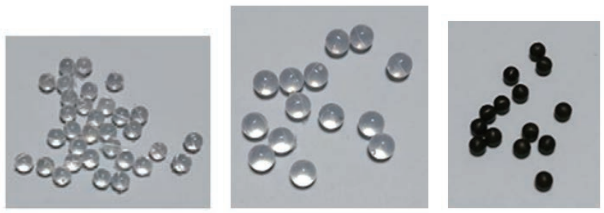

(a) (b) (c)

Photo 1 Particles used
(a) Silicone rubber, particle size 3 mm
(b) Silicone rubber, particle size 5 mm
(c) NBR, particle size 3 mm

For simulation purposes, the general coefficient of friction between rubbers of 0.5 was used as shown in Table 1.[5] In a condition for which two or more parameters are indicated in Table 1 or 2, the one in red is the reference conditions. The packing fraction refers to the ratio of particles in the particle chamber and has been determined by dividing the volume of all the particles present in the chamber by the volume of the chamber.

2.2.4 How to Calculate Generative Force

In the simulations of the particle damper with only one of the chambers filled, the total generative force can be determined, as shown in Fig. 5, by adding the compres-

sive force applied to the cylinder bottom end surface (hereinafter "the cylinder bottom") in the *z*-axis during particle compression by the piston to the frictional force of particles against the cylinder wall in the *z*-axis direction. The component of the generative force in the normal direction is attributable to viscoelasticity of particles due to their compressive deformation. The component of the generative force in the tangential direction is attributable to viscoelasticity of particles due to their shear deformation and sliding friction between particles and the cylinder wall.

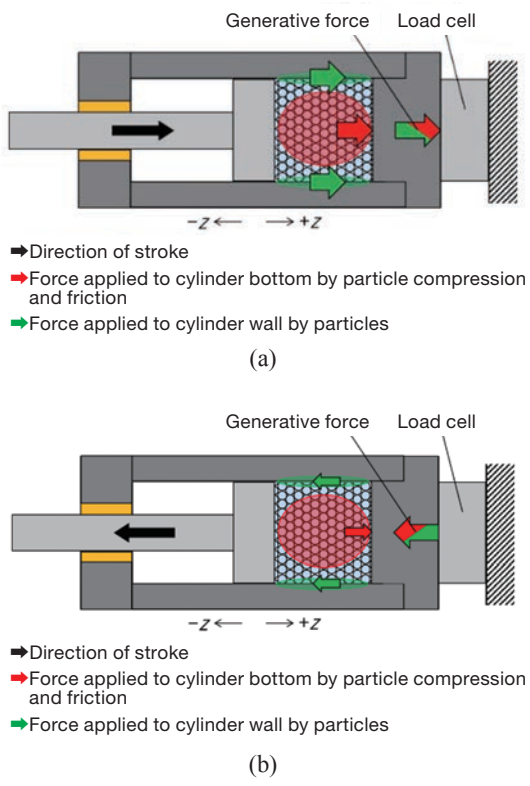

Fig. 5 Generative force in the *z*-axis direction
(a) Positive displacement, (b) Negative displacement

2.2.5 Generative Force and Its Normal and Tangential Components

The results of the simulations are plotted in Fig. 6. These curves show how the generative force and its component in the normal direction (hereinafter "the normal component") and its component in the tangential direction (hereinafter "the tangential component") change with displacement under the reference conditions (i.e., force-displacement curves). Fig. 7 shows the force-velocity curves under the same conditions. All the following figures of these kinds plot a cycle of data. The displacement refers to the piston displacement. The time development of curves is clockwise for force-displacement curves and counterclockwise for force-velocity curves.

According to Fig. 6, the generative force shows gradually hardening characteristics that the generative force increases as the displacement advances in the direction of particle compression (hereinafter "the compression process") and involves hysteresis as the piston travels in the direction opposite to the direction of particle compression (hereinafter "the retraction process"). The gradually hardening characteristics may be attributable to elastic repulsion generated by particle compression. The hysteresis may be attributable to viscosity caused by deformation of elastomer particles and/or friction between particles or between particles and the wall.

Now, let us move on to discussion about the normal and tangential components of the generative force. The normal component is related to resistance generated primarily during particle compression and the tangential component is related to shear force generated between particles or between particles and the wall as well as resistance between particles or between particles and the wall generated when particles move around.

In the compression process, both the normal and tangential components show gradually hardening characteristics as shown in Fig. 6. The normal component has a higher maximum value and lower hysteresis than for the tangential component. Since the normal component peaks at around the point of 0 m/sec. velocity as shown in Fig. 7, the effect of the viscosity attributable to compressive deformation of particles in the normal direction should be trivial, which may result in the gradually hardening characteristics and the lower hysteresis. In other words, the normal component consists predominantly of the elastic force of particles due to their compression. The tangential component also shows gradually hardening characteristics, but has higher hysteresis, resulting in a negative value that gradually becomes smaller as the displacement advances during the retraction process. Since the viscosity affecting the hysteresis depends on the velocity, the effect of viscosity on the tangential component is probably low because it peaks at around 0 m/sec. velocity as shown in Fig. 7. In addition, the force converges to 0 N at a displacement of -5 mm, which is the start point of the compression process. Therefore, the tangential component consists predominantly of frictional force, to which the normal component acts as vertical resistance. As the positive/negative sign to friction force is switched over according to the direction of displacement, the tangential

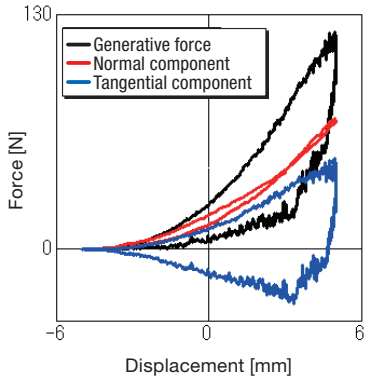

Fig. 6 Force-displacement curves of generative force and its normal and tangential components

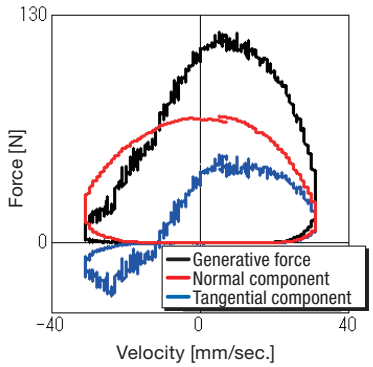

Fig. 7 Force-velocity curves of generative force and its normal and tangential components

component takes a negative value with higher hysteresis during the retraction process. The frictional force generated here refers to the friction of sliding particles against the cylinder wall.

2.2.6 Elastic and Viscous Forces in Normal/ Tangential Direction

To verify the assumption discussed in the previous section that the normal component of the generative force consists predominantly of elastic force and the tangential component consists predominantly of frictional force, this section further discusses these components by dividing them into elastic and viscous forces. Fig. 8 shows the force-displacement curves of the normal component and its breakdown into elastic and viscous forces. Fig. 9 is an enlarged view of the viscosity curve in Fig. 8. Fig. 10 shows the force-displacement curves of the tangential component and its breakdown into elastic and viscous forces.

In Fig. 8, the normal component curve generally agrees with the elasticity curve, which implies that the elastic repulsion of particles due to their compressive deformation is predominant. However, the viscosity never takes a value of zero (0). The enlarged view in Fig. 9 reveals that a minute force is always generated. Fig. 10 shows that the tangential component involves no elastic or viscous force attributable to shear deformation of particles along the cylinder wall. Rather, the tangential component only consists of friction of particles against the cylinder wall, which implies that particles are always sliding along the wall.

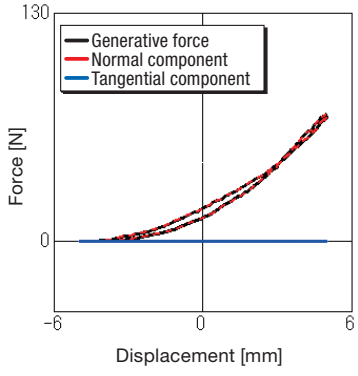

Fig. 8 Force-displacement curves of normal component and its elasticity and viscosity

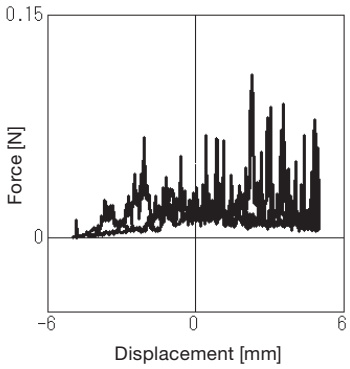

Fig. 9 Enlarged view of force-displacement curve of viscosity of normal component

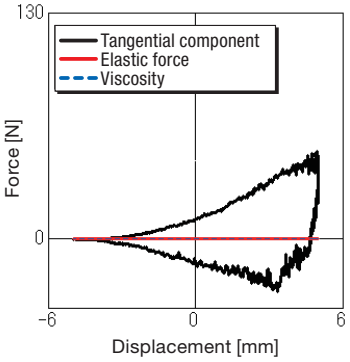

Fig. 10 Force-displacement curves of tangential component and its elasticity and viscosity

Now, the discussion above has revealed that the generative force is greatly affected by the elastic force of particles in the normal direction due to their compressive deformation and the friction of particles against the cylinder wall in the tangential direction.

2.2.7 Distribution of Particle Compression

Since the generative force heavily depends on the elastic force in the normal direction, we tried to determine the effect of the compressive force of particles filled in the damper under the reference conditions. Fig. 11 (a) to (d) show where the piston and particles are located in the damper when viewed from the section A-A in Fig. 1 and the distribution of particle compression. The compressive force on particles in these diagrams is due to the elasticity in the normal direction.

In Fig. 11 (a), many of the particles close to the piston are highly compressed during the compression process, resulting in higher particle repulsion against the piston. Near the cylinder bottom in turn many particles are not so strongly compressed. This means that the compression of the particles close to the piston has not been transferred well to the cylinder bottom. In Fig. 11 (c) for the retraction process, many of the particles close to the piston are not so strongly compressed, resulting in lower particle repulsion against the piston. However, many of the highly com-

pressed particles still remain near the cylinder bottom. This means that the compression of the particles close to the cylinder bottom has not been transferred well to the piston. It can be derived from these facts that there is a time lag between the forced excitation by the piston and the transfer of forces caused by particle deformation.

In the compression process, the particle-particle compressive force, the force pressing particles against the cylinder wall, and the friction against which these two forces act as vertical resistance increase, resulting in a higher force applied to the cylinder bottom. In the retraction process, the particle-particle compressive force and the force pressing particles against the wall become smaller, resulting in lower friction. In this case, the force applied to the cylinder bottom is the sum of the compressive repulsion of particles and the friction. Since the friction is switched from a positive value to a negative one or vice versa between the compression and retraction processes, the generative force at any given displacement during the compression process is different from that at the same displacement during the retraction process. The discussion above has revealed that the delay in the transfer of forces and the friction are one of the causes of the hysteresis of the generative force.

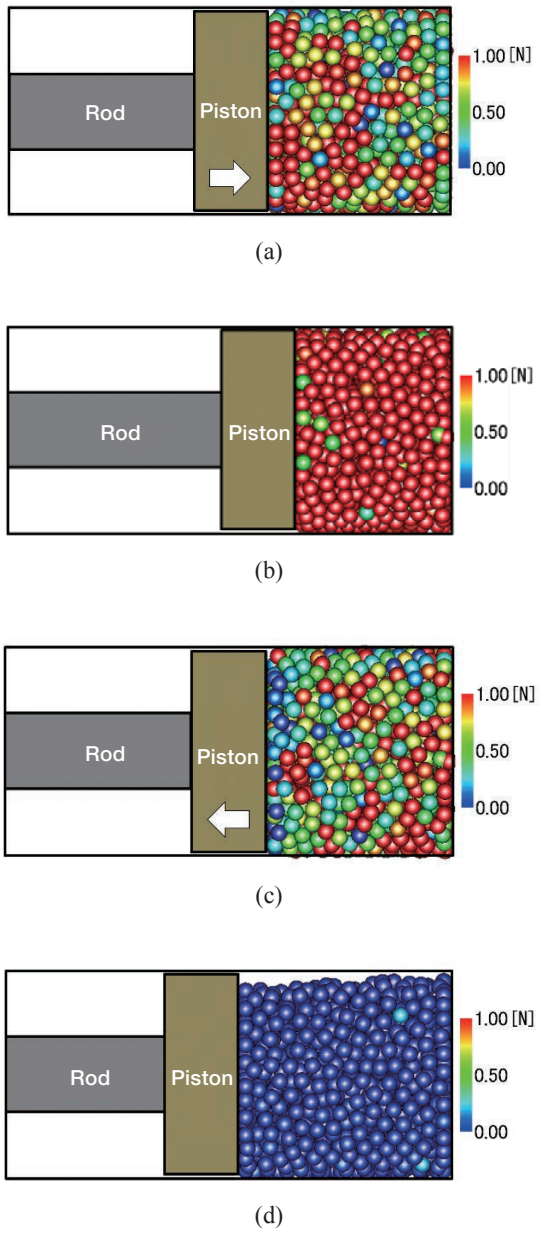

Fig. 11 Distribution of particle compression
(a) Compression process, z = 0
(b) z = 5
(c) Retraction process, z = 0
(d) z = -5

2.2.8 Comparison Between Experimental and Simulation Results

To verify the adequacy of the simulations and determine the generative force characteristics under different conditions, we conducted experiments under different conditions and compared the results with the simulation results. Figs. 12 to 16 show the generative force-displacement curves obtained from the experiments under the reference conditions as well as under another set of conditions where the packing fraction, excitation frequency, particle material and particle size were changed from the reference conditions, along with the results of the simulations. The particle material was changed from the reference conditions in that only the Young's modulus of particles was changed.

According to Figs. 12 to 16, the simulation results are in good agreement with the experimental results both qualitatively and quantitatively. Like under the reference conditions, the generative force shows gradually hardening characteristics during the compression process or hysteresis after the transition from the compression process to the retraction process, regardless of the packing fraction, excitation frequency, particle material or particle size.

Figs. 12 to 16 also show how the generative force changes under different conditions. Its peak and hysteresis substantially change with the packing fraction and the Young's modulus which affects the particle material. They do not change so much with the excitation velocity or

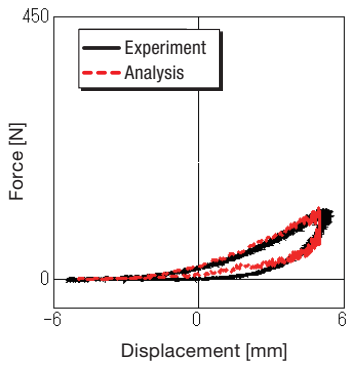

Fig. 12 Generative force-displacement curves; Experiment-simulation comparison
Under reference conditions (packing fraction 0.60, excitation frequency 1 Hz, Young's modulus 4.08 MPa, particle size φ3 mm)

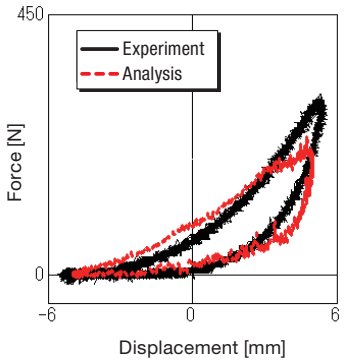

Fig. 13 Generative force-displacement curves; Experiment-simulation comparison
With packing fraction changed (0.70)

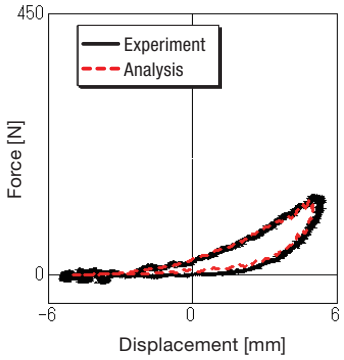

Fig. 14 Generative force-displacement curves; Experiment-simulation comparison
With excitation frequency changed (5 Hz)

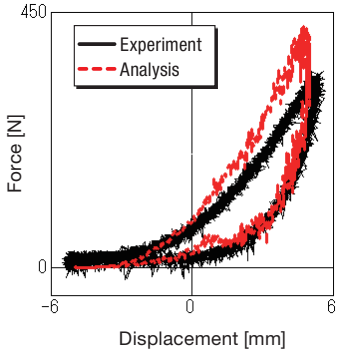

Fig. 15 Generative force-displacement curves; Experiment-simulation comparison
With material changed (Young's modulus 17.6 MPa)

particle size. The reason for the minor effect of excitation velocity is the very small effect of viscosity according to the simulation results. The reason why the particle size does not influence so much is that, if larger particles are used, the particles would have larger deformation as the displacement advances but would have lower friction of particles against the cylinder due to the lower number of particles. This lower friction was a probable cause of why the generative force did not increase so much.

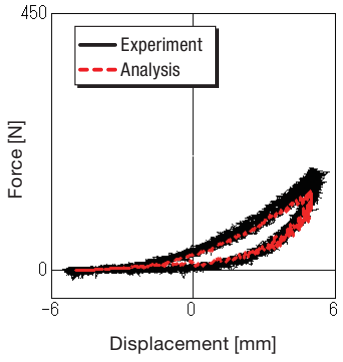

Fig. 16 Generative force-displacement curves; Experiment-simulation comparison
With particle size changed (φ5 mm)

Since the generative force characteristics are found to be qualitatively the same under the different conditions, the particles in the damper should generally behave in a same way. It can now be concluded that the simulations reliably reproduce the phenomena which occurred in the experiments.

3 Characteristics of Generative Force of Particle Damper with Both Chambers Filled

3.1 Damper Structure

Fig. 17 shows the general structure of the damper used for the simulations and experiments. The only difference from the damper described in Chapter 2 is that both chambers divided by the piston are filled with particles. In the case where both chambers are filled with particles, the chamber without the rod is called Chamber A and that with the rod Chamber B.

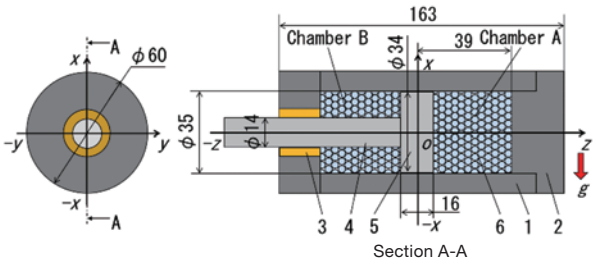

Fig. 17 Damper structure
1. Cylinder, 2. End cover, 3. Bearing, 4. Rod, 5. Piston, 6. Elastomer particles
Unit: mm

3.2 Simulations and Experiments

3.2.1 Simulation and Experimental Conditions

Table 3 shows the simulation conditions. Table 4 shows the experimental conditions. The simulation methods, primitive equations and experimental conditions described in Chapter 2 were also used in these simulations and experiments. The simulations and experiments in this Chapter were conducted only under the reference conditions described in Chapter 2 because the generative force characteristics have been generally verified in Chapter 2.

Table 3 Simulation conditions

Particle material	Silicone rubber (TSE 3466)
Particle size [mm]	3
Packing fraction [-]	0.60
Number of particles	2533
Stroke [mm]	10
Excitation frequency [Hz]	1
Time increments [sec.]	5.0×10^{-9}
Excitation waveform	Sinusoidal
Particle density [kg/m^3]	1.10×10^3
Poisson ratio of particle ν_i	0.5
Friction coefficient μ_f (wall-particles)	0.5
Friction coefficient μ_f (between particles)	0.5
Young's modulus E_w [GPa] (wall)	210
Young's modulus E_i [MPa] (particle)	4.08(TSE3466)
Viscosity coefficient α	0.5311

Table 4 Experimental conditions

Particle material	Silicone rubber (TSE 3466)
Young's modulus E_i [MPa] (particles)	4.08(TSE3466)
Particle size [mm]	3
Packing fraction [-]	0.60
Stroke [mm]	10
Excitation frequency [Hz]	1

3.2.2 How to Calculate Generative Force

In the simulations of the particle damper with both of its chambers filled, the force applied to the cylinder bottom D_z shown in Fig. 18 can be determined by adding the compressive force applied to the cylinder bottom in the z-axis during particle compression by the piston to the frictional force of particles against the cylinder wall in the z-axis direction. For simulations of a damper with both chambers filled with particles, the force applied to the rod end R_z shown in Fig. 19 can be determined by adding the compressive repulsion applied to the rod end in the z-axis during particle compression by the piston to the frictional force of particles against the rod wall in the z-axis direction. There is a balance between D_z and R_z.

The normal component of the generative force is attributable to Viscoelasticity generated by compressive deformation of particles. The tangential component of the

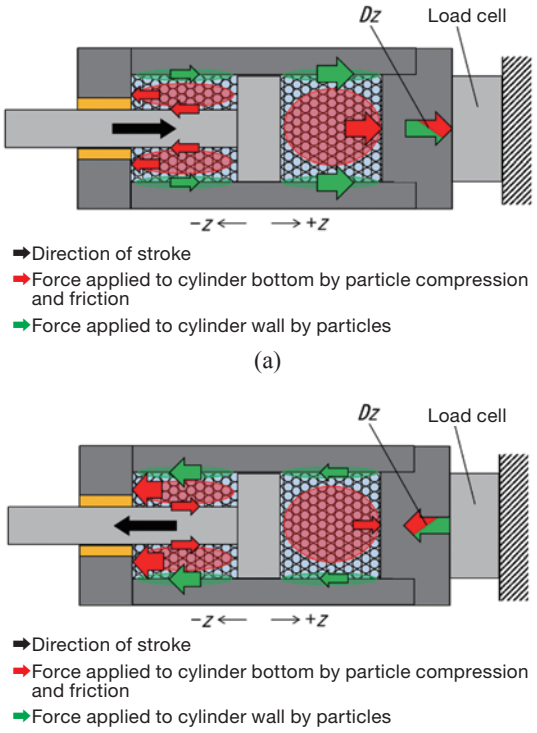

Fig. 18 Force applied to cylinder bottom in the z-axis direction
(a) Positive displacement, (b) Negative displacement

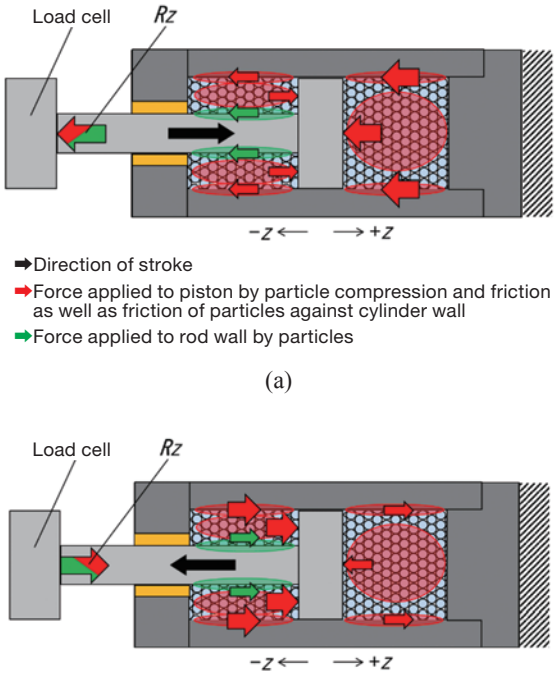

Fig. 19 Force applied to rod end in the z-axis direction
(a) Positive displacement, (b) Negative displacement

generative force is attributable to Viscoelasticity generated by shear deformation of particles and the sliding friction of particles against the cylinder or rod wall. Therefore, determining D_z will identify the friction of particles against the cylinder wall and determining R_z will identify the friction of particles against the rod wall.

3.2.3 Generative Force and its Breakdown

As shown in Fig. 18, simulations were conducted with a focus on the force applied to the cylinder wall. The simulations produced the results shown in Figs. 20 and 21. Fig. 20 shows the generative force D_z that changes with displacement under the reference conditions, the tangential component of D_z applied to the cylinder wall, and the remaining component. Fig. 21 shows the generative force D_z that changes with velocity under the same conditions. The remaining component was determined by subtracting the tangential component applied to the cylinder wall from Dz. According to Fig. 20, the generative force shows hardening characteristics and involves hysteresis after the direction of displacement changes. In general, the maximum generative force during the negative displacement in which the particles in Chamber B are predominantly compressed is larger than the maximum generative force during the positive displacement in which the particles in Chamber A are predominantly compressed. The curve of the generative force is asymmetrical with respect to the origin. Like the damper with one of the chambers filled with particles, this damper also delivers the generative force with gradually hardening characteristics probably because of the effect of the elastic repulsion due to particle compression. The hysteresis is attributable to the viscosity due to deformation of the elastomer particles and/or the effect of the particle-particle or particle-wall friction. The generative force has been plotted to be a nonlinear curve probably because, as the piston moves toward Chamber B where the rod exists to increase the displacement, the particle-rod friction increases.

The next step is to discuss the generative force characteristics based on the force applied to the cylinder wall and the remaining component. Fig. 20 indicates that, as the displacement advances in each direction, both the force applied to the cylinder wall and the remaining component increase. In this process, the force applied to the cylinder wall abruptly jumps when the direction of displacement changes. After a certain point of displacement, the force mildly increases to show gradually hardening characteristics. On the other hand, the remaining component involves this gradually hardening characteristics all the time. So, the hysteresis is considered to be greatly influenced by the force applied to the cylinder wall. The maximum generative force is attributable to the force applied to the cylinder wall and the remaining component to almost the same extent. Here again, as in Fig. 18, the generative force applied to the cylinder bottom on the side without the rod consists of the normal compression generated when the piston compresses particles, the tangential friction of particles against the rod wall, and the tangential friction of particles against the cylinder wall. The asymmetry of the generative force curve to the origin is attributable to the contact force of particles against the rod located in Chamber B. This issue will be verified later in the section discussing the results related to the generative force R_z.

Fig. 21 shows that the generative force and its normal and tangential components' peak at a point slightly shifted from the 0 m/sec. velocity. Without the influence of viscosity, the force-displacement curve should peak at the point of 0 m/sec. velocity. According to Equations (6) and (7), the velocity only affects the normal/tangential viscosity. Therefore, the maximum generative force occurs at a point slightly shifted from 0 m/sec. probably because of the effect of viscosity.

Then, another simulation was conducted with a focus on the force applied to the rod wall as shown in Fig. 19.

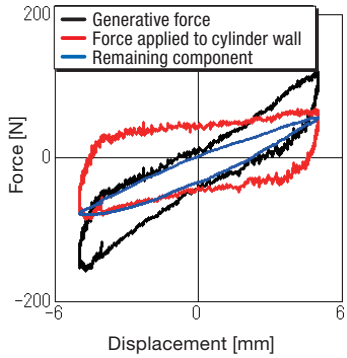

Fig. 20 Force-displacement curves of generative force D_z, force applied to cylinder wall and remaining component

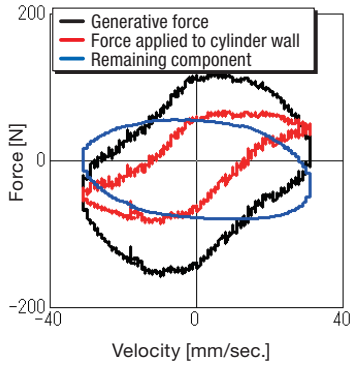

Fig. 21 Force-velocity curves of generative force D_z, force applied to cylinder wall, and remaining component

Fig. 22 shows the generative force R_z that changes with displacement under the reference conditions, its tangential component applied to the rod wall, and the remaining component. The remaining component was determined by subtracting the tangential component of the force applied to rod wall from R_z. The only difference from D_z is that the force applied to the rod wall shows gradually hardening

characteristics during the negative displacement, and increases until the displacement increases to a certain positive level and then gradually decreases until it gets down to about 0 N. The remaining component shows almost the same characteristics as those of the generative force however considerably differs from the generative force in the negative displacement region. The force applied to the rod wall shows gradually hardening characteristics as the friction of particles against the rod wall, which acts as vertical resistance, increases due to the increase in particle compression in Chamber B caused by negative displacement. During the positive displacement, the friction of particles against the rod wall decreases because the particle compression in Chamber B decreases. Furthermore, this force applied to the rod wall makes the generative force asymmetrical with respect to the origin. The gradually hardening characteristics of the remaining component is attributable to the compressive repulsion of particles and the friction of particles against the cylinder wall, which acts as vertical resistance. The hysteresis is attributable to the friction of particles against the cylinder wall.

Now the force applied to the cylinder wall shown in Fig. 20 can be compared with the force applied to the rod wall shown in Fig. 22. It is obvious that the force applied to the rod wall is smaller. This is because the rod has a smaller outside diameter than the cylinder bore. In other words, since the rod perimeter has a smaller surface area, the rod is affected by particle friction to a smaller degree than the cylinder is affected by the same.

From the above, the discussion about D_z and R_z can be summarized as follows. The generative force in Chamber A mainly consists of the normal repulsion generated during particle compression by the piston and the tangential friction of particles against the cylinder. In Chamber B, the tangential friction of particles against the rod is added to the forces stated above to constitute the generative force. Furthermore, the generative force, the force applied to the cylinder wall, and the remaining component peak at a point shifted from the 0 m/sec. velocity as shown in Fig. 21. This implies that these forces are affected by the viscous force of elastomer particles.

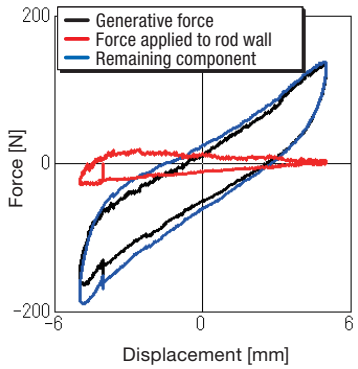

Fig. 22 Force-displacement curves of generative force R_z, force applied to rod wall, and remaining component

3.2.4 Elasticity and Viscosity of Force Applied to Cylinder or Rod Wall and of Remaining Component of Generative Force

To verify the effect of viscosity described in the previous section, the force applied to the cylinder or rod wall and the remaining component of the generative force were divided into elasticity and viscosity.

Fig. 23 shows the force-displacement curves of the force of D_z applied to the cylinder wall and its elasticity and viscosity. Fig. 24 shows the force-displacement curves of the remaining component of D_z and its elasticity and viscosity. Fig. 25 is an enlarged view of Fig. 24 showing the viscosity.

According to Fig. 23, the force applied to the cylinder wall only consists of the friction of particles against the cylinder. No elastic or viscous force is generated due to shear deformation of particles. Like the discussion about the tangential component of the generative force in the particle damper with one of the chambers filled, this damper also has sliding of particles against the cylinder in the tangential direction all the time. According to Fig. 24, the remaining component consists predominantly of elasticity with gradually hardening characteristics and hysteresis. The remaining component is generally in good agreement with the elasticity. Therefore, like the normal component of the particle damper with one of the chambers filled, this damper also delivers the generative force whose remaining component consists predominantly of the elastic repulsion due to compressive deformation of particles. The effect of the viscous force generated during particle deformation is very small. Unlike the normal component of the particle damper with one of the chambers filled, this damper delivers the generative force whose elasticity involves hysteresis. This is because the elastic modulus finally formed by the particle groups filled in chamber A and chamber B are different in each chambers. Another reason is, according to Fig. 18, that the elastic force of this damper includes the frictional force of particles against the rod. Therefore, properly speaking, this is not an elastic force or elasticity, but it is called here an elastic force or elasticity for convenience purposes. The viscous force never takes a value of zero (0). Rather, a minute viscous force is generated as shown in Fig. 25.

Fig. 26 shows the force-displacement curves of the force of R_z applied to the rod wall and its elasticity and viscosity. Fig. 27 shows the remaining component of R_z and its elasticity and viscosity. Fig. 28 shows an enlarged view of the viscosity curve in Fig. 27.

According to Fig. 26, like D_z, R_z also comes with the force applied to the rod wall only consisting of the friction of particles against the rod. No elastic or viscous force is generated by particle deformation. This means that particles around the rod are sliding all the time. According to Fig. 27, like D_z, R_z also comes with the remaining component consisting predominantly of elasticity with gradually hardening characteristics and hysteresis. The remaining

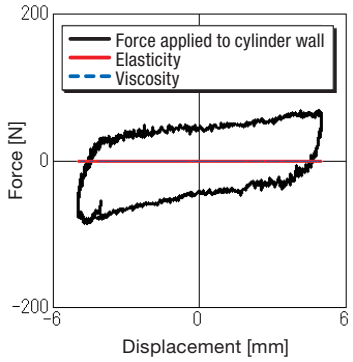

Fig. 23 Force-displacement curves of component of generative force D_z applied to cylinder wall and its elasticity and viscosity

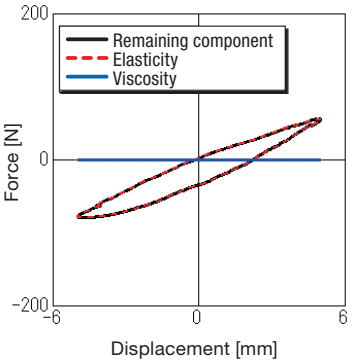

Fig. 24 Force-displacement curves of remaining component of generative force D_z and its elasticity and viscosity

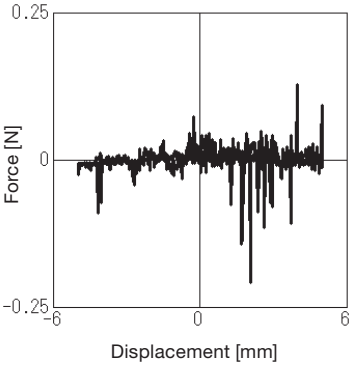

Fig. 25 Enlarged view of force-displacement curve of viscosity of remaining component (in Fig. 24)

component is generally in good agreement with the elasticity. Properly speaking, according to Fig. 19, this is not an elastic force because the elasticity in Fig. 27 consists of the elastic repulsion of particles during compressive deformation and the friction between the cylinder and particles, but it is called here an elastic force or elasticity as in the case of the force applied to the cylinder wall and the remaining component. The reason why the elastic force involves hysteresis is that, like D_z, the chambers show different non-linear Young's modulus values depending on the presence/absence of the rod. Another reason is, according to Fig. 19, that the generative force of this damper includes the friction between the cylinder and particles. Like D_z, R_z also includes a minute viscous force as shown in Fig. 28.

Now it may be useful to compare the generative force characteristics of this elastomer particle damper with the repulsion characteristics of cylindrical or other-shaped elastomer blocks during compression. When elastomer cylinders are compressed, many of them produce the generative force that depends on the displacement and involves viscoelasticity with hysteresis. In this damper in turn, friction of elastomer particles against the cylinder or

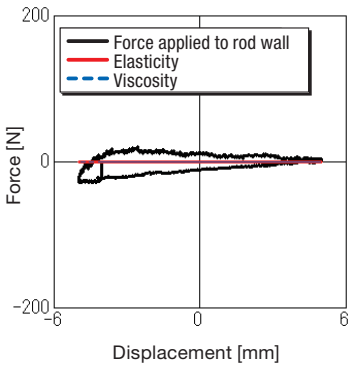

Fig. 26 Force-displacement curves of component of generative force R_z applied to rod wall and its elasticity and viscosity

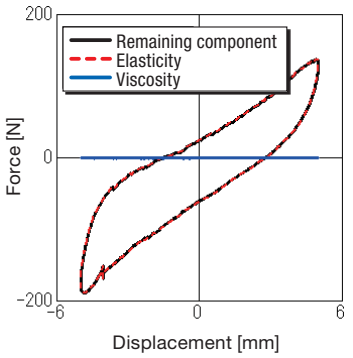

Fig. 27 Force-displacement curves of remaining component of generative force R_z and its elasticity and viscosity

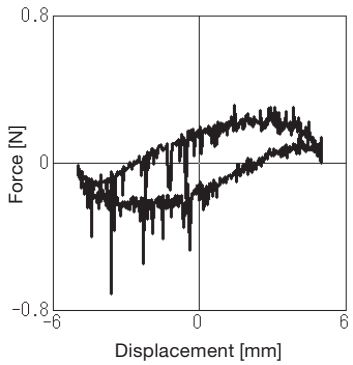

Fig. 28 Enlarged view of force-displacement curve of viscosity of remaining component (in Fig. 27)

rod wall occurs to greatly affect the generative force. Thus, the generative force of this damper shows higher hysteresis in comparison with the characteristics of the elastomer block of the same volume when it is compressed.

3.2.5 Distribution of Particle Compression

Like the particle damper with one of the chambers filled, this damper with both chambers filled also produces the generative force D_z heavily dependent on the other components than that applied to the cylinder wall, that is, particularly the elastic force in the normal direction. Then, we tried to determine the effect of the compressive force applied to particles filled in the damper. Fig. 29 (a) to (d) show where the piston and particles are located in the damper when viewed from section A-A in Fig. 17 and the distribution of particle compression. The compressive force applied to particles in these diagrams is due to the elasticity in the normal direction.

In Fig. 29 (a), as the piston travels in the direction of positive displacement, many of the particles close to the piston in Chamber A are highly compressed while many of the particles close to the cylinder bottom are weakly compressed. In Chamber B, many of the particles close to the piston are weakly compressed while many of the particles close to the cylinder bottom are highly compressed. This means that, as the piston travels in the direction of positive displacement, the force applied to the piston by the particles in the Chamber A increases while the force applied to the piston in Chamber B decreases. This phenomenon also takes place when the piston travels in the opposite direction as shown in Fig. 29 (c). However, a comparison between Figs. 29 (a) and 29 (c) reveals that Chamber B in Fig. 29 (c) has a greater number of highly compressed particles than in Chamber A in Fig. 29 (a) while Chamber A in Fig. 29 (c) has a greater number of weakly compressed particles than in Chamber B in Fig. 29 (a). This means that the compressive force applied to particles in Chamber B during displacement in the negative direction has greater influence. This is probably because Chamber B has a smaller volume than Chamber A by the volume of the rod, thereby giving particles smaller space to escape in Chamber B. As a result, particle compression in Chamber B is started at a smaller displacement than in Chamber A. In addition, a delay in the transfer of the force due to particle deformation can be found in Fig. 29 as in the case of the damper with one of the chambers filled.

3.2.6 Comparison Between Experimental and Simulation Results

To verify the adequacy of the simulations, we conducted experiments and compared the results with the simulation results. Fig. 30 shows the generative force-displacement curves obtained from the experiments and simulations.

According to Fig. 30, the simulation results are in good agreement with the experimental results both qualitatively and quantitatively. It can now be concluded that the simu-

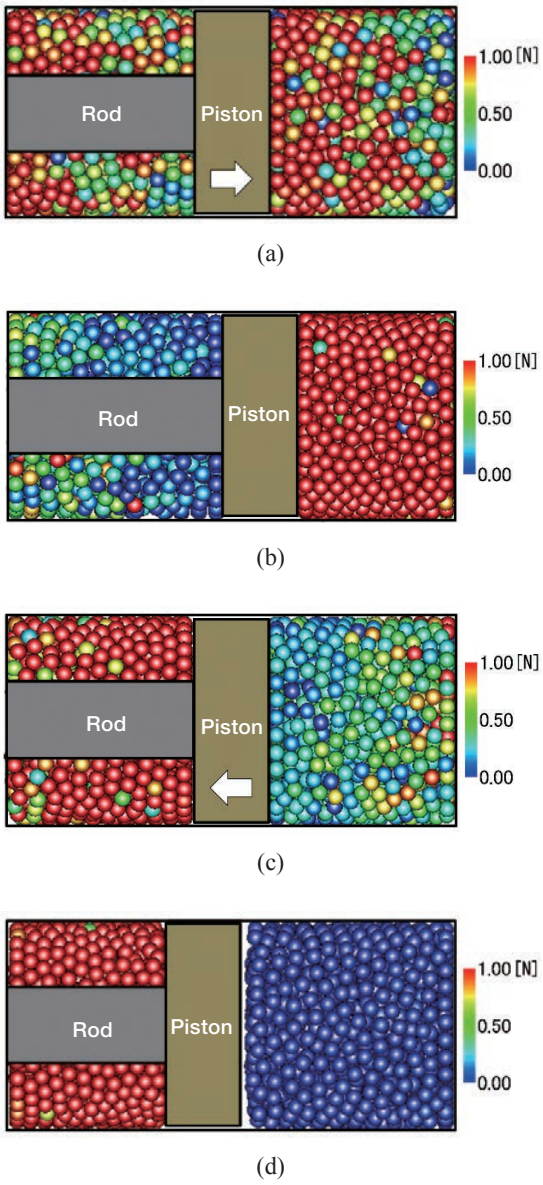

Fig. 29 Distribution of particle compression
(a) Compression process, z = 0
(b) z = 5
(c) Retraction process, z = 0
(d) z = -5

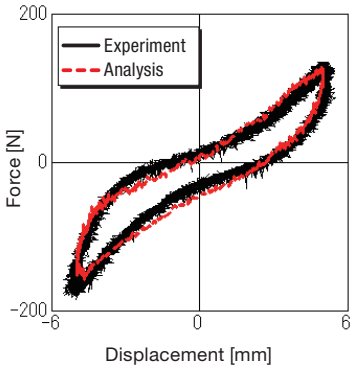

Fig. 30 Generative force-displacement curves; Experiment-simulation comparison

lations reliably reproduce the phenomena which occurred in the experiments, as in the case of the damper with one of the chambers filled.

4 Concluding Remarks

In this study, an investigation and discussions were conducted to clarify the generative force characteristics and force generation factors of a separated dual chamber single rod-type damper using elastomer particles for the two cases of one of the chambers filled and both chambers filled.

When only one of the chambers is filled with particles, the generative force shows gradually hardening characteristics along with hysteresis and is greatly affected by the elasticity in the normal direction and the friction in the tangential direction. This elasticity is mainly attributable to the compressive repulsion of particles during compression. The friction here indicates the sliding friction of particles against the cylinder. Increasing the packing fraction, the excitation frequency, the Young's modulus which affects the particle material, and the particle size will raise the maximum generative force and hysteresis. In particular, the packing fraction and Young's modulus strongly affect the generative force.

With both chambers filled with particles, the generative force shows gradually hardening characteristics along with hysteresis and is affected by the frictional force applied to the cylinder and rod walls in the tangential direction and the elasticity included in the remaining component, as in the case of the damper with one of the chambers filled. The force-displacement curve of the generative force is asymmetrical with respect to the origin because of the frictional force applied to the rod wall.

The results of DEM-based simulations of a damper with one of the chambers filled and a damper with both chambers filled were in good agreement with the experimental results both qualitatively and quantitatively. This has proved that the simulations reliably reproduce the phenomena which occurred in the experiments.

This report has now successfully clarified the generative force characteristics and force generation factors.

A future challenge is to enhance the accuracy of discussions and analyses. This report has mainly discussed the generative force based on its force-displacement curves and distribution of particle compression. Rather, we should determine the variations in elastic modulus of particles and the amount of particle deformation in the analysis process and then verify them in connection with the equations used for analysis. Furthermore, when considering to commercialize the damper, we also need to determine how the generative force changes with the size of the piston or the length of the particle chambers and to clarify advantages and disadvantages of this damper compared with other types of dampers.

Note) This report has been prepared by re-editing the FY2020 doctoral dissertation thesis in Nagoya Institute of Technology: Generative Force Characteristics of Separated Dual Chamber Single Rod-type Particle Damper Using Elastomer Particles.

References

1) IDO Y, HAYASHI K: Damping Force of Damper Utilizing a Spherical Particle Assemblage, Proceedings of 15th International Conference on Experimental Mechanics, 2012, Paper ref: 2714.
2) MORISHITA Y, IDO Y, MAEKAWA K, TOYOUCHI A: Basic Damping Property of a Double Rod Type Damper Utilizing an Elastomer Particle Assemblage, Advanced Experimental Mechanics, Vol. 1, 2016, pp. 93-98.
3) P.A. Cundall, O.D.L. Strack: A Discrete Numerical Model for Granular Assemblies, Géotechnique, Vol. 29, Issue I, 1979, pp. 47-65.
4) R.D. Mindlin: Compliance of Elastic Bodies in Contact, Transaction of ASME, Series E, Journal of Applied Mechanics, Vol. 16, 1949, pp. 259-268.
5) The Japan Society of Mechanical Engineers, JSME Mechanical Engineers' Handbook, Vol. 6, 1977, pp. 3-34, Maruzen Publishing Co., Ltd.

Author

TOYOUCHI Atsushi

Joined the company in 2009
New Products Development Sect.,
Developmental Center, Engineering
Headquarters, Automotive
Components Operations
Engaged in research and
development of particle assemblage
dampers

Technology Introduction

Construction of Case Machining Line for Piston Pump

ITOU Yuusuke

1 Introduction

PPM [Note 1)] products manufactured in KYB Sagami Plant include piston pumps (Fig. 1). The piston pump is used as a component of hydraulic excavators. One of the components of the piston pump is a pump case (Photo 1) (hereinafter "the case"), which is the core part of the pump.

With the recent rising market demand for environmental measures and energy saving, the demand for piston pumps with a load sensing control [Note 2)] is expected to increase (Fig. 2). We are thus required to manufacture competitive products of this kind. Among the piston pump manufacturing processes, the one involving the highest manufacturing cost ratio is case machining. It is therefore indispensable to reduce the cost. Then, in preparation for the establishment of a new production line, we have successfully established a level of quality, which had been hardly accomplished before, to achieve higher availability and shorter cycle time (hereinafter "CT"). We have finally built a production line that can realize lower manufacturing costs.

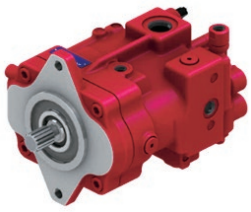

Fig. 1 Piston pump

Photo 1 Pump case

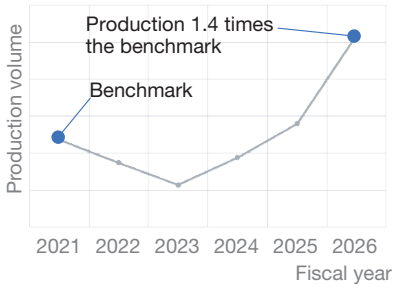

Fig. 2 Estimated production volume of piston pumps

Note 1) An abbreviation for piston pump motor

Note 2) A system that controls the pump discharge to supply the flow as much as needed

2 Line Overview and Challenges

2.1 Case Machining Line

The pump case machining line consists of machining centers (hereinafter "MC"), deburring, rough cleaning, inspection, and jet cleaning (Fig. 3).

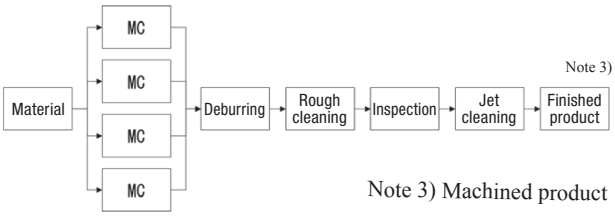

Fig. 3 Manufacturing process

2.2 Problems

The MCs can provide an integrated process [Note 4)]. Each MC can deliver finished products by itself. The problem is that, after products have been machined, they are measured on the same MC, resulting in a long cycle time. Dimensional correction is conducted as the necessity arises, which leads to lower availability. In addition, the pump case is a heavy workpiece (18 kg) to be lifted using a crane. This dangerous work is a factor in the long manual handling operation.

Note 4) A single MC can support all related processes.

3 Purpose

To improve productivity to build a production line for lower manufacturing costs.

4 Objective

Table 1 shows the target values.

Table 1 Target values

Item	Target (from the conventional level)
Production volume	33% up
Availability	6% up
Cycle time	27% down
Personnel	1 person reduced

5 Requirements

① The machining accuracy shall be improved to ensure the required quality without relying on human operation.
② The machining rate shall be increased to reduce the machining time (hereinafter "MT").
③ Work handling shall be achieved without using a crane to remove dangerous tasks.

6 Achievements

6.1 No more 100% measurement in MCs

6.1.1 Conventional Quality Problems

The case has two holes as its critical parts: one is on the front and the other on the back (Photo 2). In fact, alignment of these holes (coaxiality) was difficult to be obtained (Fig. 4), resulting in 100% manual measurement and dimensional adjustment. These additional tasks degraded the availability and productivity. The case machining was conducted by turning the machining table by 180 degrees to machine the front or the back or vice versa. Naturally, the machining quality was affected by the equipment accuracy. This was found to be attributable to variations in outside air temperature superimposed by the heat generated during continual machining, which displaced the equipment, resulting in unstable machining positions (Figs. 5 and 6). To follow any displacement of the equipment due to temperature variations, temperature sensors and temperature control systems needed to be added, which meant even higher capital investment.

(a) Front

(b) Back

Photo 2 Bore

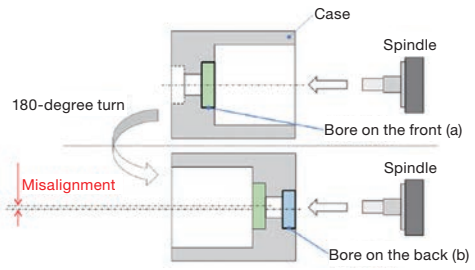

Fig. 4 Overview of front/back machining of case

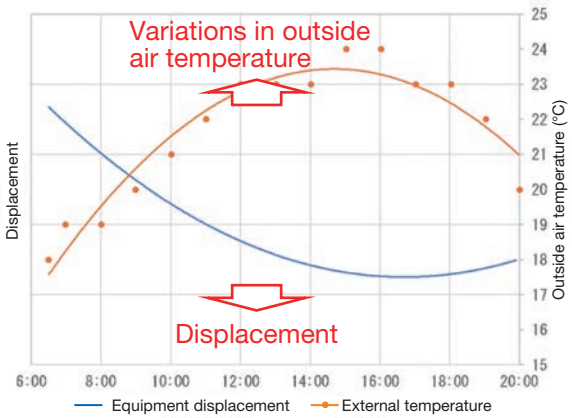

Fig. 5 Equipment displacement due to outside air temperature

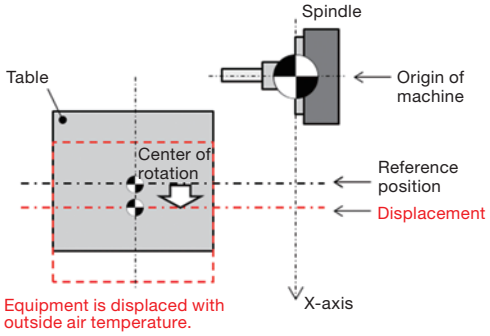

Fig. 6 Conceptual rendering of displacement

6.1.2 Internal Measurement using Touch Sensors

High capital investment leads to high manufacturing costs. So, a software program has been developed to measure displacement or deviation from the reference position using the touch sensors already mounted on the equipment and compensate for any displacement to achieve the machining target values (Fig. 7).

① Measure the position of holes provided in the jigs and then establish reference values as initial settings for equipment introduction
② Before mass production, measure the position of the holes in the jigs before machining and add any deviation from the reference value to the machining target value

If the equipment is displaced during mass production, the hole position in the jig changes. That is, the deviation

from the initially set reference value will be the displacement of the equipment.

This measurement has made it possible to satisfy the coaxial front and back machining capability. The 100% measurement during mass production is no longer necessary to achieve shorter CT. The dimensional adjustment has been also abolished to eliminate any adjustment loss, thus improving the availability.

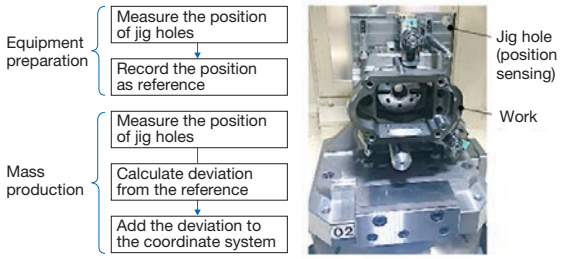

Fig. 7 Program flow and machining jig

6.2 MT Reduction with Optimal Milling Path

Among the case machining processes, milling is the most time-consuming one (Fig. 8). In the conventional milling technique, the milling cutter moves along the shortest path to accomplish the required machining. Since 50% of the perimeter of the cutter was used for milling, the cutter involves mixed operation of up milling and down milling. In fact, this resulted in unstable cutting resistance, which might cause chattering (Fig. 9). The milling machine eventually machined work at a lower speed, resulting in a prolonged MT.

To solve the problem, an optimal milling path has been developed to be suited to the complex geometry of the case (Fig. 10). The cutter has then become able to machine only with down milling being applied with cutting resistance in a fixed direction, successfully suppressing chattering. The machining speed has been doubled to reduce the MT.

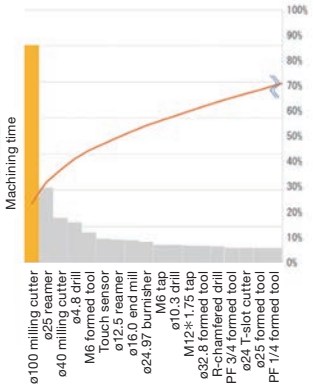

Fig. 8 Machining time of individual processes

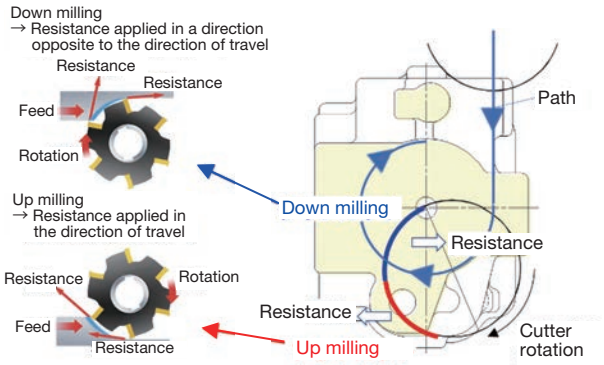

Resistance occurs in two directions, which is likely to cause chattering

Fig. 9 Milling (before change)

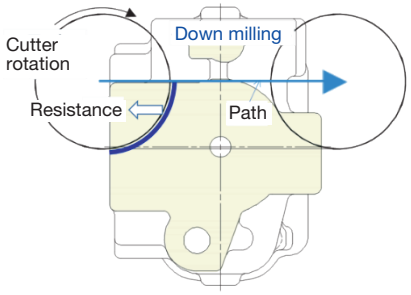

Constant resistance to suppress chattering

Fig. 10 Milling (after change)

6.3 Reduction of Manual Handling Time by Improving Jig Installability

The horizontal MC uses cross jigs for machining the case. Work must be set in position horizontally (Fig. 11). Lifting the heavy work involves danger tasks. The use of a crane makes it difficult to accurately position work, taking more time to complete attaching or detaching. As a result, the target manual handling time cannot be met.

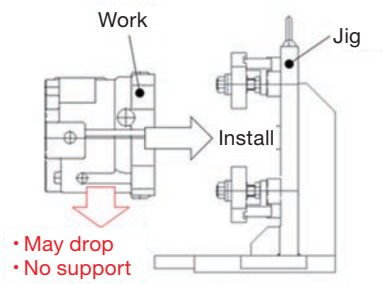

Fig. 11 Conventional way of setting work

To solve the problem, a jig that can allow the operator to set heavy work without lifting using a crane has been developed (Photo 3).

When loading, the work is slid into the jig from the carrier cart and guided by the jig for temporary positioning. The operator can just push the work to the end to accomplish final positioning with the aid of tapered pins

(Photo 4). With improved operability of jig setting, the work attach/detach time has been reduced by 50% and the manual handling time in the total production line has been reduced by 20%.

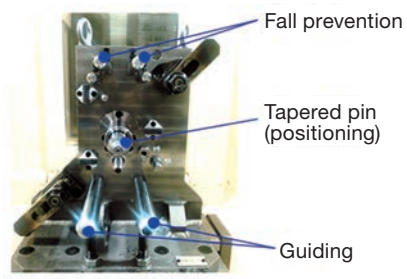

Photo 3 Jig overview

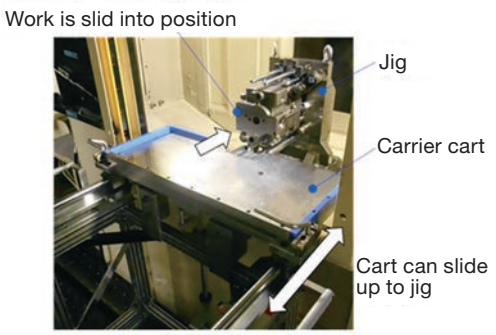

Photo 4 Work in position

7 Results

The target values have been achieved. The results are shown in Table 2.

Table 2 Results

Item	Achievements (from the conventional level)
Production volume	36% up
Availability	14.7% up
Cycle time	27% down
Personnel	1 person reduced

8 Conclusions

A new measurement method has been developed to achieve the process capability for the machining accuracy that was difficult to be achieved before. A new production line has been built to no longer involve dangerous tasks or no longer put a load on operators.

We will deploy this technique to realize new products at lower costs in future.

9 In Closing

I would like to take this opportunity to thank all those concerned from related functions who extended cooperation to the building of this production line as well as all those who gave guidance and support to us.

Author

ITOU Yuusuke

Joined the company in 2017.
Production Engineering Sect.,
Production Engineering Dept.,
Sagami Plant, Hydraulic Components Operations
Mainly in charge of design of pump manufacturing process for PPM products

Product Introduction

Development of Shock Absorbers for Snowmobile Racing

TANAKA Shin

1 Introduction

KYB Motorcycle Suspension (hereinafter "KMS") designs and manufactures shock absorbers (hereinafter "SA") for domestic and overseas motorcycle manufacturers. KMS also designs and manufactures shock absorbers for snowmobiles and ATVs and has been in business with BRP Inc. Note 1) and BRP Finland Oy. Note 2) over 30 years. They lineup snowmobiles called Ski-Doo and Lynx Note 3) known as a major brands in North America and Nordic Countries and they gained to have a majority share of the global market in 2020. [1] High-performance SA used in the high-end snowmobiles of both brands are designed and manufactured by KMS.

As snowmobiles have become technologically innovative, many state-of-the-art technologies have been reflected in their SAs. All of these technologies were originally developed for snowmobile racing and they can be found everywhere in today's mass-produced SAs for snowmobiles.

This paper introduces development of technologies that can be found in our high performance SAs.

Note 1) BRP Inc. originated with the invention of the first ever vehicle that can travel on snow by Joseph-Armand Bombardier at Valcourt in Quebec, Canada. L'Auto-Neige Bombardier Limité was established in 1942. In 1959, the Ski-Doo brand was born. In April 2003, Bombardier Inc. announced the sale of the Bombardier Recreational Products division.

Note 2) A forerunner of BRP Finland Oy was Nordtrac, which was the only snowmobile manufacturer in Nordic countries and became BRP Finland in 2005, it has continuously produced the Lynx brand. Lynx is still the only snowmobile brand in the Nordic countries.

Note 3) Ski-Doo and Lynx are the trademarks of BRP.

2 Snowmobiles Information

2.1 Vehicle Lineup

Snowmobile manufacturers offer a wide variety of vehicles that suit riders' preferences such as sport/utility models used as heavy duty work horses on snow, comfortable touring models, trail models for high-speed aggressive rides on groomed trails, crossover models that shine both on and off the trails, and deep snow models specifically designed for riding in the steep mountains covered with deep snow. Many package options are available for each model and industry's first semi-active SAs (KADS [2]) can be selected as an option for high-end package of trail and crossover models in order to have advanced shock absorption, handling and stability control. Weight savings are critical for deep snow models so lightweight high-performance SAs are chosen to improve maneuverability in the mountain terrain with steep slopes. Characteristics of snowmobile SAs required in various riding conditions are shown in Fig. 1.

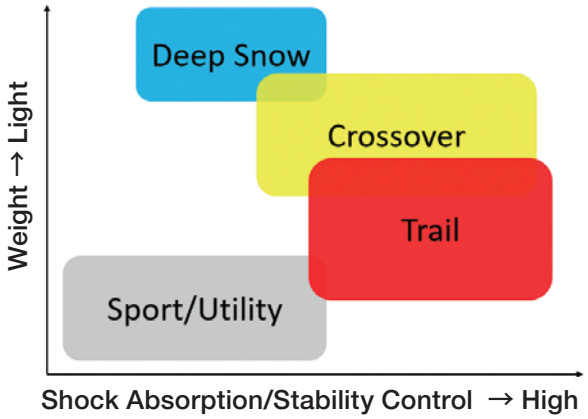

Fig. 1 Characteristics of snowmobile SAs for each models

2.2 Suspension design

Snowmobiles are quite different from motorcycles or ATVs because they have skis and track to be able to drive on the snow (Fig. 2).

The skis will float and steer a snowmobile to be able to be controlled by a handlebar on the snow. Generally, skis are suspended by double wishbone suspension. This design makes it possible to have a wider ski stance while ensuring longer suspension stroke in order to achieve higher steering stability. The right and left skis are both suspended by independent suspensions and front shocks are mounted on each side.

The track will make it drive forward on snow using its

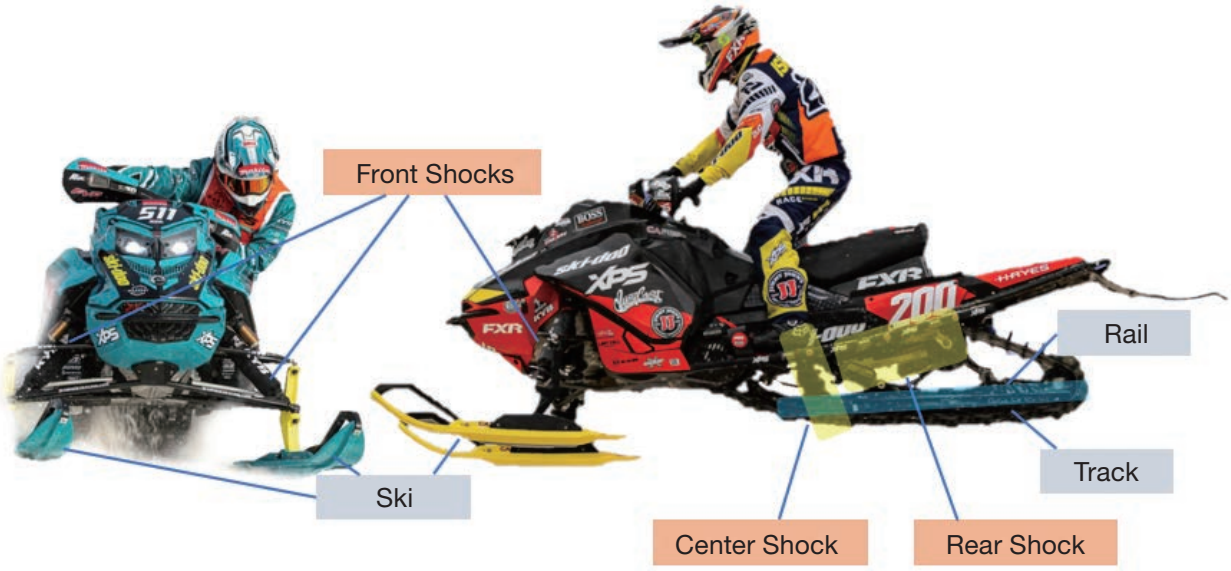

Fig. 2 Components of snowmobile suspension

lugs while keeping it floating on the snow by enlarging the contact area. There are many track styles that suit any riding conditions. Some have studs in order to have traction on hard, icy trail surfaces while some have longer lugs in the paddle form to be able to run on deep snow. Center and Rear Shocks will control the movement of the rail to keep the track in contact with rough, bumpy trails.

2.3 SA Structure

Snowmobiles are equipped with gas filled shock absorbers (hereinafter “Gas SA”) that use a steel or aluminum monotube cylinder as a standard package. (hereafter "gas SA"). All Gas SAs have Spring Preload adjuster but also some have Rebound adjuster to control Rebound Damping Force. (Fig. 3).

For the high-end package, Remote Gas SAs or Piggyback Gas SAs that have Base Valve with Compression Adjuster are equipped since much more shock absorption and stability controls are requested. (Figs. 3 and 4).

Regardless of which package they are used for, all SAs are using specially developed parts in order to be operated in specific environment conditions. The examples are in the following.

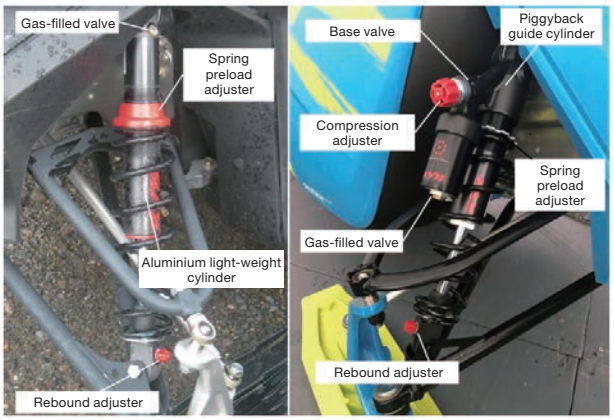

Fig. 3 Lightweight aluminium single cylinder gas SA (left) and piggyback gas SA (right)

- Ice scraper:
  Integrated Ice Scraper in the seal head to scrape off frozen snow on Piston Rod surface (Fig. 5)
- Oil:
  Specially formulated to ensure fluidity in freezing condition

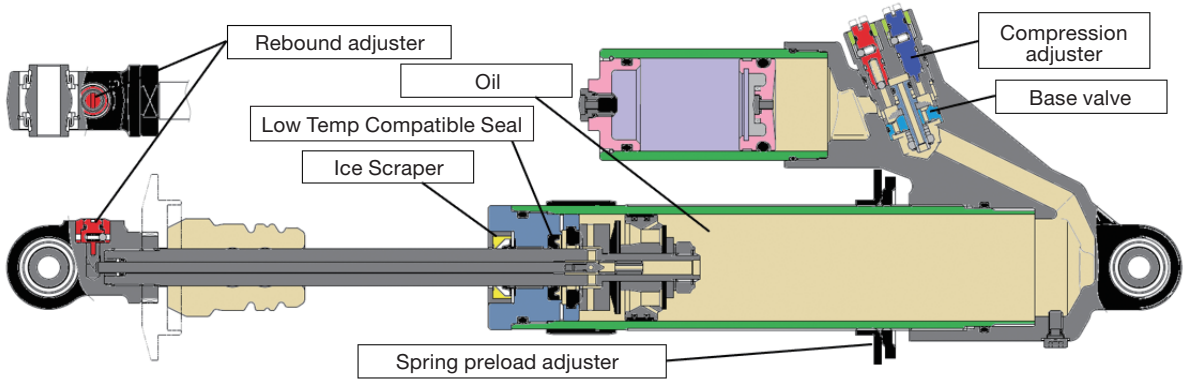

Fig. 4 Components of piggyback gas SA

- Low-temperature seal:
  Carefully chosen seal material to keep Oil in SA in freezing condition

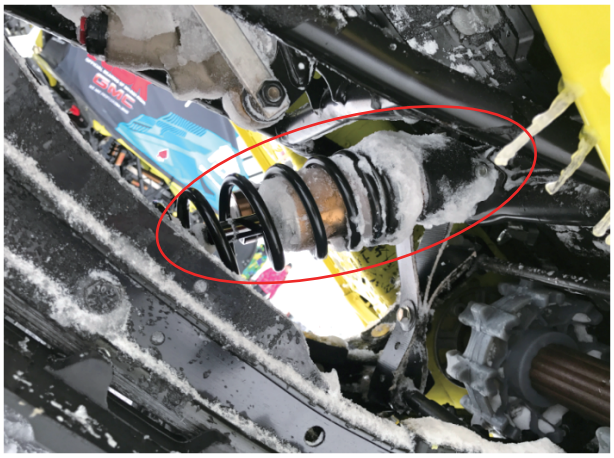

Fig. 5 Frozen ice covered Center Shock at the racing paddock

3 Types of Snowmobile Racing

There are various kinds of snowmobile races as in the case of other motorsports. The following describes major categories of snowmobile races.

3.1 Snowcross

Snowcross was derived from the sport of motocross. Like motocross, riders compete with each other on man-made racetracks with tight turns, banked corners, steep jumps and obstacles.

Today, Snowcross are held are held at many locations in North America and Nordic countries. Courses in North America include consecutive jumps and tight corners, thereby requiring harder braking and rapid acceleration. On the other hand, many of the courses in the Nordic countries make use of original natural terrains. Since these courses are usually wide, racers are likely to run at higher average speeds. The International Series of Champions (ISOC) Snocross, which are held around Great Lakes in North America, are participated in by famous competitors not only from North America but also from the Nordic countries. The world's premium race riders compete in a total of 17 races at eight racing venues every year vying with each other to clinch the championship title.

Both Ski-Doo and Lynx have lineups for the racing-ready snowmobile specific for Snowcross called 600RS that is only available for snowcross competitors (Figs. 6 and 7). They are developed based on Trail snowmobiles but equipped with a fine-tuned 600cc two-stroke engine and race-proven special suspension system.

KMS has been providing specially designed SAs called “Factory Shocks” to BRP Racing Department and joining BRP’s Racing program to develop better SAs by supporting them technically.

Fig. 6 Ski-Doo MXZx 600RS [Note 4)]

Fig. 7 Lynx Rave 600RS [Note 4)]

Note 4) MXZx, Rave and 600RS are trademarks of BRP Inc..

3.2 Hill Climb

Riders compete on how fast they can climb up ski slopes with specially modified Deep Snow snowmobiles. The most famous race is the World Championship Snowmobile Hill Climb that is held at Jackson Hole in March.

3.3 Cross-country

Competitors run a long distance toward a specified destination with the Crossover snowmobile like Dakar Rally. The most famous race is the Iron Dog in Alaska. Competitors race over 4,000 km in a week and may be required to ride on dirt, grass or skipping over frozen rivers.

3.4 Others

Oval racing competitors corner on icy oval racetracks at the highest speed with specially modified, lowered snowmobiles. Drag racing can record the highest speed on a short, straight course. Snowmobile racing is not only held in winter; Watercross is getting popular, competitors skip snowmobiles on a lake to race like snowcross.

4 Development of SA for Snowcross

The following are the major functions that are required specially for Snowcross SA.

4.1 Front Shock

To prevent rolling moment during high-speed cornering in order to keep skis in contact on the trail, Front Shocks need to provide a certain amount of damping force from lower piston speed range. In addition, Front Shocks have longer shock strokes to accommodate the larger gaps and jumps found on recent racetracks.

4.2 Center and Rear Shocks

Center and Rear Shocks will stabilize the snowmobile by controlling the rear suspension system and keep the rail tracks on bumpy racetracks. Center Shock attached to the front of the rail needs to be supple enough to help the rail to follow the rough track surface while maintaining a certain amount of Ski pressure to have good handling. However, it also needs to get stiffer to absorb energy to prevent harsh landing after jumping. Thus its damping force will have progressive characteristics that can generate less damping force at lower piston speed range but generate more damping force as it gets higher. Rear Shock is attached on the rear end of snowmobiles to control the vehicle pitching moment during acceleration and braking by providing a certain amount of damping force at lower piston speed balancing with Front Shocks. To provide higher damping force at a higher piston speed range to absorb landing impacts after jumps, it has the longest stroke than the other SAs. So it is essential to have higher rigidity construction to withstand its harsh use condition.

4.3 Adjuster

In Snowcross racing, competitors need to race all day for several rounds of races; qualifying in daytime and the final at nighttime. SAs need to have many kinds of adjusters in order to quickly adapt to any kinds of racetrack conditions because it changes depending on the weather moment to moment.

4.4 History of Development of SA for 600RS

4.4.1 Development in the Early 2000s

Before the 2000s, aluminum monotube Gas SAs were used because of its lightweight construction but they only used to have a rebound adjuster. In the early 2000s, riding style has drastically changed from old-school "sit-on seat" style to revolutionary "stand-up" style that suits modern racetracks. To adapt this, a new chassis; REV and front suspension system; RAS were developed. At that time, BRP requested to develop new Remote Gas SAs in order to improve shock absorption by adding Base Valve and Compression Adjusters that can generate higher damping force (Figs. 8 and 9).

Fig. 8 Blair Morgan's racing snowmobile built for X-Games in 2006

Fig. 9 Remote Reservoirs of Front Shocks were fixed in the hood

Later in 2004, piggyback Gas SAs were developed and introduced in all SAs years later by replacing Remote Gas SAs. To further improve shock absorption, the piston diameter got larger from 36 mm to 40 mm and rod diameter was also enlarged for higher strength and rigidity. These racing technologies developed and validated were later used in SAs for consumer models and they are still used in today's SAs.

4.4.2 Development in recent years

For the Snocross Pro Open; premier class in Snocross, it had been permitted to modify engines, pipes and chassis of racing snowmobiles to gain performance. But in 2018, the regulations were revised to limit the modification. This gained even more attention on the development of the stock racing-ready snowmobile; 600RS. Particularly, improving the suspension performance was considered as a critical challenge to ride faster on modern racetracks.

To do so, suspension linkage mechanisms were fully redesigned and more performance improvements of SAs were strongly requested. As a result, peripheral parts for suspensions have been improved every year and SAs have also been improved every year from 2018.

Following technologies were originally developed for Snocross Factory Shocks and adapted for 600RS.

① Larger diameter piston for Center and Rear Shocks

As stated above, revision of regulations were taken as an opportunity to improve performance of the rear suspension system. Larger Diameter Pistons were already introduced for Factory Center and Rear shocks but evaluation swung into high gear to find good setups. Riders soon highly valued its stability and improved impact absorption performance to prevent harsh landing after big jumps. It was adapted for Center shock of 600RS MY2018 first and for Rear shock of MY2019 later.

② Integral adjuster

An integral adjuster, originally used for motocross racing shocks, was introduced for Factory shocks to be able to be fine-tuned to rider's preferences in a tight racing schedule. It made it possible to adjust high-speed rebound damping force quickly from outside that used to be hard to adjust via conventional adjusters and normally required re-valving (Fig. 10). The characteristics of the check valve were re-calibrated for Snocross after being introduced for Snocross. As a result, it will settle shock movements to maintain a good ride height when shock rebounds from a fully stroked position which gives better handling when riders enter corners right after a jump landing. It showed its value on the racetracks with many jumps and was more useful than conventional adjusters. Finally, it was adapted in all SAs from 600RS MY2020.

③ Larger diameter piston for front shocks

Since the larger diameter piston used for center and rear shocks had been highly valued as stated above, a request arose to apply it for front shocks as well. However, it was even harder for the front shocks because they had to be fit in a very limited space around them. To solve this, related parts needed to be redesigned from ground up. A brand new guide cylinder and bearing were designed and firstly used in 2018-2019 season (Fig. 11) They reduced rider's arms fatigue by absorbing landing impact after huge consecutive jumps and provided better stability that leads to great advantage during racing. Development was further continued to find good setup and the reliability was proved on racetracks. They firstly debut for 600RS MY2021 and also selected as production shocks for high-end Lynx Trail model (Fig. 12).

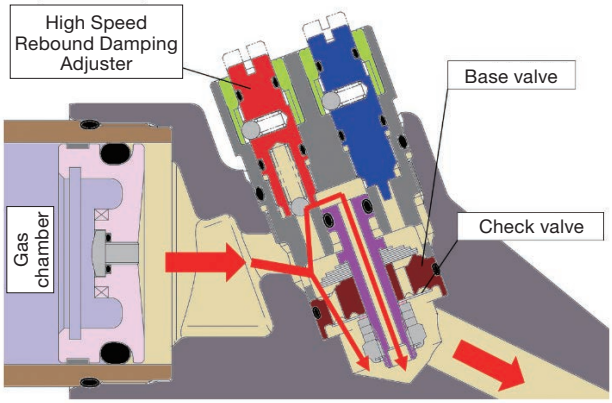

Fig. 10 Rebound Oil flows in the Integral Adjuster and High Speed Rebound Damping adjust circuit

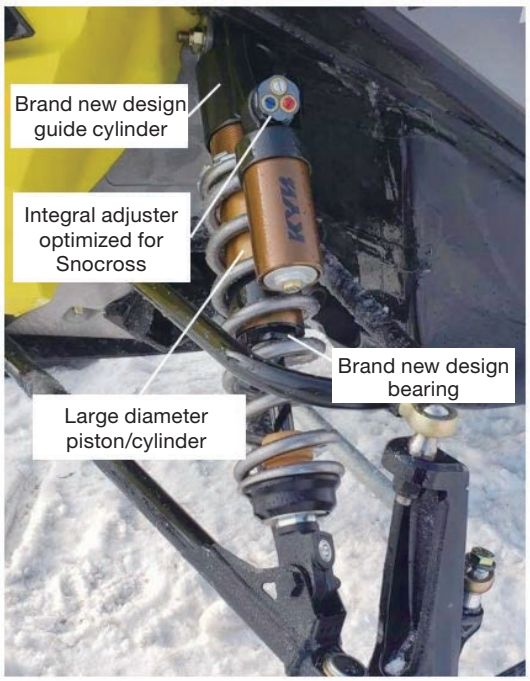

Fig. 11 A brand new Front shocks with large diameter piston debut in 2018-2019 season

Fig. 12 First production trail snowmobile adopted front shocks with large diameter piston

4.4.3 Current Development

They are equipped with new technologies that are expected to be adopted for the next generation of SAs for 600RS and production shocks. Our technologies had already been verified by great racing results as follows.

5 Major Racing Results

2020-2021 Season

#200 Elias Ishoel

Three consecutive championship in Pro Class of ISOC Snocross (Fig. 13)

Won Race 1 and finished 6th overall in FIM Snowcross World Championship 2021

Fig. 13 Elias Ishoel won the three consecutive championship along with our technicians; Tim (left) and Gilles (right)

6 In Closing

I would like to take this opportunity to thank all the engineers of BRP and BRP Finland who extended their cooperation into the development field as well as the technicians from Enzo Canada who have been joining our racing support program and provided technical support on our factory shocks for more than 20 years.

Finally, I would like to express my deep respect to our predecessors who were involved in the past development and brought those technologies of racing shocks into production that had built the foundation of today's technology and cordially thank all those from the internal related departments who extended their cooperation to us. I am committed to develop products that are even more attractive to riders all over the world and hopefully our latest technologies will be their advantage.

References

1) Power Sports Business, 2020 Market Data Book, p.61, Worldwide Snowmobile Market Share.
2) UEMURA, KOJIMA, SUGAWARA: Development of "KADS" - An Electronically -Controlled Suspension System for Motorcycles, KYB Technical Review No. 63, (October 2021).

Author

TANAKA Shin

Joined the company in 2015.
Group 2, Design Sect. No.2,
Formerly engaged in design and development of motocross racing suspensions and later engaged in design and development of SAs for snowmobiles and ATVs

Essay

Account of Residence in Czech Republic

NOMURA Norifumi

1. Introduction

I was assigned to work for KYB Manufacturing Czech s.r.o (hereinafter "KMCZ") as an expatriate for five years between April 2016 and April 2021. Before the assignment, I had been involved in the shock absorber (SA)-related quality support operation in Japan for overseas sites and in charge of ASEAN projects even while I had been preparing for the assignment. Actually, I had never been to KMCZ before. Although I had to begin my work for KMCZ rather suddenly with no specific information available, home is where you make it. I eventually developed personally thanks to a variety of experiences over those five years.

Looking back, I will outline my life there. You know many predecessors who had been sent to the Czech Republic have already talked about tourist attractions and local cuisine, but there are still many other interesting places and stories. I hope you enjoy reading my essay.

2. Information about Czech Republic

Before 1993, the Czech Republic used to be part of Czechoslovakia along with its current neighbor Slovakia. I remember in my childhood the Czech ambassador stepping onto the Sumo wrestling ring on the last day of each tournament (Senshuraku) and read out loud "hyo-sho-jo, anta-wa-erai !" in Japanese (meaning "congratulations, you are the winner") while handing a huge Bohemian glass cup to the champion. Bohemian glass is still one of the famous specialty products of the Czech Republic. Featuring high transparency and hardness, Bohemian glass used to be used for the stained glass in churches and is popularly used in a wide range of applications including flower vases and drinking glasses.

The Czech Republic is a landlocked country bordered by Germany to the west, Poland to the north, Austria to the south, and Slovakia to the southeast. Located in the center of Europe, the country is at a latitude roughly equivalent to Hokkaido. It is very cold in winter. In middle February, the temperature is below -10°C for several consecutive days. When I was in the Czech Republic, I always stayed indoors on weekends during the winter season, except going out for shopping, to spend comfortable hours in warm rooms where the temperature was controlled by a central heating system. On the contrary, the summer is comfortable with low humidity. You can spend the season without using air conditioners just by keeping the windows open.

The summer in the Czech Republic is the best season to drink beer. In front of restaurants on the street you can see tables, chairs and parasols where people can enjoy talking with their family and friends with a glass of beer in one hand. Speaking of beer, the Czech Republic is number one in the world in per capita beer consumption. Of course, the small country cannot be top in total beer consumption, but scores far ahead of others in per capita consumption. When I walked by a restaurant or bar in the early morning, I sometimes happened to see a beer tank truck parked alongside the building supplying more and more beer to the restaurant or bar. That made me understand how much beer customers drank in the restaurant last night. I recognized anew that Czechs really loved beer every time I saw such a scene.

The word Czech may also remind you of some famous traditional towns including several World Heritage sites. Not only in Prague, but also near Pardubice where I lived, there are many famous tourist sites such as Kutna Hora. The town used to prosper with silver mines and is still dotted with gorgeous traditional buildings.

Among them, the Church of St. Barbara and the Cathedral of Our Lady at Sedlec are particularly well-known. The Church of St. Barbara has Gothic architecture from the 13th to 15th centuries with various statues and paintings decorated inside the church. The historical building has three roofs at the center, around which there are several pointed columns.

The Cathedral of Our Lady at Sedlec is internally decorated using the bones of about 10,000 people. When you step into the cathedral, it is cool even during summer and may feel a little dusty. On the front of the gate there is an emblem. Inside the cathedral you can see a chandelier and several decorations on the wall. All of them are made of bones! You may be astonished by this way of using human bones, something that never happens in Japan.

Pardubice, where the KMCZ plant is located, is in East Bohemia and 100 km east of Prague. A famous event in this city is Velká pardubická, which is a cross-country

horserace or steeplechase held in October every year. Many tourists from everywhere in Europe visit the city to enjoy the race with a glass of wine in hand.

During my expat assignment in the Czech Republic, I lived in the center of Pardubice. I often ate at the plaza where the city hall was located or visited old castles nearby. The city hall was in a traditional building that had been renovated. The building exterior was decorated and lit up at night during seasonal events, which is popular among the citizens.

In addition, the Czech Republic has many other various tourist spots. Most Japanese tourists typically enter the Czech Republic from Prague and then travel to Austria via Český Krumlov.

Photo 1 Pardubice City Hall

3. KMCZ

KMCZ in 2016 finished with a plant expansion to the west (more than doubling from 15 thousand m^2 to 35 thousand m^2) since 2015 and introduced additional assembly lines. The plant had started to increase production since FY2015. With an economic boom in the Czech Republic from around that time, the country enjoyed an increase in capital investment and private consumption year by year. As the jobless rate decreased and wages increased every year, some of the employees retired from KMCZ and tried to work at another workplace on slightly more favorable terms. One of my missions during the assignment was to find substitutes for those who retired.

KMCZ introduced another manual production line for assembling single-cylinder gas SAs and standard SAs in August 2016. As the third line, an ST welding and assembly line was introduced to steadily improve the production plan in December 2017. The plant shipped 3.70 million pcs/year in 2014 before the plant expansion increased the level to 5.70 million pcs/year in 2018. Thereafter, production has increased year by year, although shipments dropped in 2019 and 2020 partly because of the effect of the novel coronavirus (COVID-19) pandemic.

Currently, on the west side of the KMCZ plant is a loading dock to receive and ship finished products including tubes. Nearby is a storage space for finished products. To the southwest are tube/rod machining lines and part warehouses. The expanded area was mainly used as a finished product yard and a preliminary machining space. To the east of the plant are an internal valve assembly line, a standard SA assembly line, and a strut SA assembly line. The production system is designed to transfer finished products to the finished product yard to the west.

KMCZ has about 700 employees. They work in three shifts for assembly lines and in four shifts for preliminary machining lines. We set up the Open House in summer and held a Christmas party in winter to allow employees to enjoy themselves with smiling faces, while they worked with their serious faces in daily production.

Photo 2 KMCZ Open House

4. Entertainment

Czech people really like to do outdoor activities. On weekends they often go hiking in the mountains, cycling, or inline skating with their family. When I was there, we also played golf on weekends. On golf courses, we often found that the husband of a typical Czech family was playing golf and his wife and children were walking their dogs following the husband. I was moved by the fact that Czechs really loved to be in nature with their family.

Sport is also a Czech favorite. The popularity of tennis may be well known to Japanese. In particular, in women's tennis, several Czech players are ranked high in the world. Many readers may have heard the names Barbora Krejcikova and Karolina Pliskova. News of their performance was reported by Czech television almost every day. It reminds me that a Czech woman won the gold medal in both skiing and snowboarding in the winter Olympics, which was quite before though. The prominence of Czech women in the world of sport is remarkable.

Photo 3 Kunětická golf course

Photo 4 A game of ice hockey

5. Ice Hockey

Ice hockey is very popular among Czechs with multiple active professional leagues. In Pardubice, where there is a professional hockey team, the arena is packed for every game with fans in the team's uniform and they roar on the team regardless of whether it is winning or losing. It was easy to figure out when a hockey game was held just by hearing the chanting on the street. I went to the arena to watch hockey games several times. In these games I saw players battling with each other for the puck or charging into each other. They had a fight once in a while. Unfortunately, I could never clearly see the scoring moment when I was watching a hockey game. Instead, I enjoyed the scoring scene by noting it with the scoring lamp and beep sound as an instant fan.

Hockey is a national sport for Czechs. They play hockey on a skate rink from childhood. Even during summer, they enjoy playing ground hockey using a stick similar to that used for ice hockey. In the PyeongChang 2018 Winter Olympics, the semifinal game was the Czech Republic against Russia. Although the Czech Republic finally lost, Czech staff members in KMCZ were always checking what was going on in the game via the Internet or the like to share information with each other, putting work to one side.

If you tell a Czech person that you are from Japan, you may be asked "Which part of Japan?". Since the Czech national hockey team won the gold medal in the Nagano 1998 Winter Olympics, the word 'Japan' reminds them of Nagano. In spite of being a hockey superpower, the Czech team had only ever won the silver medal, and it had been beaten by Russia many times. In Nagano in 1998, the Czechs were especially happy when the national team won the gold medal by beating Russia in the final. This big event for Czechs did happen at Nagano in Japan. If you talk about the Nagano Olympics, you can get friendly with Czechs very quickly.

6. Czech Food

I am often asked "What is typical Czech food?" One of the popular lunchtime dishes in KMCZ was Schnitzel, thin slices of chicken or pork that are fried. It tastes similar to cutlets in Japan. Japanese expatriates often asked the kitchen to dress Schnitzel with pork cutlet sauce and enjoyed eating it with rice. Neighboring countries including Austria and Germany also have the same dish. Schnitzel is typically served along with potato in these countries.

A kind of beef stew originating in Hungary called Goulash is another typical lunch dish. When you are in a restaurant anywhere in the Czech Republic, you can always find Goulash on the menu. This national food is a little bit salty compared to beef stew in Japan and is often served with steamed bread. I privately recommend Goulash soup in a bowl made of bread.

The next cuisine I want to introduce is Beef Steak Tartare; I do not know if you like it though. Japanese, including me, tend to have difficulty ordering this food at a restaurant because they cannot pronounce it correctly. Steak Tartare is like beef yukhoe seasoned with spices and garlic. You can put grated garlic on a piece of well-baked bread and then add an appropriate portion of Tartare on the bread before eating. Czechs, whether they are men or women, cram it into their mouths without caring about the smell of garlic. I do not know how your stomach will be next day if you eat Tartare too much.

Typical drinks in the Czech Republic include Kofola, a kind of carbonated drink. As the name implies, this is a Czech version of cola. It is said that Kofola originated during the time of Czechoslovakia when people mimicked cola. This slightly carbonated drink smells a little bit like lemon. I thought at first that it was just cola with lemon that had gone flat, but I gradually became used to the taste. It is definitely a national drink along with beer.

Photo 5 Steak Tartare

7. Czech Names

I had an opportunity to learn the typical surnames of Czechs. I want to introduce some of them as their surnames and Japanese counterparts have several things in common. Some Czech surnames are named after the natural world, such as Kopecky meaning "hill" or "mountain" and Novotony meaning "new". I thought these might be similar to the popular Japanese surnames Yamamoto (literally meaning "foot of the mountain") and Arai (literally meaning "new well"), respectively. The order of names is also common between Czechs and Japanese: the surname comes first and is followed by the "first name". This was a story I felt connected me with Czechs.

I almost forgot to say, but Czech surnames for men end a little bit differently from those for women. Most surnames for men end with "ky" or "y" while those for women end with "a". Kopecky, as mentioned above, will be Kopecka for women, and Novotony will be Novotona for women. Many surnames for women add "ova" to the surnames for men.

I found in KMCZ that a popular name for men was Jan. In Czech, "ja" is pronounced "ya". Many famous heroes are called Jan, and this should be popular among today's people too. However, its nickname is a little bit strange. Jan is nicknamed Honza, which is quite different from the original name. I did not get it at all in the early days of my stay in the Czech Republic. I remember I sometimes looked around me trying to find what people were called as I did not understand what the nickname meant. In addition, Anna, Anicka, Eva, and Evicka were also typical nicknames. I wondered why they were called by a nickname that was longer than the original name.

Another interesting story about names is that people celebrate their name day on the date corresponding to their own given name on the calendar. So, Czechs have two birthdays in one year. At first, I did not understand why they would celebrate their birthday again as they had celebrated it the previous month.

8. COVID-19 Pandemic in Europe

COVID-19 first spread as an epidemic in Italy and Spain a couple of months before the news of Japan's first infection cases on the Diamond Princess Cruise Ship were reported. Czechs seemed to look upon it as "That's not my business" in the beginning. However, as Czechs who had come home back from the designated countries were infected with the disease, the Czech Republic started to close its borders with neighboring countries and to suspend air services in March 2020. Various COVID-19 control measures including an entry ban for foreigners were taken to combat the virus in European countries.

KMCZ also took COVID-19 control measures for its employees. For example, those who had traveled to Italy or Croatia during their children's school winter holidays were recommended to voluntarily isolate. In order to cope with the problem of shortages of masks and disinfectants, the company placed orders for these goods early. It also changed the scheduled period of business trips of employees and meant those who had been sent to a foreign country had to come home before the suspension of international air services.

The situation rapidly deteriorated thereafter and was followed by a lockdown. Some customers planned plant shutdowns, and KMNA suspended production in April 2020. During the lockdown, all shops except food markets, gas stations and drug stores were closed. With no restaurants open, I had difficulty in getting food as I lived alone. Other control measures included a night curfew from 9 o'clock at night to 6 o'clock the next morning. The lighting in shops on the streets was turned off and nobody was walking on the street. Even the downtown area was quiet.

After that, the restrictions were relaxed in phases as the number of newly infected patients had changed. A cycle of lifting the ban and the spread of infection was repeated over and over again. During this period, the entry of foreigner tourists was prohibited, greatly impacting the tourism and food service industries.

I had the opportunity to visit Prague on business during the period of relaxed restrictions. The city, which had usually been crowded with tourists, was quiet and nobody was on the famous Charles Bridge (Karluv most) or on the road on the other side of the river. It felt strange the way the city was different from usual, but the scenery was still beautiful.

KMCZ also had a difficult time and struggled to secure the personnel necessary for production during the pandemic because of the increased number of newly infected patients. Some employees were infected and some others were identified as persons who had close contact with patients and were asked not to report to work. COVID-19 may still be advancing or retreating. I hope the pandemic will be over soon.

Photo 6 Prague, photographed from Letná Parks

9. In Closing

I returned to Japan after finishing with my five-year term of residence in the Czech Republic. Now I can see what difficulties my colleagues may have had during their expat assignments in foreign countries.

During my assignment in the Czech Republic, I learned a lot about corporate management as I served as site manager and was involved in management that I had never experienced in Japan. The experience of living in another culture also gave me a good opportunity to change my way of looking at things that I had never previously doubted. Particularly as I experienced living in two countries (before living in the Czech Republic, as I had been assigned to the U.S.A.), I can now compare the people, culture and economy of those countries with those of Japan, which helps me think I am a better person. I really appreciate being given such opportunities.

I would like my colleagues, if they have an opportunity to work overseas, to absorb another culture while they live in the country in addition to their daily work in Japan.

Finally, I would like to thank all those who supported me when I lived overseas. I am committed to continuously doing my best for the development of KMCZ.

Author

NOMURA Norifumi

Joined the company in 1992.
General Manager of Quality Management Dept., Quality Div.
Took present post after working in SA Quality Assurance Dept., expatriate in the U.S., Product Planning Dept., and expatriate in the Czech Republic.

Glossary

KYB-IoT Platform

Refer to Building the Foundation for MES Services in the New Era (page 8)

TAKINO Shinsuke
DX Dept.

1 Overview of KYB-IoT Platform

Recently, KYB has also become involved in many projects making use of data and digital technology.

As these projects increase in number, it is necessary to build a Data Collection Foundation that continually collects and accumulates big data and a Data Analysis Foundation for accelerating data utilization including Business Intelligence (BI) and Artificial Intelligence (AI).

So, the DX Department is promoting the building of an IoT Platform as a Data Collection/Analysis Foundation so that KYB can internally utilize digital technology widely and correctly. Fig. 1 shows a conceptual illustration of the KYB-IoT Platform.

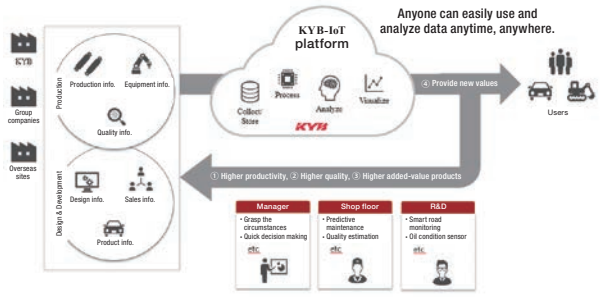

Fig. 1 KYB-IoT Platform

The cloud-shaped area in Fig. 1 represents the KYB-IoT Platform that has been implemented with the cloud service available from Amazon Web Services (AWS).

Data from the Production and Design & Development fields (e.g., plant facilities and products under development) held by KYB and its affiliates is collected, processed, analyzed and visualized to provide new values to external users or customers and to be available to internal users for improving productivity, quality and added-value products.

2 Major Functions of KYB-IoT Platform

To ensure that the KYB-IoT Platform can effectively deliver in the future, the following three technical functions are important:

① Data collection

It is essential to build a system that can quickly and continuously collect and store data from individual departments without consuming too many man-hours to analyze and utilize the big data.

② Tampering-proof

All accesses to the system should be recorded in a log.

In case of tampering, the system automatically records the event and transmits alert e-mails. This will ensure transparency around internal data management and access, providing safety and security to customers.

③ Analysis and management

In an AI development project, reproducibility can only be secured with all of the three elements: source code, data, and parameters.

Data is changing even during operation. It is essential to build a foundation for managing data in sets and for continual relearning and remodeling, in order to achieve long-term operation.

It is also needed to develop human capital for data utilization to ensure that information on the KYB-IoT Platform is accessible by anybody in the company and can be viewed in various ways as well as be analyzed in a simple way on Web browsers during daily work as standard.

Glossary

Cavitation

Refer to Research on Technology to Control Air Bubble Content in Hydraulic Fluid (page 17)

NAGASHIMA Midori
Mechanical Component Engineering Sect., Basic Technology R&D Center, Engineering Div.

1 What Is Cavitation?

A hydraulic fluid may contain bubbles for several reasons, including mixing of the air by agitation, mixing of the air due to vibration of the hydraulic circuit or tank (sloshing), and precipitation of the air dissolved in the fluid when the fluid pressure reduces to a certain level (aeration). Particularly, when the pressure reduces to below the saturated vapor pressure due to an increase in flow rate of the fluid in the hydraulic line or machinery, the fluid may vaporize to generate bubbles. This phenomenon is called cavitation (Fig. 1).

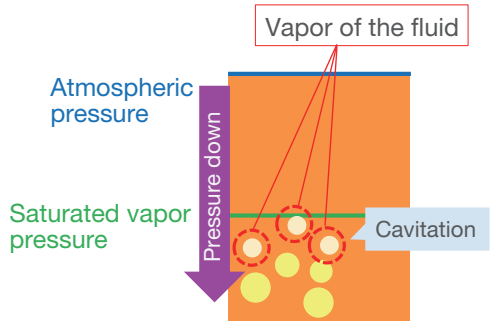

Fig. 1 How cavitation occurs

2 Problems Caused by Cavitation

Bubbles that have been generated by cavitation rapidly disappear (collapse) when the fluid pressure increases again. The collapse generates impact pressure that may damage the wall of the fluid duct and machinery components, which may cause erosion (cavitation erosion). Repeated shock waves may also lead to vibration or noise of the piping or machinery.

In addition, cavitation could be a cause of degraded products. The following introduces two examples of such products.

2.1 Hydraulic Pumps

When a hydraulic pump is run at a higher speed, the hydraulic fluid is sucked at a higher flow rate. Once the suction speed exceeds a certain level, the suction port has a local decrease in pressure, causing cavitation. When a number of bubbles are present in the fluid, the fluid accounts for less percentage of the suction volume by the same amount as the bubbles. This results in the problem of a decrease in discharge rate as shown in Fig. 2.

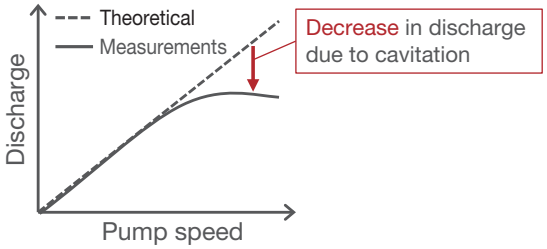

Fig. 2 Discharge characteristics

2.2 Shock Absorbers

A shock absorber as a component of an automobile (Fig. 3[(1)]) can alleviate the vibration transmitted from the surface of the road to the vehicle body. This can be achieved by a piston rod (valve) moving backwards and forwards within a cylinder filled with a hydraulic fluid. If the piston rod abruptly strokes at a higher speed, cavitation may occur to generate bubbles. When the bubbles affect the compressibility of the fluid, the intended damping characteristics may be lost as shown in Fig. 4.

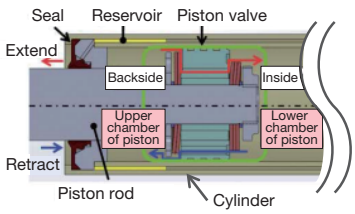

Fig. 3 Overview of shock absorber

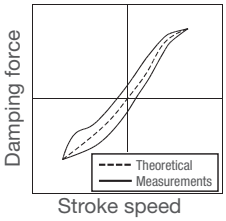

Fig. 4 Damping characteristics

References

1) SANO Yuta: Development for Analytical Technology of Shock Absorber Valve Characteristics, KYB Technical Review No. 58 (April 2019).

Editors Script

I wrote three consecutive articles in the middle of the Heisei era. At that time, I had no literary talent so proofread my articles over and over again in response to comments by editors, while complaining "Why do I have to write consecutive articles?". Fifteen years have passed since then. When I read the articles of other engineers in this Technical Review, I can recognize anew the necessity of taking a step forward, creating new things, revealing them to the public, cultivating them, and taking another step forward. It reminds me when my boss told me "A plateau is the same as a slope". He added "The difference in speed of improvement or development between us and our competitors will be the difference in profits, and you win only when you go forward faster than competitors". I expect all KYB engineers, including those who contributed to this Technical Review, will do their best even in the toughest of situations. (NOGUCHI)

Our way of living has changed dramatically during the coronavirus pandemic. Many people now take it for granted that they can work at home using the Internet and attending web meetings. Meetings of our editorial board are also held online. On holidays, going camping has become popular because of few chances to have close contact with each other. I am one of these camping converts. Still, I felt a little complicated when I learned the demand for enjoying "inconvenience" in a sense while digitization has improved convenience. KYB Technical Review is also a consequence of responding to a variety of customer and inhouse needs. I would like to continue providing information on KYB technologies and experiences. (HAYASE)

There is a trend for automobiles and construction machinery to introduce automated driving and remote control. We are always concerned with how we should cope with or follow such trend as a hydraulic component manufacturer. Against such a background, I became an editor checking articles for the Technical Review. I sometimes find a lot of helpful hints in recent KYB Technical Reviews. In spite of the tough circumstances connected to the COVID-19 pandemic, I am very proud of the engineers who have developed and produced various products in different sites. By leveraging the total engineering prowess of the overall KYB Group, I would like to further promote technical development. (KOBAYASHI)

KYB TECHNICAL REVIEW No.64

Published on April 1, 2022
Editor and Publisher: KYB Technical Review Editorial Board
Publishing Office: KYB Corporation
(KYB Corporation adopted the common name of KAYABA Corporation on April 1, 2022).
World Trade Center Building South Tower 28F, 2-4-1 Hamamatsu-cho, Minato-ku, Tokyo 105-5128, Japan
Tel: 03-3435-3511
Fax: 03-3436-6759
Published by Shobi Printing Co., Ltd. (Hakusan, Tokyo)

Notification regarding website release

Thank you for supporting KYB TECHNICAL REVIEW. Since the 50th edition (issued in April 2015), we have been releasing these reviews on our website with the aim of enabling more people to read them.
We will also continue to publish the booklets as usual, so please read the printed version and/or the website at your convenience.

<KYB website>
https://www.kyb.co.jp/
(Please click on the KYB REVIEW banner on the home page).